3rd Open Science Symposium

on Western Pacific Ocean Circulation and Climate

Handbook

May 8-10, 2018, Qingdao, China

http://oss18.csp.escience.cn/dct/page/1

Organizer Northwestern Pacific Ocean Circulation and Climate Experiment

Host Institute of Oceanology, Chinese Academy of Sciences

Northwestern Pacific Ocean Circulation and Climate Experiment (NPOCE)

NPOCE Website: http://npoce.org.cn/

Northwestern Pacific Ocean Circulation and Climate Experiment (NPOCE) is an international program endorsed by Climate Variability and Predictability (CLIVAR) in 2010, contributed by 19 institutions from 8 countries including Australia, China, Germany, Indonesia, Japan, Korea, the Philippines and the United States. The NPOCE scientific objectives are achieved through five research themes: 1. Western boundary currents; 2. Interaction with ambient circulation systems; 3. Roles in warm pool maintenance and variability; 4. Regional air-sea interaction and climatic impacts; 5. Marine biogeochemistry.

NPOCE has been successfully progressing for about seven years and made great progress through collective international effort, particularly in field experiments. NPOCE has built the largest regional scientific observing network in the tropical Western Pacific Ocean and Indonesian seas, including more than 30 subsurface moorings in water and 2 buoys near the equator. Among which, 10 subsurface moorings and the 2 buoys transmit real time data. During the 2017 annual cruise of IOCAS, 6 more subsurface moorings were deployed along 8º N and 18º N east of the Philippines, achieving a full coverage of observations in the western Pacific main current system for the first time. In addition, numerous CTD casts were made and ARGOS drifters and Argo floats were deployed. With these efforts in field observations, NPOCE community has significantly advanced scientific research into the ocean circulation and climate, strengthening conceptual findings from the past and discovering new phenomena.

➢ NPOCE participating countries

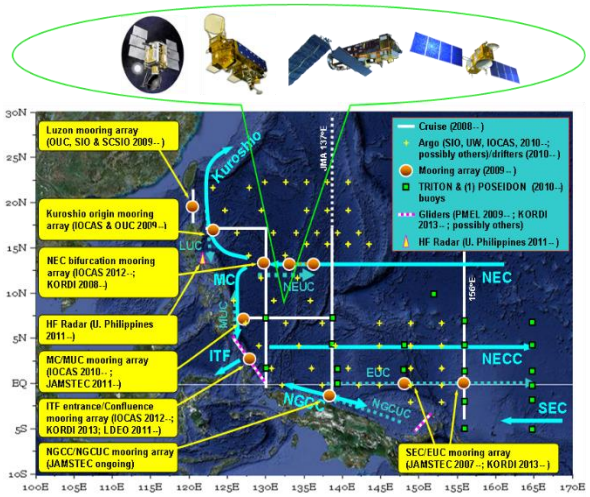

➢ NPOCE Science/Implementation Plan (Hu et al., 2011)

CONTENTS

Preface

The Western Pacific Ocean (WPO) features a complicated ocean circulation system with intensive multiscale interactions with the atmosphere and adjacent ocean basins. Understanding the dynamics of the WPO ocean circulation as well as its role in climate and biogeochemical processes is of crucial importance.

Under the auspices of NPOCE, the 3rd OSS-2018 will provide a forum for oceanographers, meteorologists and climate scientists to exchange recent progresses in their study of the WPO circulation and climate and its generality/difference with other oceans, marine biogeochemistry and ecosystem, their variability, changes and impacts, to explore opportunities for international scientific collaboration, and to promote inter-disciplinary study in the WPO.

SCIENTIFIC ORGANIZING COMMITTEE

HU, Dunxin (Co-Chair) ……..	Institute of Oceanology, Chinese Academy of Sciences, China
CAI, Wenju (Co-Chair) ……..	Centre for Southern Hemisphere Oceans Research, Australia
CHEN, Dake ……	Second Institute of Oceanography, SOA, China
DAI, Minhan ……	Xiamen University, China
DIRHAMSYAH, Dirham ……	Indonesian Institute of Sciences, Indonesia
GORDON, Arnold …….	Columbia University, USA
JIAO, Nianzhi ……..	Xiamen University, China
KESSLER, William S. ……	National Oceanic and Atmospheric Administration, USA
LEE, Jae-Hak ……	Korea Institute of Ocean Science and Technology, Korea
MU, Mu ……..	Fudan University, China
QIU, Bo ……..	University of Hawaii, USA
SAITO, Hiroaki ……	The University of Tokyo, Japan
SPRINTALL, Janet ……..	Scripps Institution of Oceanography, USA
WANG, Chunzai ……..	South China Sea Institute of Oceanology, CAS, China
WANG, Fan ……..	Institute of Oceanology, Chinese Academy of Sciences, China
WANG, Huijun ……	Nanjing University of Information Science & Technology, China
WU, Lixin ……..	Ocean University of China, China
ZHANG, Renhe ……	Fudan University, China

LOCAL ORGANIZING COMMITTEE

WANG, Fan (Co-Chair) …..	Institute of Oceanology, Chinese Academy of Sciences, China
LIN, Xiaopei (Co-Chair) ……	Ocean University of China, China
CHAI, Fei ……..	Second Institute of Oceanography, SOA, China
DAI, Minhan ……..	Xiamen University, China
DU, Yan ……..……	South China Sea Institute of Oceanology, CAS, China
QIAO, Fangli ……	The First Institute of Oceanography, SOA, China
SANTOS, Jose ……	CLIVAR
TAN, Gongke ……..	Qingdao National Laboratory for Marine Science and Technology, China
YANG, Song ……	Sun Yat-sen University, China
YIN, Baoshu ……	Institute of Oceanology, Chinese Academy of Sciences, China
ZHU, Jiang ……	Institute of Atmospheric Physics, CAS, China

AGENDA

2018.05.08 AM	**Chair: Wenju Cai**	
Time	Topic	Speaker
09:00-09:40	Opening Ceremony: Dunxin Hu, Lixin Wu, Jose Santos, Fan Wang	Dunxin Hu, Lixin Wu, Jose Santos, Fan Wang
09:40-10:00	Contribution of oceanic western boundary currents to global overturning circulation and climate	Peter Rhines (Keynote)
10:00-10:20	Global and regional high-resolution ocean and climate modeling: Meso-submesoscale dynamics	Lixin Wu (Keynote)
10:20-10:40	Makassar Strait Throughflow, 2004-2017	Arnold Gordon (Keynote)
10:40-11:00	Photo & Coffee Break	
Session 1 & 6	**Chair: Sabrina Speich**	
11:00-11:15	Transport Estimates from Moored Observations in the Exit Passages of the Solomon Sea	Janet Sprintall (Invited)
11:15-11:30	Interannual Modulations of the 50-day Oscillations in the Celebes Sea	Bo Qiu (Invited)
11:30-11:45	Constraining iron sources and pathways into the Pacific Equatorial Undercurrent	Alexander Sen Gupta (Invited)
11:45-12:00	Characteristics and Forcing Mechanisms of the NEC/NEUC: a numerical modeling study	Jianping Gan (Invited)
12:00	Lunch (buffet) 2nd floor FEAST	
2018.05.08 PM	**Chair: Fan Wang**	
Time	Topic	Speaker
14:00-14:20	Aspect of Ningaloo Niño (Niña) as an intrinsic air-sea-land coupled mode	Toshio Yamagata (Keynote)

14:20-14:40	Seven Years of Direct Observations of the Ombai Throughflow	Susan Wijffels (Keynote)
14:40-15:00	Nonlocal ocean-atmosphere interactions over the Indo-western Pacific warm pool	Shang-Ping Xie (Keynote)
15:00-15:15	Observations of the low latitude western boundary currents in 2017	Jae Hak Lee (Invited)
15:15-15:30	Connecting boundary currents: The South Atlantic and the “eddy-highway”	Sabrina Speich (Invited)
15:30-15:45	Coffee Break	
Session 1 & 6 Chair: Bo Qiu		
15:45-16:00	Thermohaline variations caused by subthermocline eddies east of Philippine	Linlin Zhang
16:00-16:15	Spatial-temporal Features of Intra-seasonal Oceanic Variability in the Philippine Sea from Mooring Observations and Numerical Simulations	Shijian Hu
16:15-16:30	Effect of Mesoscale Eddies on North Pacific Subtropical Mode Water	Yiyong Luo
16:30-16:45	Wind energy input to the surface wave and currents in the Kuroshio extension region	Yuping Guan
16:45-17:00	Origins of the Pacific Meridional Overturning Circulation	Mathias Zeller
17:00-17:15	Roles of sensible and latent heat fluxes on the wintertime atmospheric responses to the Gulf Stream	Shoshiro Minobe (Invited)
17:15-17:30	Energetics of M2 Internal Tides modulated by the Kuroshio Northeast of Taiwan	Zhenhua Xu
17:30-17:45	Effect of westward shoaling thermocline on characteristics and energetics of internal solitary waves by numerical simulation	Haibin Lv
17:45-18:45	Poster Presentation (Room: Ling Hai 3)	
19:00	Ice Breaker (Conference Room)	

2018.05.09 AM	Chair: Xiaopei Lin	
Time	Topic	Speaker
08:30-08:50	A Joint Data Assimilation System Based on Local Ensemble Transfer Kalman Filter	Asrar Ghassem (Keynote)
08:50-09:10	Towards predicting changes in the land monsoon rainfall a decade in advance	Bin Wang (Keynote)
09:10-09:25	Diversity of Surface Easterly Winds Along the Equator in El Niño and La Niña Events During 1997 to 2016	David Halpern (Invited)
09:25-09:40	Equatorial temperature effects of flow through the Solomon Sea	William Kessler (Invited)
09:40-09:55	Variability of the Pacific western boundary currents and the Indonesian Throughflow during the 2015-2016 super El Niño	Dongliang Yuan (Invited)
09:55-10:10	Coffee Break	
Session 2 & 3	**Chair: Janet Sprintall & Dongliang Yuan**	
10:10-10:25	Pacific influences on the meridional temperature transport of the Indian Ocean	Ming Feng (Invited)
10:25-10:40	Development of an Inter-basin Pacific-Indian Ocean Model: The Indonesian ThroughFlow (ITF) and the Circulation in the Banda Sea	Huijie Xue (Invited)
10:40-10:55	The Low-Frequency Processes in the Indo-Pacific Region and Their Impact on Tropical Indian Ocean	Yan Du (Invited)
10:55-11:10	Impact of a background flow on internal tides dissipation and implications for the Indonesian seas	Océane Richet
11:10-11:25	Seasonal Variability of Sea Surface Temperature Front in South China Sea	Yuntao Wang
11:25-11:40	Regional and global ocean heat content changes related to ENSO	Lijing Cheng
11:40-11:55	Seasonality and Predictability of the Indian Ocean Dipole Mode: ENSO Forcing and Internal Variability	Yun Yang
11:55	Lunch (buffet) 2nd floor FEAST	

2018.05.09 PM Session 2 & 3 Chair: William Kessler & Ming Feng		
Time	Topic	Speaker
14:00-14:15	Scale-dependence of observed wind stress response to ocean-mesoscale surface temperatures	Niklas Schneider (Invited)
14:15-14:30	The simulated large-scale oceanic circulation and mesoscale eddies in the western Pacific	Yongqiang Yu
14:30-14:45	Delineation of Thermodynamic and Dynamic Responses to Sea Surface Temperature Forcing Associated with El Niño	Xiaoming Hu
14:45-15:00	An improved ENSO simulation by representing chlorophyll-induced climate feedback in the NCAR Community Earth System Model	Ronghua Zhang
15:00-15:15	The observed impacts of two types of El Niño on the North Equatorial Countercurrent in the Pacific Ocean	Hui Zhou
15:15-15:30	Definition of extreme El Niño and its impact on projected increase in extreme El Niño frequency	Guojian Wang
15:30-15:45	Coffee Break	
Session 4 Chair: Jianping Li		
15:45-16:00	Thermal and salt variability in the South China Sea influenced by the Western Pacific Ocean	Dongxiao Wang (Invited)
16:00-16:15	The ENSO Complexity: Its Underlying Dynamics and Impacts on Western Pacific Climate	Jin-Yi Yu (Invited)
16:15-16:30	Impacts of the Atlantic Multi-Decadal Variability in the Pacific Basin and A New Large Ensemble of Decadal Prediction Simulations	Gokhan Danabasoglu (Invited)
16:30-16:45	Near-inertial waves advected by the Kuroshio from observation and simulation	Jae-Hun Park
16:45-17:00	Atmospheric dynamic and thermodynamic processes in driving the western North Pacific anomalous anticyclone	Bo Wu

17:00-17:15	Heat storage of the West Pacific warm pool (WPWP) linked to global surface warming	Yuanlong Li
17:15-17:30	Increasing persistent haze in Beijing: potential impacts of weakening East Asian winter monsoons associated with northwestern Pacific sea surface temperature trends	Lin Pei
17:30-17:45	Does extreme El Niño have a different effect on the stratosphere in boreal winter than its moderate counterpart?	Xin Zhou
17:45-18:00	A new index for identifying different types of El Niño Modoki Events	Xin Wang
18:00-19:00	Poster Presentation (Room: Ling Hai 3)	
19:00	Dinner (buffet) 2nd floor FEAST	

2018.05.10 AM	**Session 4**	**Chair: Jin-Yi Yu**
Time	Topic	Speaker
08:30-08:45	Interaction among three oceans: A review and perspective	Chunzai Wang (Invited)
08:45-09:00	Some Impacts of Indo-Pacific Warm Pool on Tropical Cyclone, Hadley circulation and Stratosphere Climate	Jianping Li (Invited)
09:00-09:15	Extreme cooling events during the past 620 years in the Western Pacific Region and its relationship with the Tibet Plateau	Yu Liu (Invited)
09:15-09:30	Laminated diatom mat deposits from the tropical West Pacific linked to global carbon and silicon cycles during the Last Glacial Maximum	Tiegang Li (Invited)
09:30-09:45	The mid-Holocene East Asian monsoon, Walker circulation, and ENSO: Insights from PMIP simulations	Dabang Jiang
09:45-10:00	Atmospheric Secondary Circulation response to ocean eddy in the winter Kuroshio Extension region	Qinyu Liu
10:00-10:15	Coupling wheels of East Asian summer monsoon and its diversity on interannual time scale	Congwen Zhu

10:15-10:30	The Interannual Dominant Co-variation Mode of Boreal Summer Monsoon Rainfall during 1979–2014	Yuqian Hao
10:30-10:45	Coffee Break	
Session 5 Chair: Fei Chai		
10:45-11:05	Anthropogenic Pb in the Western North Pacific Kuroshio Region	Edward Boyle (Keynote)
11:05-11:25	The Ocean's Biological Carbon Pump – Studies in the North Pacific as part of EXport Processes in the Ocean from Remote Sensing (EXPORTS)	Ken Buesseler (Keynote)
11:25-11:40	Deep oceans may acidify faster than anticipated due to global warming	Chen-Tung Arthur Chen (Invited)
11:40-11:55	Upper Ocean Biogeochemistry in the Ocean Desert	Minhan Dai (Invited)
11:55-12:10	Deep ventilation of the Southern Ocean and deglacial CO2 rise	Yongsheng Xu
12:10	Lunch (buffet) 2nd floor FEAST	
2018.05.10 PM Session 5 Chair: Minhan Dai		
Time	Topic	Speaker
14:00-14:15	Remote impact on decadal variability of nutrients and plankton dynamics in the Kuroshio Extension	Fei Chai (Invited)
14:15-14:30	Eco-physiological Effects of Ocean Acidification on Primary Producers	Kunshan Gao
14:30-14:45	Subduction of the North Pacific Subtropical Mode Water and its physical and biogeochemical impacts revealed by 50-year long observations along 137ºE	Eitarou Oka
14:45-15:00	Nitrous Oxide in the Southwest Pacific Ocean, an isotopic approach	Muhammed Nayeem Mullungal
15:00-15:15	Variability of particle export in the northwestern Pacific	Peng Xiu
15:15-15:30	Coffee Break	
15:30-16:10	Discussion & Best Poster Award Chair: Wenju Cai	

POSTER SESSION PLAN

Session 1: Pacific Western Boundary Currents (WBCs) dynamics and variability & **Session 6**: Characteristics, dynamics and impact of WBCs in other oceans

Co-chairs: **Bo Qiu, Sabrina Speich**

P1-1 Modelling the Seasonal Cycle of the North Equatorial Current Bifurcation in a Regional Model – Role of Eastern Boundary Conditions
Bingrong Sun, Zhaohui Chen, Lixin Wu (Physical Oceanography Laboratory/CIMST, Ocean University of China and Qingdao National Laboratory for Marine Science and Technology, Qingdao, China)

P1-2 Subthermocline eddy-induced mixing of the interhemispheric intermediate waters observed east of the Philippines
Feng Nan, Fei Yu (Institute of Oceanology, Chinese Academy of Sciences)

P1-3 The vertical structure and variability of the western boundary currents east of the Philippines: case study from in-situ observations from December 2010 to August 2014
Fujun Wang (Institute of Oceanology, Chinese Academy of Sciences)

P1-4 Seasonality of the Mindanao Current/Undercurrent System
[1]Qiuping Ren, [1]Yuanlong Li, [1]Fan Wang, [1]Chuanyu Liu, [2]Fangguo Zhai ([1]Key Laboratory of Ocean Circulation and Waves, Institute of Oceanology, Chinese Academy of Sciences, Qingdao, China, [2]College of Oceanic and Atmospheric Sciences, Ocean University of China, Qingdao, China)

P1-5 Statistical analysis of Mesoscale eddies in North Equatorial Countercurrent area
Mingkun Lv (IOCAS)

P1-6 Atlantic Multi-decadal Oscillation Controls the North Pacific Subtropical Mode Water Variability
[1]Baolan Wu, [1]Xiaopei Lin, [2]Lisan Yu ([1]Ocean University of China, [2]Department of Physical Oceanography Woods Hole Oceanographic Institution Woods Hole)

P1-7 Projected Changes of the Low-latitude North-western Pacific Wind-driven Circulation under Global Warming
[1]Jing Duan, [2]Zhaohui Chen, [2]Lixin Wu ([1]Institute of oceanology Chinese adcademy of sciences, [2]Ocean university of China)

P1-8 The observed 80-100 days variations of the subthermocline current east of Luzon Island
Qian Ma (Ocean University of China)

P1-9 Intraseasonal variability in deep current and temperature induced by Topographic Rossby Waves
[1]Qiang Ma, [1]Jianing Wang, [2]Stephen Riser, [1]Fan Wang ([1]IOCAS, [2]University of Washington)

P1-10 Horizontal and vertical thermohaline structure of mesoscale eddies in the WBCs regions of the Northern Hemisphere
Rou Hu (Ocean University of China)

P1-11 Topographic Beta Spiral and Onshore Intrusion of the Kuroshio Current
Dezhou Yang (Institute of Oceanology, Chinese Academy of Sciences)

P1-12 Response of surface winds to sea surface temperature perturbations in the Kuroshio-Oyashio Extension region

[1]Jingjing He, [1]Xiaopei Lin, [2]Lisan Yu ([1]Physical Oceanography Laboratory/CIMST, Ocean University of China and Qingdao National Laboratory for Marine Science and Technology, [2]Department of Physical Oceanography, Woods Hole Oceanographic Institution)

P1-13 Response of the Kuroshio Extension Path State to Near-Term Global Warming in CMIP5 Experiments with MIROC4h

[1]Rui Li, [2]Zhao Jing, [2]Zhaohui Chen, [2]Lixin Wu ([1]Institute of Oceanology, Chinese Academy of Sciences, [2]Ocean University of China)

P1-14 Decadal variation of the Kuroshio intrusion into the South China Sea during 1992-2016

Yicheng Chen, Fangguo Zhai (Ocean University of China)

P1-15 Baroclinic Instability of Non-zonal Flows and Bottom Slope Effects on Propagation of the Most Unstable Wave

Hengling Leng, Xuezhi Bai (Hohai University)

P1-16 Interannual and inter-decadal variability of the North Equatorial Countercurrent in the Western Pacific

[1]Xiao Chen, [2]Bo Qiu ([1]Hohai University, [2]University of Hawaii)

P1-17 Decadal variability of water transport in North Pacific using P-vector method

Shouchang Wu, Hailun He (Second Institute of Oceanography, SOA)

P1-18 Can errors/bias arising from the ignored acceleration be bounded or even controlled in the Lagrangian Argo trajectory deriving method?

[1]Tianyu Wang, [2]Sarah Gille, [1]Yan Du ([1]South China Sea Institute of Oceanology, CAS, [2] Scripps Institution of Oceanography)

P1-19 Tropical Meridional Overturning Circulation Observed by Subsurface Moorings in the Western Pacific

[1,2]Lina Song, [1,3]Yuanlong Li, [1,3]Jianing Wang, [1,3]Fan Wang*, [1,3]Shijian Hu, [1,3]Chuanyu Liu, [1]Xinyuan Diao, [1,2]Cong Guan([1]Key Laboratory of Ocean Circulation and Waves, Institute of Oceanology, Chinese Academy of Sciences, Qingdao, China, [2]Institute of Oceanographic Instrumentation, Shandong Academy of Sciences, Qingdao, China, [3]Function Laboratory for Ocean Dynamics and Climate, Qingdao National Laboratory for Marine Science and Technology, Qingdao, China)

Session 2: Interaction of WPO circulation with adjacent waters (e.g., the East and South China Seas, ITF, Indian Ocean, extra-tropical Pacific Ocean)

Co-chairs: **Janet Sprintall, Dongliang Yuan**

P2-1 Multi-decadal timeseries of the Indonesian throughflow

[1]Jun Wei, [1]Mingting Li, [2]Arnold Gordon ([1]Peking University, [2]Columnbia University)

P2-2 An Argo-derived background diffusivity parameterization for improved ocean simulations in the tropical Pacific

Yuchao Zhu, ronghua zhang (Institute of Oceanology Chinese Academy of Sciences)

P2-3 Low-Frequency Variability of the South Pacific Subtropical Gyre as Seen from Satellite Altimetry and Argo

[1]Linlin Zhang, [2]Tangdong Qu ([1]Institute of Oceanology, Chinese Academy of Sciences, [2]University of California, Los Angeles)

P2-4 Trends of Sea Surface Temperature and Sea Surface Temperature fronts in the South China Sea during 2003-2017
Yi Yu, YunTao Wang, Haoran Zhang (Second Institute of Oceanography)

P2-5 Eddy generation mechanism in the central South China Sea
Jiajia Chen, Xuhua Cheng (College of Oceanography, HoHai University)

P2-6 Long-range Radiation and Dissipation of M2 Internal Tides in the Northwestern Pacific and South China Sea
Yang Wang, Zhenhua Xu, Baoshu Yin, Hang Chang (Institution of Oceanology, Chinese Academy of Scienecs)

P2-7 Features of the Equatorial Intermediate Current associated with basin resonance in the Indian Ocean
[1]Dongxiao Wang, [1]Ke Huang, [2]Weiqing Han, [1]Weiqiang Wang, [3]Qiang Xie, [1]Ju Chen, [1]Gengxin Chen ([1]SCSIO, CAS, [2]University of Colorado, UAS, [3]Institute of Deep–Sea Science and Engineering, CAS)

P2-8 Eddy-current interaction in the Leeuwin Current off the lower-west coast of Australia
Qinyan Liu (South China Sea Institute of Oceanology)

P2-9 Decadal and long-term changes in the upper layer salinity in the South China Sea over the past five decades
Lili Zeng (South China Sea Institute of Oceanology, Chinese Academy of Sciences)

P2-10 Impact of the South China Sea Summer Monsoon on the Indian Ocean Dipole
[1]Yazhou Zhang, [1]Jianping Li, [2]Jiaqing Xue, [1]Juan Feng, [1]Qiuyun Wang, [1]Yidan Xu, and [1]Yuehong Wang ([1]Beijing Normal University, [2]State Key Laboratory of Numerical Modeling for Atmospheric Sciences and Geophysical Fluid Dynamics, Institute of Atmospheric Physics, Chinese Academy of Sciences)

P2-11 Sensitivity experiments of modeling SCSTF-ITF interactions by closing straits and passages in a 0.1° × 0.1° regional ocean model
Mingting Li, Jun Wei (Peking University)

P2-12 Wind-driven cross equator transport
[1]Junwei Chai, [1]Xiaopei Lin, [2]Jiayan Yang ([1]Ocean University of China, [2]Woods Hole Oceanographic Institution)

P2-13 Vertical propagation of mid-depth zonal currents associated with surface wind forcing in the equatorial Indian Ocean
[1]Huang Ke, [2]Michael McPhaden, [1]Weiqiang Wang, [3]Qiang Xie, [1]Dongxiao Wang ([1]South China Sea Institute of Oceanology, CAS, [2]NOAA, USA, [3]Institute of Deep−Sea Science and Engineering, CAS)

Session 3: Roles of WPO circulation variability in warm pool and ENSO variability

Co-chairs: **William S. Kessler, Ming Feng**

P3-1 Strengthened Indonesian Throughflow drives decadal warming in the Southern Indian Ocean
[1]Ying Zhang, [2]Ming Feng, [1]Yan Du, [3]Helen Philips, [3]Nathan Bindoff, [4]Michael McPhaden ([1]South China Sea Institute of Oceanology, Chinese Academy of Sciences, [2]CSIRO Oceans and Atmosphere, [3]Institute for Marine and Antarctic Studies, University of Tasmania, [4]NOAA/Pacific Marine Environmental Laboratory)

P3-2 Research on the effects of El Niño events in the typhoon
Weihui Sui ((Public Meteorological Service Center of CMA)

P3-3 Contrasting the intraseasonal variations in the Upper Equatorial Pacific Currents during the 1997-98 and 2015-16 El Niño
Yilong Lv, Yuanlong Li, Xiaohui Tang, Fan Wang (Institute of Oceanology, Chinese Academy of Sciences)

P3-4 Oceanic processes of upper ocean heat content associated with two types of ENSO
Junqiao Feng (IOCAS)

P3-5 The response of the equatorial Pacific Ocean to the winds during 2014-2015
Jing Wang (IOCAS)

P3-6 Computation of the surface wind stress response to the mesoscale SST perturbations in the Peru-Chile sea area Based on the Tikhonov regularization method
[1]Chaoran Cui, [1]Ronghua Zhang, [1]Hongna Wang, [2]Yanzhou Wei ([1]Institute of oceanology ,Chinese academy of sciences, [2]Second institute of Oceanography)

P3-7 CMIP5 model biases in the climatological mean state of the western Pacific warm pool
Yuxing Yang, Wang Faming, Zheng Jian (Institute of Oceanology, Chinese Academy of Science)

P3-8 A hybrid coupled model (HCM) of atmosphere and ocean physics and biology (AOPB) in the tropical Pacific
[1]Feng Tian, [2]Rong-Hua Zhang, [3]Xiujun Wang ([1]Institute of Oceanology, Chinese Academy of Sciences, [2]Institute of Oceanology, Chinese Academy of Sciences;Qingdao National Laboratory for Marine Science and Technology, [3]College of Global Change and Earth System Science, Beijing Normal University;Joint Center for Global Change Studies)

P3-9 The roles of atmospheric wind and entrained water temperature (Te) in the second-year cooling of the 2010–12 La Niña event
Chuan Gao, Rong-Hua Zhang (Institute of Oceanology, Chinese Academy of Sciences)

P3-10 Spatio-temporal variation of Indian summer monsoon rainfall and associated δ18O variability: Its teleconnections with ENSO
Pullabhatla Kiran Kumar, Arvind Singh, Rengaswamy Ramesh (Physical research Laboratory)

P3-11 Oceanic feedbacks in affecting ENSO asymmetry
[1]Cong Guan, [2]Michael McPhaden, [1]Shijian Hu, [1]Fan Wang ([1]Institute of Oceanology, CAS, [2]NOAA/Pacific Marine Environmental Laboratory)

P3-12 Distinct ENSO regimes enhanced by recent global warming
[1]Ning Jiang, [1]Congwen Zhu, [2]Weihong Qian ([1]State Key Laboratory of Severe Weather (LASW) and Institute of Climate System, Chinese Academy of Meteorological Sciences, [2]School of Physics, Peking University, Beijing)

P3-13 The Buoyant Equipment for Skin Temperature (BEST), A New Instrument for Measurement of Air-Sea Interactive Temperatures
Chuqun Chen, Haibin Ye, Shilin Tang (LTO, South China Sea Institute of Oceanology, Chinese Academy of Sciences)

P3-14 Sea surface temperature in the subtropical Pacific boosted the 2015 El Niño and hindered the 2016 La Niña

[1]Jingzhi Su, [1]Renhe Zhang, [1]Xinyao Rong, [2]Qingye Min, [1]Congwen Zhu ([1]Chinese Academy of Meteorological Sciences, [2]Fudan University)

P3-15 Impact of atmospheric model resolution on simulation of ENSO feedback processes: a coupled model study
Lijuan Hua (Chinese Academy of Meteorological Sciences)

Session 4: Influences of WPO on regional (e.g., monsoon, typhoon, extreme climatic events) and global climate systems and their predictability

Co-chairs: **Jianping Li, Jin-Yi Yu**

P4-1 Different impacts of two types of El Niño on the yield of early rice of Southern China
Runnan Sun, Jianping Li (Beijing Normal University)

P4-2 Causes of enhanced SST variability over the equatorial Atlantic and its relationship to Atlantic zonal mode in CMIP5
Yun Yang (Beijing Normal University)

P4-3 Mesoscale SST Perturbation-induced Impacts on Precipitation Climatology in the Kuroshio-Oyashio Extension Region, as Revealed by the WRF Simulations
Jiaxiang Gao, Rong-Hua Zhang, Hongna Wang (Institute of Oceanology, Chinese Academy of Sciences)

P4-4 Simulating the IPOD, East Asian summer monsoon, and their relationships in CMIP5
[1]Yu Miao, [1]Li Jianping, [2]Zheng Fei, [3]Wang Xiaofan, [4]Zheng Jiayu ([1]College of Global Change and Earth System Sciences, [2]Institute of Atmospheric Physics, [3] Centre for Communication and Outreach, [4]State Key Laboratory of Tropical Oceanography)

P4-5 Decadal variability of temperature in the Pacific ocean
Hongna Wang (IOCAS)

P4-6 Contrasting the impacts of the 1997–1998 and 2015–2016 extreme El Niño events on the East Asian winter atmospheric circulation
[1]Jian Zheng, [2]Qinyu Liu, [3]Zesheng Chen ([1]Institute of Oceanology, Chinese Academy of Sciences, [2]Ocean University os China, [3]South China Sea Institute of Oceanology, Chinese Academy of Sciences)

P4-7 Increasing threat of landfalling typhoons in the western North Pacific between 1974 and 2013
Shoude Guan (Key Laboratory of Ocean Circulation and Waves, Institute of Oceanology, Chinese Academy of Sciences)

P4-8 Wintertime global warming hiatus tied to negative phase of cold ocean-warm land pattern
[1]Jun-Chao Yang, [1]Xiaopei Lin, [2,1]Shang-Ping Xie, [1,2]Yu Zhang, [3]Yu Kosaka ([1]Physical Oceanography Laboratory/CIMST, Ocean University of China and Qingdao National Laboratory for Marine Science and Technology, [2]Scripps Institution of Oceanography, University of California, [3]Research Center for Advanced Science and Technology, The University of Tokyo)

P4-9 Simulating the Pacific Decadal Mode and its impact on ENSO in ACCESS model
[1]Arnold Sullivan, [2]Jing-Jia Luo, [3]Jin-Yi Yu, [4]Bodman Roger, [1]Wenju Cai, [1]Arnold Sullivan, [2]Jing-Jia Luo, [3]Jin-Yi Yu, [4]Bodman Roger, [1]Wenju Cai ([1]CSIRO oceans and atmosphere, [2]Bureau of Meteorology, [3]University of California Irvine, [4]4)School of Earth Sciences, University of Melbourne)

P4-10 Why was the western Pacific subtropical anticyclone weaker in late summer after the 2015/16 super El Niño?
Boqi Liu, Congwen Zhu, Jingzhi Su, Lijuan Hua, Yihong Duan (Chinese Academy of Meteorological Sciences)

P4-11 Biases Correction for the Simulation and Projection of Climate Change over the Kuroshio and its Extension Region in CMIP5 Models
Yan Sun (1Key Laboratory of Ocean Circulation and Waves, Institute of Oceanology, Chinese Academy of Sciences)

P4-12 Evaluating of cooling tower scheme in high resolution regional model
Miao Yu (1.Institute of Urban Meteorology, China Meteorological Administration, Beijing, China)

P4-13 A Study of Wind Wave Prediction of Binary Typhoons over the Northwestern Pacific Ocean with a Coupled Atmosphere-Ocean-Wave Model
[1]Weiwei Ding, [2]linlin qi, [2]huijie wang, [1]tianju wang ([1]National University of Defense Technology, [2]Academy of Air Force)

P4-14 Interannual variability and dynamics of intraseasonal wind rectification in the equatorial Pacific Ocean
Xia Zhao (IOCAS)

P4-15 Relationship between the western North Pacific Ocean and the East Asian summer monsoon and its non-stationarity
[1]Pei-long Yu, [1]Li-feng Zhang, [2]Quan-jia Zhong, [1]Han-xiao Yin, [1]Ming-yang Zhang ([1]College of Meteorology and Oceanography, National University of Defense Technology, [2]State Key Laboratory of Numerical Modeling for Atmospheric Sciences and Geophysical Fluid Dynamics (LASG), Institute of Atmospheric Physic, Chinese Academy of Sciences; College of Earth Science, University of Chinese Academy of Sciences)

P4-16 Atmospheric Energetic over the Tropical Indian Ocean during the IOD Event
Yuehong Wang, Jianping Li (1.College of Global Change and Earth System Sciences (GCESS), Beijing Normal University)

P4-17 Decadal variations of salinity in western tropical Pacific
Guanghui Zhou, Rong-Hua Zhang (Key Laboratory of Ocean Circulation and Waves, Institute of Oceanology, Chinese Academy of Sciences, Qingdao 266071, China)

P4-18 Evolution of the Madden–Julian Oscillation in Two Types of El Niño
[1]Xiong Chen, [2]Jian Ling, [1]Chongyin Li ([1]College of Meteorology and Oceanography, National University of Defense Technology, [2]LASG, Institute of Atmospheric Physics, CAS)

P4-19 Impact Of South Indian Ocean Dipole On Tropical Cyclone Genesis Over The South China Sea
Teng Wang, Lu Xi, Song Yang (Sun Yat-sen University)

Session 5: WPO's role in and impacts on carbon cycle, biogeochemical process, acidification, ecosystem, paleo-oceanography, and so on

Co-chairs: **Minhan Dai, Fei Chai**

P5-1 Effects of wave-current interactions on suspended-sediment dynamics during strong wave events in Jiaozhou Bay, Qingdao, China
Guandong Gao (Institute of Oceanology, Chinese Academy of Science)

P5-2 The Value of the Greenhouse Gas Monitoring System for Climate Change in the China Sea
Dan Wang, Honggang Lv, Yifei Jiang, Tiejun Ling, Dongdong Xia (Key Laboratory of Research on Marine Hazards Forecasting, National Marine Environment Forecasting Center)

P5-3 Ocean hydrography of the Yap seamount and its adjacent sea area in the tropical Western Pacific in autumn 2014
Xingyu Shi, Zhenyan Wang(Institute of Oceanography, Chinese Academy of Sciences)

P5-4 Spatial and temporal variability of surface chlorophyll and particulate organic carbon in the North Pacific Ocean during 2003-2016: Physical and biogeochemical controls
Jun Yu, Xiujun Wang (Beijing Normal University)

P5-5 Comparative study of the adaptive characteristics of zooplankton in deep (500-3500 m) and shallow (0-200 m) layers in the Western Tropical Pacific Ocean
Lei Chen, Chaolun Li, Zhencheng Tao, Fangping Cheng, Xiaocheng Wang (Institute of Oceanology, Chinese Academy of Sciences)

P5-6 Influence of the Mindanao Undercurrent on terrigenous material transport of the tropical western Pacific
Zhenyan Wang, Wei Gao (Institute of Oceanology, Chinese Academy of Sciences)

P5-7 Lead behavior in the Western Tropical Pacific
Shuo Jiang, Yan Chang, Jing Zhang (State Key Laboratory of Estuarine and Coastal Research, East China Normal University)

P5-8 Impact of Mesoscale Eddies on Bioavailability and Composition of Dissolved Organic Matter in West Pacific Ocean
Miao Zhang, Ying Wu, Fuqiang Wang (East China Normal University)

P5-9 Carbon Chemistry in the Mainstream of Kuroshio Current in Eastern Taiwan and Its Transport of Carbon into the East China Sea Shelf
Baoxiao Qu, Jinming Song, Huamao Yuan, Xuegang Li, Ning Li (Institute of Ocenology, Chinese Academy of Sciences)

P5-10 The temporal and spatial distribution and dynamic of dissolved carbon and the particulate organic carbon in the East China Sea
Lei He, Jianle Li, Kedong Yin (Sun Yat-Sen University)

SPONSORS

1. National Science Foundation of China
2. Chinese Academy of Sciences
3. Qingdao National Laboratory for Marine Science and Technology
4. Institute of Oceanology, Chinese Academy of Sciences
5. Ocean University of China
6. Xiamen University
7. Second Institute of Oceanography, SOA, China
8. South China Sea Institute of Oceanology, Chinese Academy of Sciences
9. First Institute of Oceanography, SOA, China

SECRETARIAT

JIA, Fan (general), Tel: +86 532 8289 8839, +86 13589276045, Email: jiafan@qdio.ac.cn

HU, Shijian, Tel: +86 532 8289 6260, +86 18105321381, Email: sjhu@qdio.ac.cn

ZHANG, Linlin, Tel: +86 532 8289 6260, +86 18562712171, Email: zhanglinlin@qdio.ac.cn

WANG, Jianing, Tel: +86 532 8289 8220, +86 18561681378, Email: wjn@qdio.ac.cn

USEFUL INFORMATION

Conference Venue

Room: Ling Hai, 3rd floor, Sheraton Huangdao Hotel No.1 Taihangshan Road, Huangdao District, Qingdao.

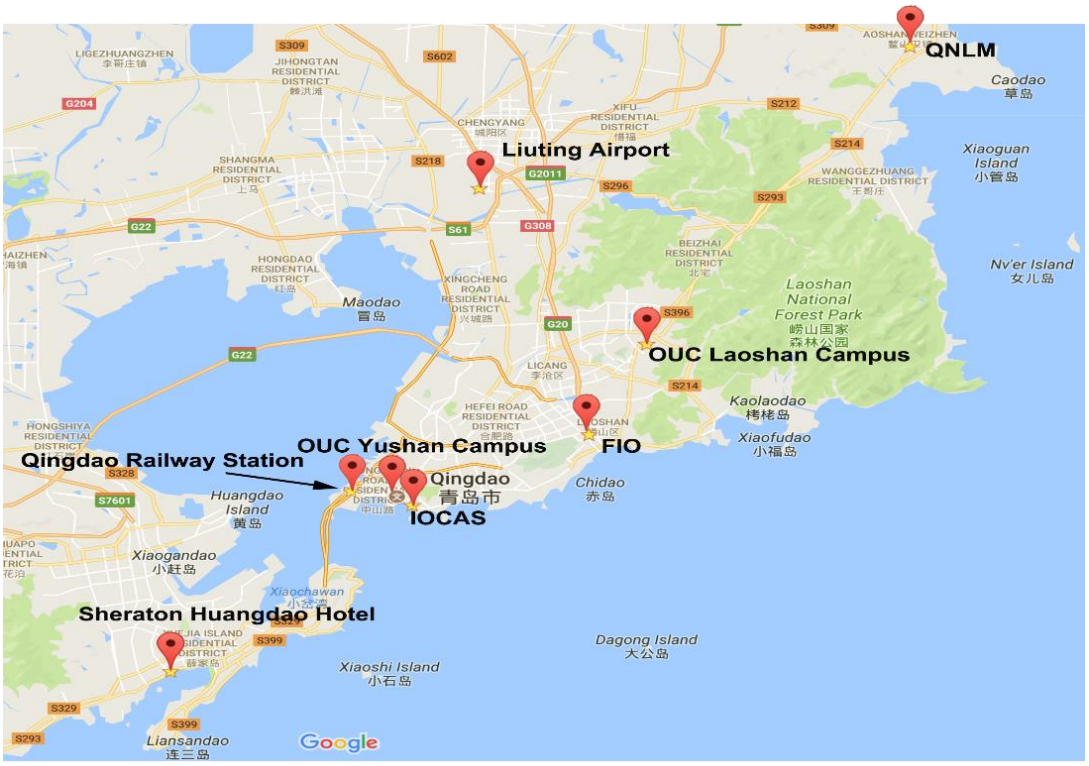

To/from airport

Taxis: A taxi ride from the airport to the Conference venue costs about 150 RMB. The taxi stand at the airport is in the basement and is clearly indicated – just follow the signs.

Shuttle Buses: There are five shuttle bus lines (http://www.travelchinaguide.com/cityguides/shandong/qingdao/getting-around.htm), transferring passengers between the airport and downtown Qingdao. The bus timetable is as follows:

From Sheraton Huangdao Hotel (please wait at the lobby door) to Qingdao Liuting Airport:

8:00, 10:00, 12:00, 14:00, 16:00, 18:00

From Qingdao Liuting Airport (please follow the signs or ask our volunteers who are waiting at the airport) to Sheraton Huangdao Hotel:

8:00, 10:00, 12:00, 14:00, 16:00, 18:00

Complimentary shuttle bus provided by conference

To facilitate participants from Qingdao institutions to join this conference, complimentary shuttle bus service will be provided, passing through Ocean University of China (Laoshan campus), SOA, IOCAS during conference days. The bus schedule is as follows:

	8th May	9th May	10th May
Depart Laoshan campus of OUC	7:00		
Depart Fushan campus of OUC	7:30		
Depart IOCAS	8:00	7:30	7:30
Depart Sheraton	20:30	20:30	16:30

Registration

May 7, Monday, 14:00 –19:00

May 8, Tuesday, 08:00 – 12:00

Venue: reception desk in the entrance hall of Sheraton Huangdao Hotel.

Participants are to collect the badge, program book and meal vouchers.

Badge

All participants are required to wear your badges to have access to conference room and ice breaker reception, and to board the complimentary shuttle bus.

Poster

The poster should be in A0 size (841 mm x 1,189 mm or 33.1” x 46.8”). Note that we do not provide poster printing service. Please look for the board marked with your poster ID (the letter and number before your title in the POSTER SESSION PLAN, such as P1-1) in the Poster Hall and display your poster. Please see the dimension design and layout of posters.

All posters should be put up before 14:00 of May 8. The poster sessions will be taking place on May 8 (17:50-18:50) and May 9 (18:00-19:00), and please make sure to present your poster on both days. All posters must be removed by 18:00 on May 10 or they will be recycled.

Exhibition

The exhibition area is located in Room Ling Hai 3 (the same room with posters). Exhibitors are expected to build up their display before 14:00 of May 8 and pull down their display by 18:00 on May 10.

Each booth contains an exhibition table (1.8m*0.6m) and a maximum area of 2m*2.5m for display. The conference provides a free booth for every sponsor. Please see the dimension

design and layout of booths.

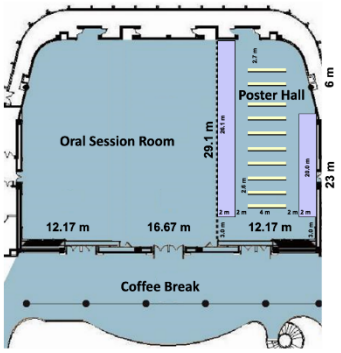

Poster (yellow):
Size: 120 cm high ×100 cm wide
Amount: 80 posters
(100 cm wide per poster)

Booth (blue):
Size: 250 cm length × 200 cm
wide (desk 180 cm × 60 cm)
Amount: 18 booths

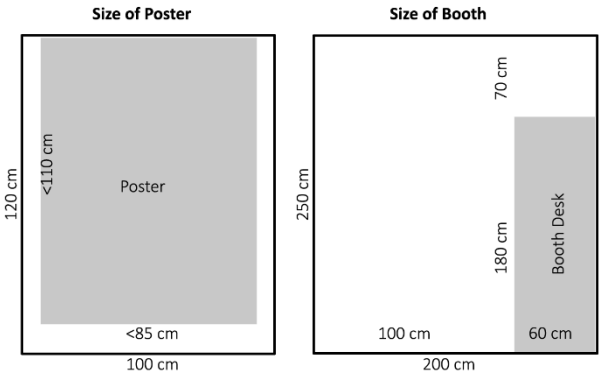

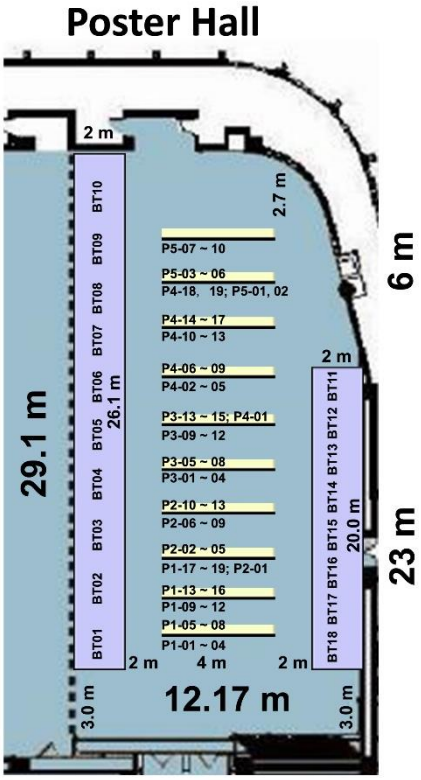

Outstanding Poster Awards

Early career scientists and students attending the 3rd OSS and presenting posters are eligible to be considered for outstanding poster awards. Two posters of each session will be identified by the corresponding session conveners as nominees during Poster Presentation session on May 8. A distinguished committee of senior and early career scientists will review and identify one First Prize winner (5000 RMB including tax), four Second Prize winners (1000 RMB/each including tax) from the nominees during Poster Presentation session on May 9.

Weather

May is in the spring and it is a mild month, but temperature differences during the day and night are significant with average daytime/nighttime temperatures (~20°C/10°C).

ABSTRACT-ORAL-MAY 8

Contribution of oceanic western boundary currents to global overturning circulation and climate

[1]Peter B.Rhines, [2]Xu Xiaobiao, [2]Eric Chassignet ([1]University of Washington, Seattle, Washington, USA, [2]Florida State University, Tallahassee, Florida, USA)

Warm western boundary currents carry heat, fresh-water anomaly and chemical tracers to high latitude, while deep, cold western boundary currents dominate the return flow from polar regions. Thus the boundary currents are dominant parts of the global meridional overturning circulation (MOC). They also carry with them the physical, dynamical tracer, the potential vorticity. Connections between these fast flowing streams and the sinking and upwelling of waters at high latitude, which drive the MOC, are not entirely known. High-resolution theory and numerical models shows how the boundary currents interact with lateral, nearly horizontal circulation gyres which steal away some of their poleward transport. The basic theory of the general circulation needs to account for these gyre/boundary current interactions in new ways.

A key property of the circulation is that water masses transform their physical and chemical properties through stirring and mixing by eddies, mesoscale and smaller. In this talk we explore the way boundary currents feed regions where intense water-mass transformation (WMT). Most studies of the MOC and its effects on climate focus on the zonally integrated velocity field as in the two-dimensional MOC streamfunction.

Yet it is important to know the full 3-dimensional fields of velocity and physical/chemical properties, to find the locations of intense WMT. While the 2-dimsional MOC stream functions from many different numerical models look similar, their 3-dimensional WMT patterns differ greatly among models. Localizing the transformations at high resolution is essential to understanding general circulation and climate dynamics, and in connecting with observations.

Here we analyze model-based time-mean velocity across potential-density surfaces (the diapycnal velocity, WD) in the northern Atlantic Ocean (the AMOC). More net WMT occurs in 3 dimensions than is evident in zonally integrated MOC (more by typically 60% in western subpolar gyre, and 40% in subtropical gyre): ‘donut’-shaped overturning cells surround dominant convective mode-water sites and ‘ribbons’ of overturning align with boundary currents. Much downward WD (‘cooling’ or salinity increase) is directly related to cold-season convection, hence related to surface-forced overturning calculated from air/sea buoyancy flux. Upward WD (‘warming or freshening’) is associated with warm-month restratification of mode waters, also in steadier sub-surface mixing across fronts in boundary currents, dense overflows, and coastal upwelling. With 1/120–latitude resolution the Hybrid Community Ocean Model (HYCOM) is forced by climatological-mean atmospheric observations, with annual cycle. The results will be model-dependent, yet point the way toward improved discovery of WMT and mixing-prone regions.

Global and regional high-resolution ocean and climate modeling: Meso-submesoscale dynamics

Lixin Wu (Physical Oceanography Laboratory/CIMST, Ocean University of China and Qingdao National Laboratory for Marine Science and Technology, Qingdao, China)

TBD

Makassar Strait Throughflow, 2004-2017

Arnold L. Gordon (Lamont-Doherty Earth Observatory of Columbia University)*

The Makassar Strait throughflow of ~12 Sv, representing ~80% of the total ITF, displays fluctuations over a broad range of time scales, from intraseasonal (Madden Julian Oscillations, Rossby and Kelvin Waves) to seasonal and interannual (ENSO) scales. We now have 13.3 years of Makassar throughflow: November 1996 - early July 1998; January 2004 - August 2011; August 2013 - August 2017.

Southward transport displays a strong seasonal signal: strongest in boreal summer, as well as interannual variability, which scales roughly to ENSO: weak southward flow with a deeper V-max during El Nino; stronger southward flow with shallower V-max during La Nina. The southward flow relaxed in 2014 and more so in 2015/16, similar though not as extreme as during the strong El Niño event of 1997. In the summer 2017 there is a return to the non-El Nino state. Since 2016 the deep layer, 300-760 m (Makassar Strait sill depth is ~680 m) southward transport increases, almost doubles to ~7.5 Sv. From mid 2016 into early 2017 the transport above 300 m and below 300 m are about equal, where they usually have a ratio of 2:1. In early 2017 the total Makassar transport increases to 'historical' highs, of over 20 Sv.

Near zero or northward flow occurs in the upper ~100 m during boreal winter, albeit with interannual variability. A particularly strong winter reversal is observed in the winters of 2014/15 and 2016/17, the latter is the strongest winter reversal revealed in the Makassar time series. In June 2016 there is a marked relaxation of the southward flow within the thermocline, dividing the summer maximum into two separate features. In July 2016 the surface layer flow, above 100m, is northward, a condition that in prior years is seen only in the boreal winter.

The Makassar southward heat flux anomaly (HFa; relative to a mean HF referenced to 0°C) increases rapidly from 2006 to 2008 with a peak of 0.13 PW in 2008 and 2009. Afterwards Makassar HFa slowly decreases to a minimum of -0.22 PW during 2015, after which southward heat flux beings to climb again. Variability in volume transport explains 56% of HFa variance, with the rest due to the temperature profile changes (deeper thermocline during La Niña). The heat content anomaly in the eastern tropical Indian Ocean, determined from Argo profiles, follows a similar pattern to the Makassar HFa (R=0.76) with a lag of 25 months.

The Pacific and Indian Ocean processes that govern the Makassar transport and its profile vary in temporal scale, with the Indian Ocean impact mainly, but not solely, confined to the higher frequencies (MJO and Kelvin Waves) while the Pacific affects seasonal and interannual fluctuations (and impinging Rossby waves). The Pacific inflow is linked to the latitude of the NEC Bifurcation and to the South China Sea throughflow. Regional topics to be explored in the western tropical Pacific include complexity of the Mindanao Current and its undercurrent, their connection to the NEC and NECC systems, as well as South Pacific water injected into the North Pacific.

The 13.3 years Makassar throughflow time series is a window to the place of the ITF and Maritime Continent to the larger scale ocean and climate systems, and presents a challenge to quantitative understanding.

**I acknowledge the contribution from colleagues: Asmi Napitu, Kandaga Pujiana, Bruce Huber and Laura Gruenburg.*

Transport Estimates from Moored Observations in the Exit Passages of the Solomon Sea

Janet Sprintall (Scripps Institution of Oceanography)

The Solomon Sea is a major pathway for the low latitude western boundary current of the south-western tropical Pacific to redistribute South Pacific thermocline waters from the subtropics to the equator. However, several key aspects of the oceanic circulation in the Solomon Sea remain poorly observed and are not properly depicted by models. Questions remain as to how much water is carried through the Solomon Sea to the equator, the pathways of the circulation and in what density range. To address this issue, under the CLIVAR supported Southwest Pacific Ocean Circulation and Climate Experiment (SPICE), an international co-operative experiment was designed to obtain a quantitative view of the properties and currents in the Solomon Sea. As part of the fieldwork, a transport array of moorings were deployed in the major outflow passages of the Solomon Sea - Vitiaz Strait, St. Georges Channel and Solomon Strait - from July 2012

until March 2014 to resolve the velocity and density fields in each strait. This presentation will review some of the recent transport estimates from this fieldwork in the Solomon Sea and discuss the relationship of the partitioning of flow between the straits to seasonal wind forcing, as well as preview ongoing and future research directions.

Interannual Modulations of the 50-day Oscillations in the Celebes Sea

[1]Bo Qiu, [2]Xiao Chen, [2]Yiquan Qi ([1]University of Hawaii, [2]Hohai University)

Intense 50-day oscillations have been previously observed at the entrance of Celebes Sea and their formation has been suggested to be a result of Rossby wave resonance where the frequency of cyclonic eddy shedding by the intruding Mindanao Current matches that of the gravest Rossby mode of the semi- enclosed Celebes Sea basin. Using the ocean state estimate of 1993-2016 from the Estimating the Circulation and Climate of the Ocean, Phase II (ECCO2), we detected strong interannual modulations in the shedding of cyclonic eddies at the Celebes Sea entrance. Active eddy sheddings occurred during 1992- 93, 2002-03, 2006-10, and 2013-2015. Southward shifting of the wind-driven North Pacific tropical gyre and the concurrent weakening of the North Equatorial Countercurrent (NECC) in these years are found to be inducive for the generation of cyclonic eddies intruding into the Celebes Sea. Modulated by the activity of eddy sheddings, the upper ocean water mass properties in both the Celebes Sea and Makassar Strait exhibit noticeable interannual changes with less saline waters appearing in the 50-200m layer during the active eddy shedding years.

Constraining iron sources and pathways into the Pacific Equatorial Undercurrent

[1]Alexander Sen Gupta, [1]Xuerong Qin, [1]Laurie Menviel , [2]Eric van Sebille ([1]Climate Change Research Centre and ARC Centre of Excellence for Climate Systems Science, University of New South Wales, Sydney, Australia, [2]Utrecht University, The Netherlands)

The Eastern Pacific is one of the few high chlorophyll, low productivity regions of the world, where new primary production is thought to be primarily limited by the supply of the micronutrient Iron. Previous work suggests that much of this iron is derived from the margins of Papua New Guinea, where it becomes entrained into the fast-flowing New Guinea Coastal Undercurrent (NGCU) that feeds into the Equatorial Undercurrent (EUC). The EUC transports water and iron along the equator, across the width of the Pacific basin, which is ultimately upwelled in the eastern equatorial Pacific. However, there is a sparsity of iron observations which means that other western Pacific source regions and boundary currents systems may also be important.

In this work we have developed a Lagrangian iron model that tracks the evolution of iron concentration along particle trajectories between a number of potential source regions and the eastern Pacific. By conducting sensitivity experiments varying the concentration of iron at these multiple source regions and comparing simulated and observed concentrations long the EUC, the model suggests that that the NGCU alone cannot explain the magnitude and distribution of EUC iron concentrations. Inputs from the Mindanao current and the western boundary currents to the east of the Solomon Islands may also play important roles. Moreover, the presence of multiple source regions can help to explain how ENSO related variations in the strength of the western boundary currents can modulate eastern Pacific productivity on interannual time scales.

Characteristics and Forcing Mechanisms of the NEC/NEUC: a numerical modeling study

Junlu Li, Jianping Gan (The Hong Kong University of Science and Technology)

In the Western Pacific Ocean (WPO), the North Equatorial Current (NEC) bifurcates from its core position at ~13°N northward into the Kuroshio (KC) and southward the Mindanao Current (MC) off Philippines. This NKM current system governs the water/energy transport in the WPO and greatly influences conditions in China Sea. Beneath the wind-driven NEC, the eastward North Equatorial Undercurrent (NEUC) transports intermediate water eastward, and inter- acts dynamically with the NEC. However, the physical process and controlling mechanisms of the NEUC remains largely unclear. Based on realistic and physics-oriented modeling studies, we investigate the underlying distinct forcing processes of the NEC and NEUC. We find that the magnitude of both NEC and NEUC decrease from the west to the east. However, the seasonality of the NEC and NEUC is longitude-dependent and longitude-independent, respectively. The NEC intensity is affected by local wind dynamics and comparable remote wave dynamics, while the strength of the NEUC is largely dominated by the wind-induced effect. In order to isolate dynamics in different spatial scales, we decompose the velocity profile of the NEC/NEUC into large-scale and mesoscale patterns. The large-scale variability of the NEC correlates significantly with meridional barotropic pressure gradient force (PGF_BT), while the variability in the NEUC reflects the effect of baroclinic PGF (PGF_BC). Beneath the PGF_BT-controlled westward NEC, the vertical velocity shear induced by the meridional density gradient forms the eastward NEUC when the PGF_BC overcomes the PGF_BT. The variation of the PGF_BT and PGF_BC are correlated with the spatiotemporal variability of wind stress curl, and the tilting of pycnocline associated Ekman pumping dynamics. For the mesoscale variability, the NEUC al- ternative jets is well simulated, which are coherent with the strong variation of SSH anomaly induced by westward propagating eddies. Other forcing factors of the NEUC as well as its dynamical correlation with the adjacent undercurrent (e.g., the Luzon Undercurrent and the Mindanao Undercurrent) will also be discussed.

Aspect of Ningaloo Niño (Niña) as an intrinsic air-sea-land coupled mode

Toshio Yamagata and collaborators (Application Lab, Japan Agency for Marine-Earth Science and Technology)

Recently discovered Ningaloo Niño (Niña) is the regional climate mode along the west coast of Australia. In particular, the Ningaloo Niño event in 2010/11 was the unprecedented marine heat wave which influenced severely marine ecosystem of fishery and coral reef. The term was actually coined based on the similarity between the devastating coastal warm event and the tropical warm event of El Niño. The Ningaloo Niño (Niña) may be classified into a kind of coastal Niño (Niña) just like the Benguella Niño (Niña), California Niño (Niña) and Dakar Niño (Niña). The coastal Niño (Niña), occurs normally in an upwelling region associated with a cold coastal current along the eastern boundary of subtropical oceans. Along the west coast of Australia, however, the warm Leeuwin Current flows poleward and the situation is very different from the other analogs. Therefore we need to understand carefully how the regional climate mode of Ningaloo Niño (Niña) develops. Here we show that the mixed-layer depth variation plays a key role in the initiation of Ningaloo Niño (Niña) by use of OGCM forced by the NCEP/NCAR reanalysis data. We also show importance of local air-sea-land coupled processes in the subsequent evolution. Then, using a coupled GCM, we demonstrate that the regional climate mode may develop even without any influence of the basin-wide climate mode of ENSO. This hinders us at the present stage from predicting the occurrence of Ningaloo Niño (Niña) events which are independent of ENSO events.

Seven Years of Direct Observations of the Ombai Throughflow

[1,2] Susan Wijffels, [1]Bernadette Sloyan ([1]Centre for Southern Hemisphere Ocean Research, CSIRO Oceans and Atmosphere, [2]Woods Hole Oceanographic Institution)

Ombai Strait carries roughly 30% of the Indonesian Throughflow into the Indian Ocean. Comprising two mean flow cores – one at ~150m depth in the thermocline and a deep core around 900m. Flow variability is dominated by remotely forced Kelvin waves transmitted from the Indian Ocean to the Strait

along the Nusa Tengarra coastal wave guide. The Ombai Throughflow was measured during the INSTANT campaign from 2004-2006. The Strait was them re-instrumented from May 2001- October 2015 as part of the Australian Integrated Marine Observing System. Here we report on the new insights gained from now having over seven years of observations of this key flow, particularly focusing on the behaviour of the near surface shear and low frequency changes.

Nonlocal ocean-atmosphere interactions over the Indo-western Pacific warm pool

Shang-Ping Xie (Scripps Institution of Oceanography, UCSD, USA)

El Niño-Southern Oscillation (ENSO) induces coherent climate anomalies over the Indo-western Pacific warm pool, and these anomalies outlast sea surface temperature (SST) anomalies of the equatorial Pacific by a season, with major effects on the Asian summer monsoon. Specifically, a large-scale anomalous anticyclone (AAC) is a recurrent pattern in post-El Niño summers, spanning the tropical Northwest Pacific and North Indian Oceans. Regarding the ocean memory that anchors the summer AAC, competing hypotheses emphasize either SST cooling in the easterly trade wind regime of the Northwest Pacific or SST warming in the westerly monsoon regime of the North Indian Ocean and South China Sea. Recent studies reveal a coupled ocean-atmosphere mode that builds on both mechanisms in a two-stage seasonal evolution. In spring when the northeast trades prevail, the AAC and Northwest Pacific cooling are coupled via wind-evaporation-SST feedback. The Northwest Pacific cooling persists to trigger a summer feedback that arises from the interaction of the AAC and North Indian Ocean warming, enabled by the westerly monsoon wind regime. This Indo-western Pacific ocean capacitor (IPOC) explains why El Niño stages its last act over the monsoonal Indo-Northwest Pacific and casts the Indian Ocean warming and AAC in leading roles.

Conflicting views exist regarding the climatic role of the Indo-western Pacific warm pool. Some argue for a disproportionately important role as mean SSTs there well exceed the threshold for deep convection. By citing weak local correlations between SST and rainfall, on the other hand, the opposing camp argues that SST variability there is passive and of limited atmospheric effect. The talk will trace historical developments in the study of Indo-western Pacific warm pool variability. Recent studies consistently show that the warm pool is coupled with the atmosphere, but this coupling is not always local, rendering the local SST-rainfall correlation a poor metric. While ENSO is a dominant forcing, regional ocean-atmospheric coupling and feedback select preferred patterns of the regional response. Such regional modes (e.g., the IPOC and Indian Ocean dipole) are important in determining the season and spatial pattern of predictable climate variability. The remote effect on summer rainfall over eastern China will be discussed.

Observations of the low latitude western boundary currents in 2017

[1]Jae Hak Lee, [2]Hong Sik Min, [2]Chang Woong Shin, [2]Chang Su Hong, [2]Dong Guk Kim, [2]Gyu Nam Baek, [2]Fuad Azminuddin, [3]Cesar Villanoy, [4]Shaun Dolk ([1]Korea Institute of Ocean Science and Technology (KIOST), [2]KIOST, [3]MSI, University of the Philippines, [4]AOML, NOAA)

Field observations including deployment of ADCP moorings and satellite-tracked surface drifters using the R/V Isabu were carried out in the southwestern Philippine Sea in November and December of 2017 to observe the low latitude western boundary currents. The velocity data measured by lowered Acoustic Doppler Current Profiler (LADCP) and vessel mounted ADCP clearly show the Mindanao Current (MC) with a maximum speed > 1 m/s and the Mindanao Undercurrent with a maximum speed > 0.5 m/s. The strong southward flow near the sea surface appeared in the area from the Philippine coast to 129°E along 8°N. Both geostrophic velocity and LADCP data indicate that the current thickness exceeds 2000 m. Drifter trajectories revealed the Mindanao Eddy (ME) and Halmahera Eddy (HE) in the Mindanao Current and the New Guinea Coastal Current retroflection area, respectively, in the 2017-2018 winter sea- son. The result with other drifter trajectories support the possible seasonal displacement of the ME in the meridional direction.

Connecting boundary currents: The South Atlantic and the "eddy-highway"

Sabrina Speich, Remi Laxenaire, Tonia Capuano, Emanuela Rusciano (LMD/IPSL, CNRS, ENS, PSL Research University, 75231, Paris, France)

The global ocean is filled with mesoscale eddies that, as a consequence, should have a strong impact on the ocean circulation. These eddies are very efficiently detected and tracked (including their splitting and merging with other eddies) with the newly TOEddies algorithm developed at LMD-IPSL. Here we present an original study that show how long-lived mesoscale eddies in the South Atlantic materialize the climatically important link between the eastern and western boundary of the basin. The study is based on multisatellite sea-level data, Argo floats and high-resolution ship surveys that gives access to the subsurface velocity and hydrographic structure of such eddies. We will show that both, anticyclonic and cyclonic eddies, originating in the Cape Basin, follow a rather similar propagation route. In particular Agulhas Rings form an intense "eddy-highway" that connects the South Indian and South Atlantic western boundary currents. Agulhas rings are made by anticyclonic eddies that do not remain isolated vortices, but they split and merge with other eddies a number of times in their life span. Near the eastern boundary, their water cores undergo to in-route transformations under the influence of intense air-sea interactions. When leaving the eastern region, these low stratified core are sufficiently deep to prevent further water modifications and a well-developed anomaly is released at the western boundary where these eddies merge either with the South Brazil Current or other anticyclonic eddies. Some of them are tractable until the Zapiola Gyre, at the southern limit of this current. We will show that very quickly after their injection in the South Atlantic, Agulhas Rings are subsurface eddies, with maximum velocity at 200 m or deeper depth. This is why their signature in the surface dynamic height decrease, biut they remain intense mesoscale structures while crossing the Atlantic basin.

Thermohaline variations caused by subthermocline eddies east of Philippine

Linlin Zhang, Dunxin Hu (Institute of Oceanology, Chinese Academy of Sciences)

Intensive intraseasonal variations below the thermocline with period of 70-120 days east of Philippine has been reported by previous studies based on mooring observations and numerical models, which is proposed to be related to strong subthermocline eddy activities in that area. In this work, we investigated the thermohaline variations caused by subthermocline eddies east of Philippine based on mooring CTD measurements combined with Argo float profiles. Two cyclonic eddies are detected by mooring and Argo measurements, which appear to carry high salinity North Pacific Tropical Water in the thermocline and low salinity North Pacific Intermediate Water below the thermocline to the south, playing an important role in the water mass balance in the western Pacific. Thermohaline transport caused by these subthermocline eddies was estimated with numerical model outputs.

Spatial-temporal Features of Intra-seasonal Oceanic Variability in the Philippine Sea from Mooring Observations and Numerical Simulations

[1]Shijian Hu, [2]Janet Sprintall, [1]Cong Guan, [1]Bowen Sun, [1]Fan Wang, [3]Guang Yang, [1]Fan Jia, [1]Jianing Wang, [1]Dunxin Hu, [4]Fei Chai ([1]IOCAS, [2]Scripps Institution of Oceanography, University of California San Diego, [3]Center for Ocean and Climate Research, First Institute of Oceanography, State Oceanic Administration, [4] State Key Laboratory of Satellite Ocean Environment Dynamics, Second Institute of Oceanography, State Oceanic Administration)

The Philippine Sea is located at the pathway of the Madden–Julian oscillation (MJO) and the destination of north Pacific mesoscale oceanic eddies and waves, and characterized by striking intra-seasonal variability (20–90 days; ISV) that plays a key role in bridging weather and climate. Spatial pattern and temporal feature of intra-seasonal oceanic variability along the Philippine coast are investigated using multi-source mooring observations and outputs from an eddy-resolving general circulation model. Result shows that the SLA ISV intensity decreases from the northern and coastal

Philippine Sea to the south and interior Pacific Ocean. By contrast, eddy kinetic energy (EKE) features a northward decreasing gradient with a maximum at about 6 N. The meridional distribution of SLA and EKE spectra indicates that the ISV period increases with latitudes and is symmetrical about the equator. Mesoscale eddies in the up- per layer are tracked to explore its statistical distribution. Westward propagating mesoscale eddies and intraseasonal Rossby waves related to dynamic in- stability are found to be an important source of the oceanic ISV in the Philippine Sea and explain the latter's spatial and temporal patterns. Clear coastal propagation of ISVs related to coastal Kelvin waves is detected in the south of about 14 N. Composite analysis shows that the MJO is another important forcing in forming the spatial feature of Philippine ISV intensity and contributes close to half of the observed total ISV.

Effect of Mesoscale Eddies on North Pacific Subtropical Mode Water

Fei Shi, Yiyong Luo, Lixiao Xu (Ocean University of China)

The effect of eddies on the subtropical mode water (STMW) in the North Pacific is investigated through an analysis of the high-resolution OGCM solutions. Results show that both anticyclonic eddy (AE) and cyclonic eddy (CE) have strong stretching and squeezing effect on the STMW. In particular, the AE with lens-shaped structure encompasses thick STMW, while the AE without lens structure (the CE) deepens (Lifts) the STMW in its core. The eddy-trapped STMW moves essentially westward and makes a significant contribution to total STMW volume transport in the region. This study highlights the importance of eddy contribution to the STMW distribution in the North Pacific.

Wind energy input to the surface wave and currents in the Kuroshio extension region

Yuping Guan, Qian Yang, Yu Zhang (South China Sea Institute of Oceanology,CAS)

The winds and tides not only play a vital role in driving the upper-ocean variability, but also are the sole possible source of mechanical energy to drive the interior mixing. On the other hand, the energy exchanged between the ocean and the atmosphere is one key parameter for understanding the Earth's climate as well. One way to quantify this energy exchange is calculated the work done on the ocean by the wind. According to the interaction between ocean surface currents and surface wind stress, wind energy input to a number of ocean surface current components can be used to decompose wind work calculations. Previous studies show that wind energy input to the world ocean are patch distributions rather than uniform everywhere, Kuroshio extension is one of such region, due to ocean–atmosphere interaction is exceptionally strong over the Kuroshio and its extension. Here based on the SODA data, we present wind energy input to surface wave, surface current and surface geostrophic current and their secular trends, in the Kuroshio extension region.

Origins of the Pacific Meridional Overturning Circulation

[1]Mathias Zeller, [1]Shayne McGregor, [2]Paul Spence ([1]Monash University, [2]University of New South Wales)

Our study focuses on the shallow overturning circulation in the Pacific Ocean, known as the subtropical cells (STCs). The STCs extend from the tropics to the subtropics in both hemispheres and are thought to modulate the background state that the El Nino – Southern Oscillation (ENSO) operates in. This back- ground state modulation is important as it impacts the frequency and intensity of ENSO events along with its teleconnections. Therefore, understanding what drives STC variability and exactly how it modifies the tropical Pacific mean state would be a big step towards better understanding Pacific Ocean decadal variability and its potential predictability. We use a high-resolution ocean general circulation model to investigate the transports that are associated with the STC branches along 5ºN and 5ºS.

Based on a simulation driven by atmospheric re-analysis, we find that on interannual time scales the Northern hemisphere (NH) STC exhibits a slightly stronger variance than the Southern hemispheric (SH) STC. Moreover, the NH STC appears to lead the SH STC by 3 months (lagged corr: 0.75). Also on decadal time scales, the evolution of the NH STC clearly differs from that of the SH STC, specifically in the recent decades where the NH STC shows a much weaker increase than the SH STC. We next investigate the mechanisms driving the STC variability on both time scales and ask how much ENSO itself can drive the modelled STCs and their hemispheric differences. Therefore, winds that are linearly and non-linearly related to ENSO are identified and used to force the ocean model. Firstly, we find that the winds associated with ENSO can explain 56% of the total STC variability, with the two STCs being represented about equally well. The hemispheric differences in interannual variance and covariability are both reasonably well rep- resented by the ENSO forced STCs, while the winds non-linearly related to ENSO play a crucial role to explain these differences. However, the decadal STC variability represented by the linear trends of two distinct periods is not captured by the ENSO forcing suggesting different mechanisms to be responsible for the existence of these trends.

Roles of sensible and latent heat fluxes on the wintertime atmospheric responses to the Gulf Stream

[1]Togo Ida, [2,3]Kohei Takatama, [1,4]Shoshiro Minobe ([1]Department of Natural History Sciences, Graduate School of Science, Hokkaido University, Sapporo, Japan, [2]RIKEN Advanced Institute for Computational Science, Data Assimilation Research Team, Kobe, Japan, [3]International Pacific Research Center, SOEST, University of Hawaii, Honolulu, Hawaii, [4]Department of Earth and Planetary Science, Faculty of Science, Hokkaido University, Sapporo, Japan)

The roles of sensible and latent heat fluxes in the wintertime atmospheric responses over the Gulf Stream were investigated. In order to assess respective effects of two components of turbulent heat fluxes, we conducted numerical experiments in which sea surface temperatures that are used for air-sea heat flux calculations are smoothed separately for sensible heat flux and latent heat flux. Comparison among simulations indicates that sensible and latent heat flux contributes differently to the atmospheric responses over the Gulf Stream. Sensible heat flux contributes dominantly to diabetic heating in the boundary layer. By enhancing low (high) sea level pressure anomaly and destabilizing (stabilizing) atmosphere over the Gulf Stream (cold shelf water to the north of it), sensible heat flux strengthens surface wind convergence and cyclonic wind rotation over the Gulf Stream. Sensible heat flux enhances upward motion from the boundary layer to the lower free-troposphere. In addition, sensible heat flux contributes to sharpening the structure of meridional eddy wind variance, especially near the surface. On the other hand, latent heat flux mainly contributes atmospheric responses in the free troposphere. Latent heat flux enhances precipitation over the Gulf Stream. The released latent heat leads to an enhancement of upward motion in the free troposphere and extremely strong upward motion both in the boundary layer and the free troposphere. Latent heat flux suggested to be contribute more strongly to enhancing the intensity of storm track, especially near the surface.

Energetics of M2 Internal Tides modulated by the Kuroshio Northeast of Taiwan

Zhenhua Xu, Hang Chang, Baoshu Yin, Yijun Hou (Institute of Oceanology, Chinese Academy of Sciences)

The Luzon Strait and the area northeast of Taiwan are both prominent sources of internal tides among global ocean. The M2 internal tides originated from Luzon Strait and their radiation processes into the South China Sea have attracted much attention, but few studies have been conducted on the area to the northeast of Taiwan. In the present study, generation, propagation and dissipation processes of M2 internal tides to the northeast of Taiwan are revealed through high-resolution numerical simulations. The Kuroshio are found to play important roles in modulating the lifecycle of M2 internal tides in this area. Interference

processes and various topographical features clearly enhance M2 internal tide dissipation and induce strong, inhomogeneous vertical mixing, which is an important factor in energy cascading processes.

Effect of westward shoaling thermocline on characteristics and energetics of internal solitary waves by numerical simulation

Haibin Lv (Huai Hai Institute of Technology)

An internal gravity wave (IGW) model is employed to simulate the generation of internal solitary waves (ISWs) over a sill by tidal flows. A westward shoaling thermocline parameterization scheme derived from a three parameter model is adopted for characteristics and energetics of ISWs. Ten numerical experiments were designed and the results were compared. It is found that, with the westward shoaling thermocline, the horizontal current velocity in the upper and lower layers of the thermocline, number of ISWs, total barotropic kinetic energy and baroclinic energy in packet A are reduced. When the thermocline thickness is increased, the depth of turning point, ISW amplitude, number of ISWs, phase speed of ISWs, total barotropic kinetic energy, total baroclinic energy and ratio of baroclinic kinetic energy (KE) to available potential energy(APE) in packet A decrease, whilst depth of isopycnal undergoing maximum dis- placement and the ratio of baroclinic energy to barotropic energy increase; when the density difference is reduced, the depth of turning point, ISW amplitude, phase speed of ISWs, total barotropic kinetic energy, the ratio of baroclinic energy to barotropic energy, total baroclinic energy in packet A decrease, whereas depth of isopycnal undergoing maximum displacement increase; when the isopycnal slope angle is increased, number of ISWs, phase speed of ISWs, total baroclinic energy in packet A increase, however, the depth of turning point almost remains unchanged; when the vertical depth of westward shoaling thermocline is reduced, the depth of turning point, depth of isopycnal undergoing maximum displacement, phase speed of ISWs, ratio of baroclinic energy to barotropic energy, total baroclinic energy in packet A decrease, whilst ISW amplitude, total barotropic kinetic energy, ratio of KE to APE in- crease.

ABSTRACT-ORAL-MAY 9

A Joint Data Assimilation System Based on Local Ensemble Transfer Kalman Filter

G. R. Asrar, Y. Liu, N. Zeng, M. Chen and E. Kalnay (University of Maryland, College Park & Pacific Northwest National Laboratory)

We have developed a joint data assimilation system (JDAS) to be used in integrated Earth system modeling framework, a.k.a. coupled assimilation mode. This JDAS is based on Local Ensemble Kalman Filter (LETKF), and is capable of estimating the ocean and land carbon fluxes (e.g. seasonal cycle at grid scale), which are essential for better understanding and quantifying the carbon sources and sinks for carbon cycle research and analysis. Based on some preliminary research, we find the JDAS to be capable of reproducing the seasonal cycle of surface carbon fluxes, in an Observing System Simulation and Assimilation (OSSA) mode. We also found the JDAS to perform best with an optimum combination of a short assimilation window and a long observation window. We used a combination of CO2 measurements from surface- and space-based platforms to test the JDAS performance. The assimilation products capture very well CO2 seasonal cycle and spatial patterns, a pre-requisite for understanding the magnitude and variability of CO2 sources and sinks, at regional and global level.

Towards predicting changes in the land monsoon rainfall a decade in advance

Bin Wang (Department of Atmospheric Sciences, School of Ocean and Earth Science and Technology, University of Hawaii at Manoa, Honolulu, HI 96822, USA, Earth System Modeling Center, Nanjing University of Information Science and Technology, Nanjing, 210044, China)

Predictions of changes of the land monsoon rainfall (LMR) in the coming decades are vitally important for sustainable economic development. The intensity change of the Northern Hemisphere LMR (NHLMR) not only reflects the changes in global hydrology and tropical circulation, but also represents the changes in the regional land monsoon rainfall over northern Africa, India, East Asia, and North America, potentially impacting some two-thirds of the global population. However, the current global climate models have shown little skill in the direct prediction of decadal variability of the NHLMR. The physical basis and predictability for such predictions remain largely unexplored. Using the observed data from 1901 to 2014, we show that the decadal predictability of the NHLMR is rooted primarily in decadal variations of the north-south hemispheric thermal contrast in the Atlantic-Indian Ocean sector and augmented by an east-west thermal contrast in the Pacific. The former features a dipolar SST anomaly pattern between the North Atlantic and South Indian Ocean. This assertion is supported by a 500-year coupled climate model simulation and a suite of numerical experiments. A 51-year, independent decadal hindcast with a hybrid dynamic-conceptual model and using the SST anomalies predicted by a multi-climate model ensemble suggests that the decadal changes in the NHLMR can be predicted approximately a decade in advance with significant skills. The results here open a promising way forward for decadal predictions of regional land monsoon rainfall worldwide.

Diversity of Surface Easterly Winds Along the Equator in El Niño and La Niña Events During 1997 to 2016

David Halpern (Scripps Institution of Oceanography)

Continuous satellite surface wind vector measurements captured two super El Niño events (May 1997 to May 1998 and March 2015 to May 2016), four typical El Niño events, and four La Niña events. Both super El Niño events had similar sea surface temperature anomaly intensities. In the average typical El Niño event, the westward wind speed collapsed over 135°E-165°E with longitudinal-averaged eastward wind speed of about 1.0 m s-1. In June-November 1997, a major collapse of the easterly wind substantially occurred over 153°E-170°W, with a longitudinal-averaged eastward wind speed of about 2 m s-1 and maximum speed of 4.1 m s-1 at 168°E. A similar easterly wind collapse did not occur in the 2015-2016 super El Niño event. During the latter six months of the 1997-1998 event, the wind direction was westward throughout the Pacific with a uniform speed of about -3.0 m s-1 from the far west Pacific to 130°W, where the speed declined linearly, more or less, to approximately zero at 90°W. The average westward wind speeds at 150°W associated with the 1997-1998, 2015-2016 and typical El Niño events were 3.2, 4.6 and 6.0 m s-1, respectively, which indicated a large diversity among El Niño events. Correlations between inferences of Ekman vertical motions in the upper ocean at the equator and fluctuations in satellite measurements of near-surface phytoplankton abundance and in model-generated depths of the thermocline will be discussed.

Equatorial temperature effects of flow through the Solomon Sea

William S. Kessler, Hristina Hristova, Russ Davis and Jeff Shermann (NOAA)

Gliders have made regular coast to coast sections across the Solomon Sea since 2007, for a total of 103 coast-to-coast sections to date. Annual and interannual Solomon Sea transport variability have similar magnitude (RMS about 6Sv), but most of the annual cycle occurs as a shallow subtropical inflow, while lower-frequency signals arrive from the coast of Australia as a western boundary current. Much of the

ENSO-timescale variability can be traced to wind curl variability over the Coral Sea, including curl signals extending beyond 20S. These pump mass towards the western boundary during the mature phase of El Ninos, and away from the boundary during La Ninas, with this signal modulating Solomon Sea transport via the WBC along the coast of Australia. A linear (Rossby wave/Time-dependent Island Rule) analysis accounts for much of the variability, and allows separating the forcing regionally and by frequency.

An estimate of interannual temperature advection into the basinwide equatorial band is constructed from four pieces: (1) Glider data for the Solomon Sea, (2) Argo temperature and geostrophic currents at 9.5S across the Pacific east of the Solomon Islands to South America and (3) across the Pacific at 9.5N, (4) CCMP winds for the Ekman contribution. (Indonesian Throughflow variability is a residual). The method of Lee et al., (2004) provides a means to isolate the Solomon Sea part of this system. Of these four, the Solomon Sea is the largest contribution to temperature advection variability into the equatorial band, accounting for much of the observed temperature tendencies within the band.

Variability of the Pacific western boundary currents and the Indonesian Throughflow during the 2015-2016 super El Niño

Dongliang Yuan, Xiang Li, Zheng Wang, Yao Li, Hui Zhou, Jing Wang, Xiaoyue Hu, Shuwen Tan, Ya Yang (Institute of Oceanology, Chinese Academy of Sciences, Qingdao, China)

Adhitya Wardana, Dewi Surinati, Adi Purwandana, Mochamad Furqon Azis Ismail, Praditya Avianto, Dirhamsyah, Zainal Arifin (Research Center for Oceanography, Indonesian Institute of Sciences, Jakarta, Indonesia)

The mooring observations deployed in the Maluku Channel of the Indonesian Seas during December 2012 through November 2017 show significant interannual variations of the Indonesian Throughflow through the eastern Indonesian seas during the 2015-2016 strong El Niño. The amplitudes of the interannual variations are as large as or larger than the mean transport through the Makassar Strait, suggesting the importance of the ITF transports through the eastern Indonesian seas in the total ITF interannual variability. In comparison, the interannual transport through the Halmahera Sea during the peak of the 2015-2016 El Niño is very small, smaller than the seasonal variations, suggesting that the interannual Rossby waves are blocked by the western boundary currents offshore of the New Guinea coast. The interannual variations of the ITF in the eastern Indonesian seas during a strong El Niño are measured for the first time in history.

Using observations from ship-board acoustic Doppler current meters, we show that the Kuroshio transport increases and the MC transport decreases by 10 and 25 Sv (1 Sv= 106 m3 s-1), respectively, during the 2015-2016 El Niño. During the 2010 strong La Niña peak in comparison, geostrophic calculations also suggest that the Kuroshio transport decreases by more than 10 Sv and the Mindanao Current transport increases by more than 5 Sv. The dynamics of the WBC interannual variations are suggested to be associated with the Kelvin wave propagation around the Philippines and the MC regime shift. The results suggest the importance of the WBCs in the discharge and re-charge of the western Pacific warm pool during strong ENSO events.

Pacific influences on the meridional temperature transport of the Indian Ocean

Ming Feng, Jie Ma, Bernadette Sloyan (CSIRO)

In this study, the interannual-decadal variations of the meridional temperature transport in the Indian Ocean and their mechanisms are examined using an eddy-resolving global ocean circulation model for the period 1979-2014. The first empirical orthogonal function (EOF) mode of the meridional temperature transport of the Indian Ocean is found to be highly influenced by remote forcing from El Niño–Southern Oscillation (ENSO) in the Pacific through both oceanic waveguide and atmospheric teleconnection, with stronger southward temperature transport during La Nina events and weaker southward temperature

transport during El Nino. ENSO influences the southeast Indian Ocean steric height anomalies along the oceanic waveguide, whereas ENSO atmospheric teleconnection induces opposite steric height anomalies in the southwest tropical Indian Ocean, which act together to drive the meridional temperature transport of the southern Indian Ocean. In the tropical South Indian Ocean between Equator and 10°S, the steric height anomalies off Java and Sumatra is driven by the wind stress anomalies along the equatorial Indian Ocean and off Java and Sumatra, and the resultant geostrophic transport over- comes the direct Ekman contribution to drive meridional temperature transport across the Indian Ocean; in the tropical North Indian Ocean, the interannual-decadal variations in the meridional temperature transport are primarily associated with surface Ekman transport, driven by co-varying Indian Ocean Di- pole wind variability with ENSO. The meridional temperature transport variability is significantly associated with the leading mode of Indian Ocean meridional overturning streamfunction, which corresponds to a deep circulation cell extending from 27°S across the Equator to about 20°N. A dynamical decom- position of the meridional streamfunction supports the different mechanisms of variability with latitude.

Development of an Inter-basin Pacific-Indian Ocean Model: The Indonesian ThroughFlow (ITF) and the Circulation in the Banda Sea

Linlin Liang, Huijie Xue (South China Sea Institute of Oceanology)

The tropical Pacific Ocean and the Indian Ocean are connected via a labyrinth of passages through the Indonesian Archipelago. The Indonesian Through- Flow (ITF) is a key component of the global conveyer belt, and it has profound influences on the ocean general circulation and climate change. However, exceedingly complicated topography of the Indonesian Archipelago exerts great difficulties in both observations and numerical modeling. In this work, the Regional Ocean Modeling System (ROMS) is implemented for the western Pacific and northern Indian oceans to depict the 3-D circulation inside the Indonesian Archipelago and its relationship to the throughflow.

The model results show that the Pacific's low latitude western boundary currents are the sources of the ITF. The inflow through the Celebes Strait then the Makassar Strait originates from the Mindanao Current, while the flow entering the Halmahera Sea originates from the New Guinea Coastal Current. The ITF exits the Indonesian Archipelago mainly through the Lombok Strait, Ombai Strait and Timor Passage. While topography smoothing changes the partition among these three exiting passages, the sea level difference between the western Pacific and the eastern Indian Ocean appears to determine the total ITF transport, which can be significantly modified by including tide in the model. Moreover, the principal in- and outflows all show three-layer structures in the vertical. Similarly, there is a three-layer circulation in the Banda Sea: clockwise-counterclockwise-clockwise in the top (< 500m)-middle (500-2250m)-bottom (> 2250m) layers. The three layers in the Banda Sea are linked vertically by the upward (downward) flux from the middle layer to the top (bottom) layer, which are balanced by the net inflow of 2.12 Sv to the middle layer and the net outflow of 1.08 and 1.04 Sv from the top and bottom layer, respectively.

The Low-Frequency Processes in the Indo-Pacific Region and Their Impact on Tropical Indian Ocean

Yan Du (South China sea insititute of Oceanology, CAS)

The Indo-Pacific Region is a noteworthy area with the sophisticated ocean and atmosphere (O-A) system. Here, we focus on the low-frequency signals related to the O-A variation and its impact on dynamic and thermodynamic processes in this region. The oceanic waveguide, as the ocean dynamic linkage, connects two basins in the Indonesian Seas. The wave signals generated by off-equatorial wind curl in the tropical Pacific dominate the decadal SSH variations in the south IO. For the thermodynamic processes, we find that the sea surface salinity in the tropical IO features a meridional dipolar variation on multi-timescale,

named by Salinity Indian Ocean Dipole mode (S-IOD). It is highly correlated with O-A pathways, affected by precipitation, sea level changes and advection in the Indo-Pacific Region. We also identify a decadal Indian Ocean Dipole (IOD) pattern of SST in the tropical IO. It modulates the interannual IOD characteristics, such as frequency of occurrence and O-A coupled efficiency. Summarily, our studies suggest that multi-timescale teleconnections exist in the Indo-Pacific Region and implicate that considering low-frequency signals would be meaningful to the climatic prediction.

Impact of a background flow on internal tides dissipation and implications for the Indonesian seas

Océane Richet (CSIRO)

The Indonesian seas is a region characterized by strong tides. The generation of internal tides, their propagation, breaking and the induced mixing play a leading role to set the main characteristics of the Indonesian Throughflow [Koch-Larrouy 2007]. These internal waves are mainly generated in narrow straits [Nagai & Hibiya 2015], by interaction between barotropic tides and sills, where background flow is strong, subsurface intensified and variable in time.

In the presented study, we investigate the interaction and the dissipation of internal tides in the presence of a background flow. We use a high-resolution two-dimensional nonhydrostatic numerical model (the MITgcm), with idealized topography. We find that the mean flow induces a Doppler shift on the internal waves frequencies modifying their scales and hence their probability to break near the generation site or remotely in the interior Indonesian seas. This study is directly related to the Indonesian seas where ocean mixing influences the Indonesian Throughflow temperature and property transport, and the sea surface temperature in the region on seasonal time scales. Determining how the internal wave field is modulated by the mean flow is potentially Important to improving our understanding of the role of mixing on the intra-seasonal to interannual behavior and characteristics of the Indonesian seas.

Seasonal Variability of Sea Surface Temperature Front in South China Sea

Yuntao Wang, Han-Ran Zhang (Second Institute of Oceanography, SOA)

High resolution satellite observation for sea surface temperature (SST) was used to derived the daily SST fronts and monthly frontal probability (FP) in the South China Sea. The spatial pattern of overall mean SST front agreed well the feature of SST gradient. More fronts were identified in the region where SST gradient is larger. The FP was characterized by large seasonal variability with highest (lowest) values found in winter (summer). The temporal variability was confirmed by using EOF method and the largest variability was identified along the coast of Vietnam and China, to the northwest of Luzon Island. Wind and river discharge played important role in determining the variability of SST fronts. The northeast monsoon during winter drove onshore Ekman transport near the coast of China, which converged with Pearl River plume. Thus, more fronts were generated in the region. The southwest monsoon during summer induced offshore transport, which brought upwelling near the coast of southeast Vietnam. There were fronts generated between upwelled and offshore water. The interannual variability of front was described in EOF3, which was impacted by ENSO signal. The ENSO was two months leading the variability of front indicating a clear imprint of atmospheric influence.

Regional and global ocean heat content changes related to ENSO

[1]Lijing Cheng, [2]Kevin Trenberth, [2]John Fasullo, [3]Michael Mayer, [3]Magdalena Balmaseda, [1]Jiang Zhu, [4]Karina von Schuckmann ([1]Institute of Atmospheric Physics, Chinese Academy of Sciences,

[2]National Center for Atmospheric Research, Boulder, Colorado, USA, [3]European Centre for Medium Range Weather Forecasts, Shinfield Park, Reading RG2 9AX, UK, [4]Mercator Océan)

As the strongest inter-annual perturbation to the climate system, the El Niño Southern Oscillation (ENSO) dominates the inter-annual variability of the ocean energy budget. Here we combine ocean analysis, re-analysis, Earth system model simulations and surface flux datasets to better understand the re- gional and global evolution of ocean heat related to ENSO.

A robust cooling of the climate system and global ocean is identified during and after El Niño, as seen from multiple datasets. This negative ocean heat content tendency (OHCT) is dominated by the net cooling of the tropical Pacific Ocean through enhanced air-sea heat fluxes driven by high sea surface temperatures. The adiabatic redistribution of heat, both laterally and vertically, in the tropical Pacific and Indian Ocean dominates their local OHCT: for ex- ample, heat content increases in the West Indian and East Pacific Ocean before El Niño, reflecting the effects of weakened Pacific trade winds and related walker circulation changes. Heat also discharges from tropics (i.e. 20S-5oN) into off-equatorial regions (5-20oN) during and after El Niño.

The tropical Atlantic is found to experience a net warming during El Niño and the North (South) Pacific Ocean warms (cools) and then cools (warms) after El Niño. Consistency between OHCT and the net surface flux in these regions indicates that atmospheric teleconnections play a main role in observed changes. In contrast, OHCT in the Indian ocean is found to be out of phase with surface flux, indicating a strong modulation of ocean transport: i.e. Indonesian Throughflow. There is insignificant net ocean heat change in the North and South Atlantic Ocean.

A combination of OHC and surface flux analyses allow ocean Meridional Heat Transport (MHT) to be estimated as a residual. Significant regulation of MHT by ENSO is found in the Indo-Pacific basin.

Seasonality and Predictability of the Indian Ocean Dipole Mode: ENSO Forcing and Internal Variability

Yun Yang (Beijing Normal University)

This study evaluates the relative contributions to the Indian Ocean Dipole (IOD) mode of interannual variability from the El Niño-Southern Oscillation (ENSO)forcing and ocean-atmosphere feedbacks internal to the Indian Ocean. The ENSO forcing and internal variability is extracted by conducting a 10-member coupled simulation for 1950-2012 where sea surface temperature (SST) is restored to the observed anomalies over the tropical Pacific but interactive with the atmosphere over the rest of the world ocean. In these experiments, the ensemble mean is due to ENSO forcing and the inter-member difference arises from internal variability of the climate system independent of ENSO. These elements contribute one third and two thirds of the total IOD variance, respectively. Both types of IOD variability develop into an east-west dipole pattern due to Bjerknes feedback and peak in September-November. The ENSO forced and internal IOD modes differ in several important ways. The forced IOD mode develops in August with a broad meridional pattern, and eventually evolves into the Indian Ocean Basin mode; while the internal IOD mode grows earlier in June, is more confined to the equator and decays rapidly after October. The internal IOD mode is more skewed than the ENSO forced response. The destructive interference of ENSO forcing and internal variability can ex- plain early-terminating IOD events, referred to IOD-like perturbations that fail to grow during boreal summer.

Our results have implications for predictability. Internal variability, as represented by pre-season sea surface height anomalies off Sumatra, contributes to predictability considerably. Including this indicator of internal variability, together with ENSO, improves the predictability of IOD.

Scale-dependence of observed wind stress response to ocean-mesoscale surface temperatures

Niklas Schneider (International Pacific Research Center and Department of Oceanography University of Hawai'i at Mānoa, Honolulu, Hawai'i, USA)

Ocean-mesoscale sea surface temperatures (SST) leave a strong imprint on surface wind stress. To explore the dependences of underlying dynamics on length-scale and on large-scale wind direction and speed, we represent the spatial co-variability of wind stress and SST by spectral transfer functions. These relate spectral amplitudes of winds and SST as a function of wave numbers aligned with, and perpendicular to, large-scale winds. Together with the large-scale wind speeds, the former defines the downwind Rossby number. Application in the Southern Ocean shows distinct sensitivities to the direction and speed of the large-scale winds. For large Rossby numbers, ocean-mesoscale SST induced wind speeds are large and include, for swift large-scale winds, a lagged component. This suggests modulation of vertical mixing as underlying process. SST induced changes of wind speed peak are largest for Rossby numbers of order one, and suggest advection, rotation and SST induced vertical mixing pressure gradients are important. For large wave--numbers perpendicular to background winds, responses of wind speed and direction reflect vertical mixing and pressure gradients. Conversions of wind components to wind divergence and curl shows the former dominated by large Rossby numbers, while the latter is significant for large wave-numbers perpendicular to large-scale winds.

The simulated large-scale oceanic circulation and mesoscale eddies in the western Pacific

Yongqiang Yu, Hailong Liu, Pengfei Lin, Bo An (LASG, Institute of Atmospheric Physics, Chinese Academy of Sciences)

The present study described high-resolution climate modeling efforts including oceanic, atmospheric and coupled general circulation model (GCM) at the state key laboratory of numerical modeling for atmospheric sciences and geophysical fluid dynamics (LASG), Institute of Atmospheric Physics (IAP). The high-resolution OGCM is established based on the latest version of the LASG/IAP Climate system Ocean Model (LICOM3.0), but its horizontal resolution and vertical resolution are increased to 1/10° and 55 layers, respectively. Forced by the surface fluxes from the reanalysis and observed data, the model has been integrated for approximately more than 80 model years. Compared with the simulation of the coarse-resolution OGCM, the eddy-resolving OGCM not only better simulates the spatial-temporal features of mesoscale eddies and the paths and positions of western boundary currents but also reproduces the large meander of the Kuroshio Current and its interannual variability. Another aspect, namely, the complex structures of equatorial Pacific currents and currents in the coastal ocean of China, are better captured due to the increased horizontal and vertical resolution. The high-resolution LICOM is also coupled with an atmospheric model CAM4 with horizontal resolution about 25km, in which the meso-scale air-sea interaction processes are better captured than stand-alone OGCM.

Delineation of Thermodynamic and Dynamic Responses to Sea Surface Temperature Forcing Associated with El Niño

[1]Xiaoming Hu, [2]Ming Cai, [1]Song Yang, [2]Zhaohua Wu ([1]Sun Yat-Sen University, [2]Florida State Universtiy)

A new framework is proposed to gain a better understanding of the response of the atmosphere over the tropical Pacific to the radiative heating anomaly associated with the sea surface temperature (SST) anomaly in canonical El Niño winters. The new framework is based on the equilibrium balance between thermal radiative cooling anomalies associated with air temperature response to SST anomalies and other thermodynamic and dynamic processes. The air temperature anomalies in the lower troposphere are mainly in response to radiative heating anomalies associated with SST, atmospheric water vapor, and cloud anomalies that all exhibit similar spatial patterns. As a result, air temperature induced thermal radiative cooling anomalies would balance out most of the radiative heating anomalies in the lower

troposphere. The remaining part of the radiative heating anomalies is then taken away by an enhancement (a reduction) of upward energy transport in the central-eastern (western) Pacific basin, a secondary contribution to the air temperature anomalies in the lower troposphere. Above the middle troposphere, radiative effect due to water vapor feedback is weak. Thermal radiative cooling anomalies are mainly in balance with the sum of latent heating anomalies, vertical and horizontal energy transport anomalies associated with atmospheric dynamic response and the radiative heating anomalies due to changes in cloud. The pattern of Gill-type response is attributed mainly to the non-radiative heating anomalies associated with convective and large-scale energy transport. The radiative heating anomalies associated with the anomalies of high clouds also contribute positively to the Gill-type response. This sheds some light on why the Gill-type atmospheric response can be easily identifiable in the upper atmosphere.

An improved ENSO simulation by representing chlorophyll-induced climate feedback in the NCAR Community Earth System Model

Rong-Hua Zhang (Institute of Oceanology, Chinese Academy of Sciences)

The El Niño-Southern oscillation (ENSO) simulated in the Community Earth System Model of the National Center for Atmospheric Research (NCAR CESM) is much stronger than in reality. Here, satellite data are used to derive a statistical relationship between interannual variations in oceanic chlorophyll (CHL) and sea surface temperature (SST), which is then incorporated into the CESM to represent oceanic chlorophyll -induced climate feedback in the tropical Pacific. Numerical runs with and without the feedback (referred to as feedback and non-feedback runs) are performed and compared with each other. The ENSO amplitude simulated in the feedback run is more accurate than that in the non-feedback run; quantitatively, the Niño3 SST index is reduced by 35% when the feedback is included. The underlying processes are analyzed and the results show that interannual CHL anomalies exert a systematic modulating effect on the solar radiation penetrating into the subsurface layers, which induces differential heating in the upper ocean that affects vertical mixing and thus SST. The statistical modeling approach proposed in this work offers an effective and economical way for improving climate simulations.

The observed impacts of two types of El Niños on the North Equatorial Countercurrent in the Pacific Ocean

Hui Zhou (Institute of Oceanology, Chinese Academy of Sciences)

This study investigates the inter-annual variations of the North Equatorial Counter Current (NECC) associated with the Eastern-Pacific (EP) type and the Central-Pacific (CP) type of El Niños in the Pacific Ocean by using identification method of Kao and Yu (2009). Our analysis suggests that during both types of El Niños, the amplitudes of wind field anomalies are comparable with each other accompanied by distinct spatial structures, which results in significant and distinct fluctuations of the NECC during EP and CP El Niños respectively. During the EP-El Niños, the NECC starts to shift southerly in the central-eastern Pacific and extends west as the development of El Niños. However, during the CP-El Niños, the southerly displacement and strengthening of the NECC are confined in the western-central Pacific. These discrepancies can be attributed to the different modulations of equatorial Kelvin wave and tropical Rossby wave propagation as well as Ekman pumping forced by the unique wind stress field during the two types of El Niños, which are verified by using a 1.5-layer reduced gravity model.

Definition of extreme El Niño and its impact on projected increase in extreme El Niño frequency

Guojian Wang (CSIRO)

During extreme El Niño, the Intertropical Convergence Zone (ITCZ) moves to the normally cold and dry east equatorial Pacific, resulting in a nonlinear rainfall increase with sea surface temperature (SST) in the region. An arbitrary threshold value of boreal winter total rainfall (e.g., 5 mm day-1) in the east equatorial Pacific is used to capture this feature. Under greenhouse warming, the extreme El Niño frequency is projected to increase, so is the mean east equatorial Pacific rainfall. Is the projected frequency increase a consequence of the mean rainfall increase? Using various definitions, here we show that the projected increase in extreme El Niño frequency is only weakly influenced by the increased mean rainfall. Instead, the increased frequency accounts for approximately 50% of the mean rainfall increase, and results from an increased probability of atmospheric deep convection in the eastern equatorial Pacific, because the region warms faster than the surrounding regions.

Thermal and salt variability in the South China Sea influenced by the Western Pacific Ocean

Dongxiao Wang (South China Sea Institute of Oceanology, CAS)

The thermal and salinity variability in the South China Sea is influenced by the western Pacific Ocean. First, associated with two types of El Nino, the evolution of SST in SCS is different, such as amplitude and oscillation periods. The net heat flux is major contribution to the significant difference between EP and CP EN in autumn; Second, two extreme subsurface warm events were identified during 1998/99 and 2006/07, but there were no extreme surface warm events except in 1998. Extreme subsurface warm events in the SCS is likely to be related to the PDO phase rather than to the ENSO; Last, The subsurface salinity in the northern SCS also shows distinct decadal variability in its horizontal and vertical structures, and salinity budget suggests that entrainment from the mixed layer played a more important role in the freshening periods than in the salinifying period which was dominated by salinity advection through the Luzon Strait.

The ENSO Complexity: Its Underlying Dynamics and Impacts on Western Pacific Climate

Jin-Yi Yu (Department of Earth System Science, University of California, Irvine, CA, USA)

Not all El Niño–Southern Oscillation (ENSO) events are the same. One event may have its sea surface temperature (SST) anomalies initially develop in the eastern or central Pacific, propagate eastward or westward afterward, and decay into a neutral state or into an event of the same- or opposite-phase.

In this talk, a new framework will be presented to explain the possible sources of these complex ENSO behaviors. In this framework, ENSO complexity is linked to three key atmosphere-ocean coupling mechanisms crucial to ENSO. The interplay of these processes results in different ENSO types (Central Pacific type vs. Eastern Pacific type), different ENSO evolutions (cycles, episodes, and multi-year events), and El Niño-La Niña asymmetries.

The climate impacts produced by this ENSO complexity on the Western Pacific will also be discussed. One example is the changing importance of the Maritime Continent and Indian Ocean in modulating variability in the western Pacific subtropical high and tropospheric biennial oscillation.

Impacts of the Atlantic Multi-Decadal Variability in the Pacific Basin and A New Large Ensemble of Decadal Prediction Simulations

Gokhan Danabasoglu, Steve Yeager, Yohan Ruprich-Robert, Frederic Castruccio, Rym Msadek, and Thomas Delworth

In the first part of the presentation, we will focus on the impacts of the Atlantic Multi-decadal Variability (AMV) on the Pacific Basin via atmospheric teleconnections. We use an ensemble set of coordinated coupled simulations in which the model North Atlantic sea surface temperatures are restored towards time-independent anomalies corresponding to an estimate of the internal component of the observed AMV. A robust finding is that the warm phase of the AMV produces a Pacific Decadal Variability (PDV)-like response in its negative phase which in turn impacts the occurrence frequency of El Nino or La Nina events. The PDV-like response comes from changes in the Walker Circulation and can be largely attributed to the tropical part of the AMV. In the second part, we will introduce a new and improved ensemble of Decadal Prediction (DP) simulations with the Community Earth System Model (CESM). The new DP set (CESM-DP-LE) is comprised of 40-member ensemble simulations that are integrated forward for 10 years following initialization on 01 November of each year between 1954 and 2015. CESM-DP-LE represents the initialized counterpart to the CESM Large Ensemble (CESM-LE): both simulation sets are large ensembles, and they use identical model code and radiative forcings. Comparing CESM-DP-LE to CESM-LE highlights the impacts of ocean initialization on prediction skill. In particular, we highlight how better initialization of the tropical Pacific Ocean leads to improved predictions. CESM-DP-LE exhibits significant and potentially useful prediction skill for a wide range of fields, regions, and timescales. We show the level of skill in predicting surface temperatures and precipitation with a focus on the Pacific Basin as well as for El Nino events in comparison to persistence and CESM-LE. We will close with a summary of our future DP activities within the newly-formed International Laboratory for High-Resolution Earth System Prediction (iHESP).

Near-inertial waves advected by the Kuroshio from observation and simulation

[1]Chanhyung Jeon, [1]Jae-Hun Park, [2]Hirohiko Nakamura, [2]Ayako Nishina, [3]Xiao-Hua Zhu, [4]Dong Guk Kim, [4]Hanna Na, [4]Hong Sik Min, [5]Naoki Hirose ([1]Inha University, [2]Kagoshima University, [3]Second Institute of Oceanography, [4]Korea Institute of Ocean Science and Technology, [5]Kyushu University)

Advection of near-inertial waves (NIWs) by background currents has been predicted using numerical simulations, while supporting in-situ observations were rare. A pair of tall current moorings, deployed around 25°N and 125°E in Okinawa Trough from June 2015 to June 2016, provides a clear evidence exhibiting NIWs advected by the Kuroshio. Energetic NIWs are observed after two-typhoon passages in early August and late September 2015. Both typhoon passages occurred across the Kuroshio east of Taiwan upstream of the observation sites about 250 km southwestward with a difference of about 2-degree in latitude. One site (KCM1), relatively close to the center of the Kuroshio axis, exhibits more energetic NIWs than near the edge of the Kuroshio (KCM2), ~40 km away from KCM1. The frequency of NIWs are shifted to the lower band from the local inertial frequency (0.91f), inferring propagation from the south. Data-assimilative three-dimensional numerical model simulates that local NIW generation is weak at observation sites during and after typhoon pas- sages, while its generation in the Kuroshio upstream is energetic. In addition, the model simulates patterns and characteristics of the advecting NIWs similar to the observations, strongly supporting that the observed features of NIWs are caused by their advection to the northeastward by the Kuroshio.

Atmospheric dynamic and thermodynamic processes in driving the western North Pacific anomalous anticyclone

Wu Bo (Institute of Atmospheric Physics)

In the study, we explored the mechanisms responsible for the formation and maintenance of the western North Pacific anomalous anticyclone (WNPAC). This is the part one, which focuses on the maintenance of the WNPAC during El Nino mature winter and following spring. Detailed moisture and moist static energy analyses and idealized numerical experiments indicates that the WNPAC is primarily maintained by the remote forcing from the equatorial central-eastern Pacific (CEP), while the local cold sea surface

temperature anomalies (SSTAs) play a secondary role. The key forcing mechanism is that the El Nino-related positive precipitation anomalies over the equatorial CEP generate twin Rossby-wave-like cyclonic anomalies straddling along the equator to the west. The northerly component to the western flank of the northern branch of the twin cyclonic anomalies advects dry (low moist enthalpy) air into the tropical WNP, which suppresses convection over there. Meanwhile, the enhanced convection over the equatorial CEP causes the entire tropical free tropo- sphere warming through Kelvin-wave-related dynamics. The warm anomalies tend to enhance the gross moist stability over the tropical WNP and thus also have contributions to the suppressed convection there. The suppressed convection further drives the Rossby-wave-like WNPAC to the northwest. In addition, two atmospheric internal positive feedbacks in situ, that is convection-cloud-radiative-forcing feedback and wind-moist enthalpy advection-convection feedback, tend to further amplify the remote forcing effects from the equatorial CEP to the WNPAC.

Heat storage of the West Pacific warm pool (WPWP) linked to global surface warming

Yuanlong Li, Fan Wang (Institute of Oceanology, Chinese Academy of Sciences)

Subsurface ocean heat redistribution plays an important role in modulating the Global surface warming rate. In this study, we show that the West Pacific warm pool (WPWP) region plays a critical role in determining global mean surface temperature (GMST) warming rate on interannual-to-decadal timescale. More (less) heat is stored in the thermocline of the WPWP when the GMST warming is decelerated (accelerated). The El Nino-Southern Oscillation (ENSO) and Interdecadal Pacific Oscillation (IPO) are the primary regimes controlling interannual and decadal variabilities of the WPWP heat storage, respectively, which is mainly through wind-driven ocean dynamical processes. Variations of the Pacific trade winds by ENSO and IPO causes anomalous heat transports of the upper-ocean circulation through oceanic wave adjustments. During El Nino or positive IPO condition, the weakened westward-flowing South Equatorial Current and the strengthened eastward-flowing North Equatorial Countercurrent lead to surface divergence and upwelling motion in the WPWP, which is partly attenuated by the weakened eastward Equatorial Undercurrent. In comparison, meridional heat transports by the western boundary currents, including the Indonesian through-flow toward the Indian Ocean, play a minor role. The opposite scenario occurs during La Nina and negative IPO condition.

Increasing persistent haze in Beijing: potential impacts of weakening East Asian winter monsoons associated with northwestern Pacific sea surface temperature trends

[1]Pei Lin, [2]Yan Zhongwei ([1]Institute of Urban Meteorology, China Meteorological Administration, Beijing, China, [2]2RCE-TEA, Institute of Atmospheric Physics, University of Chinese Academy of Sciences, Beijing, China)

Over the past decades, Beijing, the capital city of China, has encountered increasingly frequent persistent haze events (PHE). While the increased pollutant emissions are considered as the most important reason, changes in regional atmospheric circulations associated with large-scale climate warming also play a role. In this study, we find a significant positive trend of PHE in Beijing for the winters from 1980–2016 based on updated daily observations. This trend is closely related to an increasing frequency of extreme anomalous southerly episodes in North China, a weakened East Asian trough in the mid-troposphere, and a northward shift of the East Asian jet stream in the upper troposphere. These conditions together depict a weakened EAWM system, which is then found to be associated with an anomalous warm and high-pressure system in the mid-lower troposphere over the northwestern Pacific. A practical EAWM index is defined as the seasonal meridional wind anomaly at 850 hPa in winter over North China. Over the period 1900–2016, this EAWM index is positively correlated with the sea surface temperature anomalies over the northwestern Pacific, which indicates a wavy positive trend, with an enhanced positive phase since the mid-1980s. Our results suggest an observation-based mechanism linking the increase in PHE in Beijing with large-scale climatic warming through changes in the typical regional atmospheric circulation.

Does extreme El Niño have a different effect on the stratosphere in boreal winter than its moderate counterpart?

[1]Xin Zhou, [2]Jianping Li, [2]Fei Xie, [3]Quanliang Chen, [1]Ruiqiang Ding, [3]Yang Li ([1]Institute of Atmospheric Physics, Chinese Academy of Sciences, [2]Beijing Normal University, [3]Chengdu University of Information Technology)

A robust impact of El Niño on the Northern Hemisphere (NH) polar stratosphere has been demonstrated by previous studies, although whether this applies to extreme El Niño is uncertain. The time evolution of the response of the NH stratospheric vortex to extreme El Niño, compared with that to moderate Eastern Pacific El Niño, is addressed by means of composite analysis using the NCEPDOE reanalysis dataset from 1980 to 2016. Lead–lag analysis indicates that the El Niño signal actually leads the stratospheric response by ~2 months. Considering the time lag, the signal of December–January–February El Niño in the NH stratospheric vortex should mature in the February–March–April season (late winter/early spring). The patterns of circulation and temperature for late winter/early spring during extreme and moderate El Niño events are significant, exhibiting similar structure. The results are confirmed with the WAC- CM4 model, which is forced with observed SSTs of extreme and moderate El Niño in winter (December–January–February) to analyze the day-to-day propagation of their signals. Note that the magnitudes of the stratospheric responses are much larger in the case of extreme El Niño, as stronger upward propagation of planetary waves leads to a weaker northern polar vortex than during moderate El Niño events.

A new index for identifying different types of El Niño Modoki Events

[1]Xin Wang, [2]Wei Tang, [1]Chunzai Wang ([1]SCSIO, CAS, [2]First Institute of Oceanography, State Oceanic Administration)

El Nino Modoki events can be further classified into El Nino Modoki I and II in terms of their opposite impacts on southern China rainfall (Wang and Wang, J Clim 26:1322–1338, 2013) and the Indian Ocean dipole mode (Wang and Wang, Clim Dyn 42:991–1005, 2014). The present paper develops an index to identify the types of El Nino events. The El Nino Modoki II (MII) index is defined as the leading principle component of multivariate empirical orthogonal function analysis of the normalized El Nino Modoki index, Nino4 index and 850 hPa relative vorticity anomalies averaged near the Philippine Sea during autumn. The MII index exhibits dominant variations on interannual (2–3 and 4–5 years) and decadal (10–20 years) timescales. El Nino Modoki II events can be well identified by using the MII index value being larger than 1 standard deviation. Further analyses and numerical model experiments confirm that the MII index can portray the major oceanic and atmospheric features of El Nino Modoki II events. The constructed MII index along with previous ENSO indices can be used for classifying and identifying all types of El Nino events. Because of distinct impacts induced by different types of El Nino events, the implication of the present study is that climate prediction and future climate projection under global warming can be improved by using the MII index and other indices to identify the types of El Nino events.

ABSTRACT-ORAL-MAY 9

Interaction among three oceans: A review and perspective

Chunzai Wang (South China Sea Institute of Oceanology, CAS)

All of the Pacific, Atlantic and Indian Oceans play important roles in climate variability and climate change. The ocean-atmosphere coupling over these three oceans forms and produces various climate phenomena. As a result, the Pacific hosts the El Nino-Southern Oscillation (ENSO) and Pacific decadal oscillation (PDO); the Atlantic has the Atlantic Nino, Atlantic multidecadal oscillation (AMO) and Atlantic meridional overturning circulation (AMOC); and the Indian Ocean owns the Indian Ocean basin (IOB) mode and the Indian Ocean dipole (IOD) mode. These climate phenomena can all affect regional climate, extreme weather events and even global warming. Indeed, interaction among these three oceans together with the ocean-atmosphere coupling can initialize and modulate climate variability and then change our traditional views of climate and climate change. This talk synthesizes and summarizes climate variability and mechanisms induced by inter-ocean interaction during the past. Because this topic is relatively new and promising, it is hoped that further study and focus may greatly advance our understanding and prediction of global climate. This talk also discusses issues and questions that need to be ad- dressed in the future, providing a global perspective of climate.

Some Impacts of Indo-Pacific Warm Pool on Tropical Cyclone, Hadley circulation and Stratosphere Climate

[1,2]Jianping Li, [1]Qiuyun Wang, [4]Xin Zhou, [1,2]Juan Feng, [1]Fei Xie, [1]Cheng Sun, [3]Ruiqiang Ding, and [4]Wenshou Tian ([1]College of Global Change and Earth System Science, Beijing Normal University, Beijing 100875, China, [2]Laboratory for Regional Oceanography and Numerical Modeling, Qingdao National Laboratory for Marine Science and Technology, Qingdao 266237, China, [3]State Key Laboratory of Numerical Modeling for Atmospheric Sciences and Geophysical Fluid Dynamics, Institute of Atmospheric Physics, Chinese Academy of Sciences, Beijing 100029, China, [4]College of Atmospheric Sciences, Lanzhou University, Lanzhou 730000, China)

Some recent progresses of impacts of Indo-Pacific warm pool (IPWP) on tropical cyclone, Hadley circulation and stratosphere climate are reviewed from the following aspects:

- Modulation of tropical cyclogenesis location, frequency and tracks over the Indo–Western North Pacific by the intraseasonal Indo–western Pacific convection oscillation (IPCO) during the boreal extended summer.

- Long-term variation of the principal mode of Hadley circulation linked to SST over the indo-pacific warm pool.

- IPWP area expansion and its influences on tropical cold-point tropopause temperature (CPTT) variations.

- Influences of warm pool (WP) El Niño on tropical ozone changes since the 1980s.

- Effects of the IPWP on the stratosphere and comparison with the effect of ENSO.

Extreme cooling events during the past 620 years in the Western Pacific Region and its relationship with the Tibet Plateau

Yu Liu, Changfeng Sun, Qiufang Cai, Qiang Li, Ying Lei (Institute of Earth Environment, Chinese Academy of Sciences)

A complete understanding of the past millennium of temperature variations in the low-latitude region of East Asia suffers from a lack of annual or better resolution continuous temperature records. Here we present a tree-ring width based February-October mean temperature reconstruction from Taiwan, in the low-latitude region, at the time span from 1380 to 2007 AD. During the past six centuries, the highest temperature along with the largest variability appeared in the 20th Century, and is closely related to human

activities. A spatial correlation analysis reveals that this temperature reconstruction can represent the sea-land temperature change in the Western Pacific Region and also provides good contrast with the temperature series in the Tibet Plateau and elsewhere in the Northern Hemisphere. The Taiwan constructed temperature series, compared with other Asian temperature sequences is apparently higher, and includes several cold events. Therefore, we argue that the Asian constructed temperature series can represent that in the low-latitude region of East Asia.

Laminated diatom mat deposits from the tropical West Pacific linked to global carbon and silicon cycles during the Last Glacial Maximum

Tiegang Li, ZhifangXiong (Key Laboratory of Marine Sedimentology and Environmental Geology, First Institute of Oceanography, SOA, Qingdao 266061, PR China; Laboratory for Marine Geology, Qingdao National Laboratory for Marine Science and Technology, Qingdao 266061, PR China)

Giant marine diatoms, blooming or aggregating within deep chlorophyll maxima under stratified conditions, can generate substantial production and a large export flux of organic carbon from surface waters. However, their role in regulating glacial-interglacial variation in atmospheric pCO2 remains unclear.Herelaminated diatom mats (LDMs), found in a series of cores recovered in the eastern Philippine Sea(EPS), provide the unique document to test their role in global climate change, and carbon and siliconbiogeochemical cycles.

LDMs, deposited during the Last Glacial Maximum (LGM) in the EPS, are dominated by fragmented valves of the mat-forming diatom Ethmodiscus rex (Wallich) Hendey in near-monospecific assemblages. E. rex utilized eolian silicon, bloomed in the stratified seawater with the stimulation of dust Fe and then deposited to LDMs by the way of ‘fall dump’. E. rex used up all the silcic acid in surface water. With respect to the nutrient silicic acid, the surface EPS appeared under an oligotrophic sate during the LGM, the same as at present. Elevated levels of primary productivity during LDM deposition are comparable to high-productivity regions of the modern ocean, thus exerting an important impact on the distribution, transfer and burial of carbon in the ocean upper and deep waters. For the surface ocean, elevated primary productivity and, to a lesser extent,intensified water-column stratification resulted in the EPS switching from being a strong CO2 source during DC deposition to a weak CO2 sink during LDM deposition, which may have contributed to the drive of glacial-interglacial atmosphericpCO2 cycles.For the deep ocean, enhanced primary productivity and more reducing bottom waters during LDM deposition indicate a larger respired carbon pool in the deep EPS, which may have been part of a larger-scale modulation of atmospheric pCO2 variation during Pleistocene glacial-interglacial cycles by deep-ocean carbon storage.These observations highlight the potential role of giant marine diatoms in the sequestration of atmospheric CO2 during the LGM and, hence, supportchanges in biogenic silica fluxes as a potential cause of lower glacial atmospheric CO2.

The mid-Holocene East Asian monsoon, Walker circulation, and ENSO: Insights from PMIP simulations

Dabang Jiang, Zhiping Tian (Institute of Atmospheric Physics, Chinese Academy of Sciences, Beijing, China)

Using all available numerical experiments within the framework of the Paleoclimate Modeling Intercomparison Project (PMIP), we present an analysis of the East Asian summer (June–July–August) and winter (December–January–February) monsoons, Walker circulation, and El Niño–Southern Oscillation (ENSO) during the mid-Holocene approximately 6,000 calendar years ago. Compared to the preindustrial period, both the summer and winter monsoons were intensified over East Asia during the mid-Holocene, which was due to an orbitally driven enhancement of land–sea thermal contrast and in turn sea level pressure gradient between the East Asian continent and adjacent oceans. The annual mean of the Pacific Walker circulation strengthened and shifted westward for its western edge and center, which

were closely related to an overall increase in the equatorial Indo-Pacific east–west sea level pressure difference and low-level trade winds over the equatorial Pacific. Consistent with geologic records, the simulated mid-Holocene ENSO amplitude was weaker than at preindustrial. Such a weakening was primarily attributed to the decrease in the Bjerknes thermocline feedback, while the meridional advective feedback also played a role.

Atmospheric Secondary Circulation response to ocean eddy in the winter Kuroshio Extension region

Qinyu Liu, Longjing Chen and Yinglai Jia (Ocean University of China)

In the winter Kuroshio Extension region, the atmospheric response to oceanic eddies is studied. The detected eddies are mostly under the force of northwesterly wind, with the sea surface temperature (SST) anomaly located within the eddy. According observation data we found that most response sights (about 60%) is characterized by significant sea surface wind convergence and divergence at the edge of oceanic eddy and a vertical secondary circulation (SC) aloft, which is called by the “Vertical Mixing Mechanism” (VMM) type response. But other response sights to eddy (about 10%) is characterized by surface wind divergence, sea level pressure and vertical speed of the SC anomaly in the oceanic eddy center, which is called by the “Pressure Adjustment Mechanism” (PAM) type response. Numerical experiments provided when relative speed between the background sea surface wind and oceanic eddy is less 0.5m/s, atmosphere response to eddy can transport from VMM type to PAM type in 6 hours. For VMM type response, eddy-driven Asymmetry atmospheric SC: the top of SC on anticyclonic eddies (AEs) is over 500 hPa, but those on cyclonic eddies (CEs) are limited to 700 hPa, because the climbing process is corresponding to larger latent heat release in atmosphere boundary layer due to the upward moisture transport when northwesterly wind passes the warmer center of AE. This result points out that the Eddy-driven SC is not only in atmosphere boundary layer, but also in free atmosphere and this response is Asymmetry.

Coupling wheels of East Asian summer monsoon and its diversity on interannual time scale

Congwen Zhu (Chinese Academy of Meteorological Sciences)

The East Asian summer monsoon (EASM) is characterized by a three-dimensional coupling wheels in circulation regime, which can be described as the coactions of low-level western Pacific anticyclone (WPA), the upper-level South Asian high (SAH), and the Mongolian cyclone (MC) over North Asia. They act as three coupled dynamical wheels via the upper-level westerly jet over North China and the vertical shear of the meridional monsoonal flow over Southeast Asia. In present study, we applied the EOF and K-means cluster analysis and revealed the dominant modes of EASM in wind and rainfall anomalies during 1979–2015. The first mode shows a coupling wheels between MC and SAH with a passive response of WPA. The second mode, however, is featured by the coupling wheels between WPA and SAH with a passive response of MC. These two distinct coupling modes revealed the diversity of EASM regimes on inter-annual time scale. The strong or weak EASM correspond two distinct circulation regimes, implying that a perfect prediction of monsoon index may causes the failure of rainfall prediction.

The Interannual Dominant Co-variation Mode of Boreal Summer Monsoon Rainfall during 1979–2014

Yuqian Hao, Boqi Liu, Congwen Zhu, Shuangmei Ma (Chinese Academy of Meteorological Sciences)

The boreal summer monsoon (BSM), which includes the monsoons over India (IND), the western North Pacific (WNP), East Asia (EA), North America (NAM) and North Africa (NAF), shows prominent interannual variation (IAV) in summer precipitation and affects the areas with the largest populations in the world. In the present, we used the EOF analysis to extract the BSM dominant co-variation mode during 1979–2014. This mode is featured by the out-of-phase rain- fall IAV over the WNP to the other BSM members. The BSM co-variation mode is closely associated with the upper- and lower-level coupled circulations, which are characterized by two anomalous zonal circulations over the tropical oceans coupled near the dateline and an abnormal meridional cell over the WNP and EA regions, respectively. Furthermore, the strength of this mode depends on the phase relationship of rainfall IAV between the WNP and NAM monsoon regions, which is modulated by the seasonal evolution of ENSO events and its resultant SSTAs in tropical Indian Ocean (TIO). The weaker mode is accompanied by the in-phase rainfall IAV between these two regions, along with the persisting ENSO events and stronger SSTA in the TIO from winter to summer. While in the years with fast-decaying ENSO events and the related weaker TIO SSTA, the out-of-phase rainfall IAV between the WNP and NAM re- gion takes place to enhance this mode. A series of AGCM sensitivity experiments could reproduce the anomalies of atmospheric circulation related to the distinct seasonal evolution of ENSO events.

Anthropogenic Pb in the Western North Pacific Kuroshio Region

[1]Ed Boyle, [2] Mengli Chen ([1]Earth Atmospheric and Planetary Sciences, Massachusetts Institute of Technology, Cambridge MA USA 02139, [2]EOS, Nanyang Technological University, Singapore 639798)

There are relatively few data for anthropogenic Pb concentrations in the western North Pacific Ocean, although there has been a very strong temporal evolution in Pb inputs during the past ~50 years, with Pb gasoline emissions rising and then falling, but totalh Pb emissions rising due to increased industrialization and coal consumption (e.g. see 170 year coral history from the South China Sea reported by Chen et al., Geophys. Res. Lett. 43:4490). The transition between these sources is expected to have been accompanied by significant changes in Pb isotope composition, although there is even less data than there is for Pb concentrations. Here we report data for Pb concentrations from 6 stations in the Kuroshio Current occupied by the Japanese research vessel Hakuho Maru in October 2015 and compare them to other information on Pb in the western North Pacific. Carrying water from further south with less industrial influence, Pb concentrations in the Kuroshio are ~50 pmol/kg in the surface waters increasing to ~65 pmol/kg in subsurface waters at 200-500m depth, where higher Pb water from further north is transported following subduction. Below that, Pb concentrations decrease to 15-30 pmol/kg in the 1000-3000m depth range, although near the bottom of two high-turbidity stations the Pb concentrations are as low as ~10 pmol/kg, likely due to adsorption of particle-reactive Pb on resuspended sediments.

The Ocean's Biological Carbon Pump – Studies in the North Pacific as part of EXport Processes in the Ocean from Remote Sensing (EXPORTS)

Ken Buesseler (Woods Hole Oceanographic Institution)

Ocean ecosystems play a critical role in the Earth's carbon cycle and the quantification of their impacts for both present conditions and for predictions into the future remains one of the greatest challenges in oceanography. The goal of the EXport Processes in the Ocean from Remote Sensing (EXPORTS) Science Plan is to develop a predictive understanding of the export and fate of global ocean net primary production (NPP) and its implications for present and future climates. The first US EXPORTS field study will take place at the time-series station Papa in the NE Pacific in August 2018. This two ship process study will include a combination of ship and robotic field sampling, satellite remote sensing and numerical modeling. Prior studies suggest that the biological pump is generally more efficient at transferring organic C to the deep sea at the NW Pacific time-series K2 site than at station Papa. The reasons for these differences is less well known. The EXPORTS goals and field plans can be seen as a

model for future international studies at other sites. Our understanding of the mechanisms that control the export of carbon from the euphotic zone as well as its fate in the underlying “twilight zone” will improve by studying contrasting ecosystems and seasonal variations in export processes.

Deep oceans may acidify faster than anticipated due to global warming

[1,2]Chen-Tung Arthur Chen, [1,3]Hon-Kit Lui, [1]Chia-Han Hsieh, [4]Tetsuo Yanagi, [5]Naohiro Kosugi, [5]Masao Ishii and [6]Gwo-Ching Gong ([1]Department of Oceanography, National SunYat-sen University, Kaohsiung 80424, Taiwan. [2]State Key Laboratory of Satellite Ocean Environmental Dynamics, Second Institute of Oceanography, Hangzhou, China. [3]Taiwan Ocean Research Institute, National Applied Research Laboratories, Kaohsiung 80143, Taiwan. [4]Research Institute for Applied Mechanics, Kyushu University, Kasuga 816-8580, Japan. [5]Meteorological Research Institute, Japan Meteorological Agency, Tsukuba, 305-0052, Japan. [6]Institute of Marine Environmental Chemistry and Ecology, National Taiwan Ocean University, Keelung 20224, Taiwan.)

Oceans worldwide are undergoing acidification due to the penetration of anthropogenic CO2 from the atmosphere. The rate of acidification generally diminishes with increasing depth. Yet, slowing down of the thermohaline circulation due to global warming could reduce the pH in the deep oceans, as more organic material would decompose with a longer residence time. To elucidate this process, a time-series study at a climatically sensitive region with sufficient duration and resolution is needed. Here we show that deep waters in the Sea of Japan are undergoing reduced ventilation, reducing the pH of seawater. As a result, the acidification rate near the bottom of the Sea of Japan is 27% higher than the rate at the surface, which is the same as that predicted assuming an air–sea CO2 equilibrium. This reduced ventilation may be due to global warming and, as an oceanic microcosm with its own deep- and bottom-water formations, the Sea of Japan provides an insight into how future warming might alter the deep-ocean acidification.

Upper Ocean Biogeochemistry in the Ocean Desert

Minhan Dai, Chuanjun Du, Zhiyu Liu and Zhimian Cao (State Key Laboratory of Marine Environmental Science, Xiamen University, China)

The oligotrophic ocean, mostly located in subtropical regions occupies ~40% of the Earth surface and has been conventionally regarded as an ocean desert. It is characterized by permanent stratification, nutrient depletion and extremely low net biological production, and hence, contributes little to carbon export from surface to deep waters at per unit area. Emerging evidence has shown that this oceanic system has a much larger dynamic range of nutrient inputs from different sources in addition to those from depth. These differently sourced nutrients with differing stoichiometry may stimulate biological productions in different community structures and drive the carbon export at various depth horizons within the sunlit euphotic zone (EZ). Hence, the EZ is better characterized by a two-layered structure with a nutrient nutrient-depleted layer (NDL) above the nutricline and a nutrient replete layer (NRL) across the nutricline to the base of the EZ. Based on simultaneous turbulence microstructure and high-resolution chemical measurements, we quantified diapycnal fluxes of nitrogen, phosphorus, silicon, and carbon in the oligotrophic South China Sea showing a negligibly low diapycnal dissolved inorganic nitrogen (DIN) flux in the NDL where other nutrient supplies sustain the new production. Here, higher phosphate and silicate fluxes relative to DIN than Redfield stoichiometry further indicate N-limited biological productivity and additional removal of DIN by diatoms. In the NRL, the DIN flux is sufficiently large in supporting the export production therein. Here, higher dissolved inorganic carbon (DIC) flux relative to DIN than Redfield stoichiometry further infers DIC excess in the upper ocean of oligotrophic nature. Considering the new understanding of the biogeochemistry of the oligotrophic ocean, we attempt to propose an improved framework of nutrient-determined and biologically mediated carbon export in the ocean desert.

Deep ventilation of the Southern Ocean and deglacial CO2 rise

Yongsheng Xu, Chao Huang (Key Laboratory of Ocean Circulation and Waves, Institute of Oceanology, Chinese Academy of Sciences)

Increasing evidence shows that release of CO2 from the Southern Ocean was blocked during last ice age, leading to the sequestration of an aged, car- bon-rich water mass in the abyssal ocean. Dissipation of this CO2 reservoir should help us to understand the glacial termination, but its mechanism is still unclear. Paleoclimatic and palaeoceanographic data are used to trace the change of the deep ventilation of the Southern Ocean during the last glacial-interglacial transition, and modern observation network is used to investigate the deep ventilation at the present age. We find that the deep across- density upwelling in the modern Southern Ocean can rapidly dissipate the presumed old carbon reservoir within about four thousand years, twenty times shorter than the time span of the last ice age. We propose a physical mechanism that can reconcile a wide range of debates and explain seemingly disparate observations in the last deglaciation.

Remote impact on decadal variability of nutrients and plankton dynamics in the Kuroshio Extension

[1]Pengfei Lin, [1]Jinfeng Ma, [2]Fei Chai ([1]Institute of Atmospheric Physics, Chinese Academy of Sciences, [2]Second Institute of Oceanography, State Oceanic Administration)

The Pacific decadal climate variability not only affects on physical ocean conditions, but also has impact on marine ecosystems in the North Pacific Ocean. The mechanisms that affect decadal variations of nutrients and plankton dynamics in the Kuroshio Extension (KE) are investigated by comparing satellite observation and a biological-physical coupled model simulations. The biological-physical coupled model is based on Regional Ocean Model System (ROMS) and Carbon, Silicate, and Nitrogen Ecosystem (CoSiNE) for the entire Pacific Ocean. The ROMS-CoSiNE model captures the spatial distribution and decadal variation of the key biological variables in the Northwest Pacific, which includes nutrients, nutrient transports, phytoplankton and zooplankton bio- mass in the upper ocean. The decadal variation of nutrients and plankton dynamics in the Northeast Pacific is mainly caused by the westward-propagating Rossby waves that originate from the central and eastern North Pacific.

Eco-physiological Effects of Ocean Acidification on Primary Producers

Kunshan Gao (Xiamen University)

The oceans are taking up over one million tons of fossil fuel CO2 per hr, but, have been acidified by 30% since the industrial revolution, and will be further acidified by 150% (IPCC RCP8.5) by the end of this century. Typical chemical changes associated with the ocean acidification (OA) are increased concentrations of pCO2、H+ and HCO3- and decreased concentration of CO32- and CaCO3 saturation state, with different extents in different regions or waters.

When exposed to CO2 concentrations projected for the end of this century, surface-water phytoplankton assemblages in the South China Sea (SCS) responded with decreased photosynthetic carbon fixation, increased non-photochemical quenching (NPQ) and declined abundance of diatoms. When diatoms were grown at different CO2 concentrations under varying levels (5-100%) of solar radiation, growth rates in the high CO2-grown cells were inversely related to light levels, and exhibited reduced thresholds at which PAR becomes excessive, leading to higher NPQ. That is, elevated CO2 concentrations (lowered pH) impaired the specific growth rate of diatoms at high levels, but enhanced it at low to moderate levels of solar irradiances. These puzzling results are explained as follows: elevated CO2 concentrations down-regulate the uptake capacity (CO2 concentrating mechanisms) of the cells for dissolved in- organic carbon, so that energy, which is used for the active uptake mechanism, is

saved and the diatoms' growth at low irradiances is augmented; on the other hand, at high levels of solar radiation, the saved light energy could add to enhance photoinhibition, resulting in reduced growth rate and enhanced NPQ.

Additionally, OA increases contents of phenolic compounds in phytoplankton and in zooplankton assemblages fed with OA-grown phytoplankton cells. The observed accumulation of the toxic phenolic compounds in primary and secondary producers can have profound consequences for marine ecosystem and seafood quality, with a possibility that fisheries industries could be influenced due to progressive ocean changes.

(based on the results published at Nat Clim Change, Nat Comm, for the full papers: http://mel.xmu.edu.cn/staff_publications.asp?tid=35)

Subduction of the North Pacific Subtropical Mode Water and its physical and biogeochemical impacts revealed by 50-year long observations along 137ºE

Eitarou Oka (Atmosphere and Ocean Research Institute, The University of Tokyo)

The 137ºE repeat hydrographic section of the Japan Meteorological Agency across the western North Pacific was initiated in 1967 as part of the Cooperative Study of the Kuroshio and Adjacent Regions and has been continued biannually in winter and summer for more than 50 years. The publicly available data from the section have been widely used to reveal seasonal to decadal variations and long-term changes of currents and water masses, biogeochemical and biological properties, and marine pollutants in relation to climate variability such as the El Niño−Southern Oscillation and the Pacific Decadal Oscillation. For the detailed history and scientific achievements of the section, please see our recently published review paper (Oka et al., J. Oceanogr., in press).

In my talk, after introducing the brief history of the 137ºE section, I present two topics related to the North Pacific Subtropical Mode Water (STMW) revealed from the section. The first topic is the decadal variability of STMW subduction and its impact on biogeochemistry (Oka et al., 2015, J. Oceanogr.). Argo profiling float data during 2005−2014 clarified decadal variability of STMW in relation to that of the Kuroshio Extension (KE) system, which is associated with the Pacific Decadal Oscillation. Specifically, the formation and subduction of STMW decreased (increased) during unstable (stable) KE periods. This affected not only physical but also biogeochemical structure at the 137ºE section with a lag of 1 year. After 2010, enhanced subduction of STMW during the stable KE period consistently increased dissolved oxygen, pH, and aragonite saturation state and decreased potential vorticity, apparent oxygen utilization, nitrate, and dissolved inorganic carbon.

The second topic is the rapid freshening in the upper main thermocline/halocline in the western subtropical gyre, which began in mid-1990's and persisted for the last 20 years (Oka et al., 2017, J. Oceanogr.). This freshening trend observed at the 137ºE section originated in the winter mixed layer in the KE region and was transmitted southwestward to 137ºE 1−2 years later in association with the subduction and advection of STMW. The mechanism of surface freshening in the source region is unclear and needs to be clarified.

Nitrous Oxide in the Southwest Pacific Ocean, an isotopic approach

[1]Muhammed Nayeem Mullungal, [2]Russell D Frew, [2]Robert Van Hale, [2]Cliff S Law ([1]Qatar University,University of Otago,New Zealand, [2]University of Otago)

Nitrous oxide (N2O) is a powerful greenhouse gas and a precursor of stratospheric ozone depletion. Although a 30% of natural emissions of N2O to the atmosphere comes from the ocean, still there is a paucity of data concerning the oceanic distribution and emissions. In the ocean, N2O is majorly produced through nitrification and denitrification; however, there exist uncertainties about the major

pathways responsible for its production. Here we present sur- face and vertical profiles of N2O that include the highest reported N2O concentrations in Southwest Pacific surface waters surrounding New Zealand. Regional flux estimates indicate a total annual N2O emission of 1.85 Tg N2O/yr from SWP. It is also estimated that the contributions to the global open ocean flux (3.2- 3.8 Tg N/yr, IPCC) is 29-34 % and to the global oceanic Flux (5.4 Tg N/yr, IPCC) is 24 % from the study regions. The contribution from the New Zealand Coastal regions to the global continental shelf emissions (1.5 Tg N/yr, IPCC) were estimated to 6 %. The dissolved oxygen, nutrients and stable isotope results suggest that the nitrification process (through NH2OH followed by NO oxidation) are mainly responsible for the N2O production. It was further confirmed by 15N labelled isotope incubation experiments. An additional contribution to N2O source from nitrifier denitrification at subsurface layers were evident from the intramolecular distribution of isotopomers of 15N (Site preference).

Variability of particle export in the northwestern Pacific

[1]Peng Xiu, [2]Fei Chai ([1]South China Sea Institute of Oceanology, [2]Second Institute of Oceanography)

The variability and controlling mechanism of particle sinking flux in the northwestern Pacific were investigated by using data from a moored sediment trap and a coupled physical-biogeochemical model. The sediment trap was located at the S1 location (30oN, 145oE) and the particle flux data collected during 2010-2013 at three depths (200 m, 500 m, and 4810 m) were analyzed. Strong seasonal variability in particulate organic carbon (POC) flux was found at all three depths, in a relatively consistent pattern with vertical fluxes of particulate iron, opal, and lithogenic matters. In order to elucidate dominant mechanisms, we incorporated the iron cycling process into an existing biogeochemical model, CoSiNE, and coupled it with a one-dimensional physical model con- figured at the S1 location. This new CoSiNE-Fe model can explicitly simulate iron and ligand dynamics, as well as the dust deposition process. The model results and sensitivity studies indicate that dust deposition into the northwestern Pacific may play an important role in driving the vertical POC export at depth.

ABSTRACT-POSTER-SESSION 1 & 6

P1-1 Modelling the Seasonal Cycle of the North Equatorial Current Bifurcation in a Regional Model – Role of Eastern Boundary Conditions

Bingrong Sun, Zhaohui Chen, Lixin Wu (Physical Oceanography Laboratory/CIMST, Ocean University of China and Qingdao National Laboratory for Marine Science and Technology, Qingdao, China)

The role of eastern boundary conditions in modelling the seasonal cycle of North Equatorial Current Bifurcation Latitude (NBL) is studied based on a simplified reduced-gravity model and Hybrid Coordinate Ocean Model (HYCOM). The seasonal cycle of modeled NBL is significantly affected by eastern boundary conditions in regional model such as the locations of boundary as well as the data input at the boundary.

It is demonstrated that the seasonal cycle of NBL can be well reproduced by regional models wherever the eastern boundary is as long as the boundary conditions are nested from respective Basin Run (full Pacific). However, the seasonal variations of NBL in terms of its south-north migration and phase are not properly simulated if we apply the reanalysis products like SODA as boundary conditions despite that the reanalysis data is much closer to observations. The bad performance from SODA Run may be attributed to the lack of self-consistency in parameter space which leads to dynamical mismatch between boundary condition and the numerical system. This kind of boundary/forcing mismatch will enhance numerical noises and eventually disorder the simulated seasonal variations of NBL at western boundary.

Further experiments indicate that the modelled seasonal cycle of NBL is less sensitive to the data input at boundary if regional model extends farther east- ward even we use reanalysis products as the boundary input. Considering the dominant dynamic process which affect seasonal variations of NBL, the regional models are suggested 1) set open boundary far away from the western boundary as much as possible, or 2) use the nested boundary condition provided by the respective basin runs if we want to get a more realistic NBL seasonal cycle. This can be further extended to the simulations of low-latitude western boundary currents.

P1-2 Subthermocline eddy-induced mixing of the interhemispheric intermediate waters observed east of the Philippines

Feng Nan, Fei Yu (Institute of Oceanology, Chinese Academy of Sciences)

Both sporadic observations and modeling studies suggest that there exist energetic subthermocline eddies east of the Philippines, where the interhemispheric waters meet. However, the eddy effect on water masses mixing has never been observed. Here, based on mooring and buoy data deployed in the front region of the interhemispheric water masses, we show for the first time that subthermocline eddy acts as “underwater mixer” enhancing isopycnal mixing of the North and South Pacific Intermediate Waters. Subthermocline eddies have typical swirl speeds of 0.1~0.4 m s−1 at 200~600 m depth with periods of ~90 days. Stirred by the energetic subthermocline eddies, intermediate water changes indicated by salinity variations at 26.3~27.1 σθ also has a period of ~90 days, lagging the eddy speed by 8 days. Horizontal eddy mixing length (λ) and diffusivity (κh) are estimated using a mixing-length frame- work. Maximum λ and κh appear at surface, decrease with depth, and exhibit subthermocline maxima at ~26.8 σθ. The estimated κh based on observations can be used to parameterize eddy stirring in this region for climate model.

P1-3 The vertical structure and variability of the western boundary currents east of the Philippines: case study from in-situ observations from December 2010 to August 2014

Fujun Wang (Institute of Oceanology, Chinese Academy of Sciences)

The vertical structure and variability along the western boundary of Philippines are investigated using direct observations from acoustic Doppler current profiler (ADCP), Doppler volume sampler (DVS) and Aanderaa Seaguard, which are mounted on a subsurface mooring deployed at 8°N, 127°3′E. In climatology, the southward Mindanao Current (MC) and northward Mindanao Undercurrent (MUC) play a dominant role in the upper layer. The mean currents at 1200 and 3500 m flow northward, whereas those at 2500 and 5600 m flow equatorward. The power spectrum density (PSD) shows that an intraseasonal signal of 60-80 days is common from sea surface to the bottom. The semiannual signals are strongest in the MUC layer, and then its amplitude decreases with depth to 3500 m. The seasonal variability at 2500 and 5600 m is similar with each other, suggesting a southward current in winter and northward flow in autumn. The current at 3500 m exhibits a northward direction in spring and the southward in winter. In addition, the linear correlations between mooring data and altimetry products indicated that the variations of surface meridional currents along the western boundary of Pacific Ocean could reach to the bottom via low frequency processes. The vertical mode decomposition for observations indicates that the first four modes could effectively capture the original data. The relative contributions of different modes exhibit seasonal variability. The first baroclinic mode plays a dominant role in spring and autumn. In winter and summer, its contribution decreases and becomes comparable with the other modes.

P1-4 Seasonality of the Mindanao Current/Undercurrent System

[1]Qiuping Ren, [1]Yuanlong Li, [1]Fan Wang, [1]Chuanyu Liu, [2]Fangguo Zhai ([1]Key Laboratory of Ocean Circulation and Waves, Institute of Oceanology, Chinese Academy of Sciences, Qingdao, China, [2]College of Oceanic and Atmospheric Sciences, Ocean University of China, Qingdao, China)

Seasonality of the Mindanao Current (MC)/Undercurrent (MUC) system is investigated using moored acoustic Doppler current profiler (ADCP) measurements off Mindanao (8°N, 127.05°E) and ocean model simulations. The mooring observation during December 2010-August 2014 revealed that the surface-layer MC between 50-150 m is dominated by annual-period variation and tends to be stronger in spring (boreal) and weaker in fall. Prominent semiannual variations were detected below 150 m. The lower MC between 150-400 m is stronger in spring and fall and weaker in summer and winter, while the northward MUC below 400 m emerges in summer and winter and disappears in spring and fall. In-phase and out-of-phase current anomalies above and be- low 150 m were observed alternatively. These variations are faithfully reproduced by an eddy-resolving ocean model simulation (OFES). Further analysis demonstrates that seasonal variation of the MC is a component of large-scale upper-ocean circulation gyre, while current variations in the MUC layer are confined near the western boundary and featured by shorter-scale (200-400 km) structures. Most of the MC variations and approximately half of the MUC variations can be explained by the 1st and 2st baroclinic modes and caused by local wind forcing of the western Pacific. Semiannual surface wind variability and superimposition of the two baroclinic modes jointly give rise to the enhanced subsurface semiannual variations. The pronounced mesoscale eddy variability in the MUC layer may also contribute to the seasonality of the MUC through eddy-current interaction.

P1-5 Statistical analysis of Mesoscale eddies in North Equatorial Countercurrent area

Mingkun Lv (Institute of Oceanology, Chinese Academy of Sciences)

With the development of ocean technology, more and more mesoscale ocean processes have been revealed. Mesoscale eddies are an important mesoscale ocean process that has been the subject of

much research in recent decades. However, research on the spatial distribution, seasonal variation, and movement characteristics of mesoscale eddies in the tropical northwestern Pacific is lacking. In this study, we statistically analyzed the spatial distribution of eddies in the northwestern tropical Pacific using the eddy dataset provided by Chelton. We found that more eddies are generated in the North Equatorial Countercurrent (NECC) area (A zone, 120°–180°E, 4°–6°N) where less research effort has been focused. Moreover, in this area, the eddy radii, amplitudes, lifecycles, and nonlinear intensities are larger, the movement distances are farther, and the meridional eddy movement distances obey a gamma distribution. Most eddies move southward in the region close to the western boundary, and most move northward far away from the western boundary. The quantity of eddies generated in NECC area exhibits obvious seasonal variation, which is mainly affected by the shear intensity of the currents. At the same time, eddy formation is affected by the ENSO in this area, and its mechanism requires further study.

P1-6 Atlantic Multi-decadal Oscillation Controls the North Pacific Subtropical Mode Water Variability

[1]Baolan WU, [1]Xiaopei LIN, [2]Lisan YU ([1]Ocean University of China, [2]Department of Physical Oceanography Woods Hole Oceanographic Institution Woods Hole)

Mode waters play an important role in contributing to mass, heat, nutrient transport and climate variability. Previous studies attribute the decadal variability of North Pacific Subtropical Mode Water (NPSTMW) to the Pacific Decadal Oscillation (PDO). Here we show that the decadal to multi-decadal variability of NPSTMW is more related with the Atlantic Multi-Decadal Oscillation (AMO) rather than PDO. The NPSTMW temperature has very good correlation with AMO for 1945-2012, moderate during 1950-1960, relatively lower during 1975-1985 and higher during 2000-2010. The PDO only has good correlation with the NPSTMW temperature after 1976-77 regime shift. Besides, the core depth of NPSTMW also shows consistent variability with AMO. Although PDO is dominant in the North Pacific decadal variability, it has little impact on sea surface temperature (SST) anomaly in the Western Pacific Ocean, where it is the formation and subduction region of NPSTMW. The AMO could induce strong SST anomaly through the tele-connection as revealed by recent study (Sun et al., 2017). This is important for the decadal prediction since mode water is the climate memory.

P1-7 Projected Changes of the Low-latitude North-western Pacific Wind-driven Circulation under Global Warming

[1]Jing Duan, [2]Zhaohui Chen, [2]Lixin Wu ([1]Institute of oceanology Chinese adcademy of sciences, [2]Ocean university of China)

Based on the outputs of 25 models participating in the Coupled Model Inter comparison Project Phase 5, the projected changes of the wind-driven circulation in the Low-latitude north-western Pacific are evaluated. Results demonstrate that there will be a decrease in the mean transport of the North Equatorial Current (NEC), Mindanao Current, and Kuroshio Current in the east of the Philippines, accompanied by a seasonal south-north migration amplitude. Numerical simulations using a 1.5-layer nonlinear reduced-gravity ocean model show that the projected changes of the upper ocean circulation are predominantly determined by the robust weakening of the north-easterly trade winds and the associated wind stress curl under the El Niño-like warming pattern. The changes in the wind forcing and intensified upper ocean stratification are found equally important in amplifying the seasonal migration of the NBL.

P1-8 The observed 80-100 days variations of the subthermocline current east of Luzon Island

Qian Ma (Ocean University of China)

An obvious 80-100 days period of meridional velocity was found in the thermocline at the Luzon Undercurrent (LUC), origin of Kuroshio (18°N,122°E, east of the Luzon Island) by analyzing the mooring data from November,2010 to October,2012. It is not affected by the surface water and may be related to sub-thermocline eddies. To get more evidence to prove this assumption and find the resource of this phenomenon, a list of long-term model data are analyzed. The 80-100 days period is found in the hycom data at the same position and the velocity of CFS matched well with the mooring data. This phenomenon is believed to play an important role in heat, salt, and freshwater transport in the region and it even affects the Kuroshio.

P1-9 Intraseasonal variability in deep current and temperature induced by Topographic Rossby Waves

[1]Qiang Ma, [1]Jianing Wang, [2]Stephen Riser, [1]Fan Wang ([1]IOCAS, [2]University of Washington)

Direct measurements of deep current and temperature from moorings deployed near the channel between East and West Mariana Basins revealed intraseasonal (30-90 days) intensified fluctuations towards the bottom. These bottom intensified fluctuations were analyzed to be induced by Topographic Rossby Waves (TRWs) since the vertically coherence with similar phase were shown in each first frequency domain empirical orthogonal function mode, and the major axis amplitude of currents and the root-mean-square of isothermal depth could be well fitted by the wave solution function. Energetic surface eddies could dominant the whole water column and supplant TRW motions, and the vertical trapping scales of TRWs inferred from the currents and temperature were comparative only if the time series of eddy part was removed. TRWs are related with the topographic roughness, and may play a significant role in deep ocean circulation and water-exchange between different layers.

P1-10 Horizontal and vertical thermohaline structure of mesoscale eddies in the WBCs regions of the Northern Hemisphere

Rou Hu (Ocean University of China)

Satellite measurements from the Soil Moisture Active Passive (SMAP) and the Optimum Interpolation Sea Surface Temperature (OISST) acquired from March 2015 to April 2017 in the WBC regions of the North Pacific and the North Atlantic are used to reveal the sea surface salinity (SSS) and sea surface temperature (SST) structure of mesoscale eddies with an unprecedented space and time resolution. Combined with in situ Argo profile measurements and satellite-derived surface currents, SMAP and OISST observations are shown to coherently delineate salty- (warm-) and fresh- (cold-) core eddies pinching off from the WBCs. By comparing the three WBC regions (the Oyashio Extension, Kuroshio Extension and Gulf Stream), three distinctive features are shown. First, salinity anomaly is proved to be a better indicator of the existence and characteristic of the eddy, especially in summer. Second, unlike the Gulf Stream, the vertical salinity anomalies change their plus-minus below a certain depth in the OE and KE as a result of salinity minimum of the North Pacific Immediate Water (NPIW). Lastly, the seasonal variation of the SST and SSS anomalies in the GS are much weaker than those in OE and KE. Relations between SSH, SSS, SST are also examined in the above regions. Summertime SST in all regions are not aligned with SSH due to surface heat flux. SSH in the OE presents the weakest seasonal variation than the others, because of strong density compensation between the temperature and salinity variations. The relations between SSS and SSH reveal different mechanisms affecting SSS in different regions. The SSS of KE eddies is mainly controlled by oceanic dynamics since its SSS and SSH show perfect consistence. SSS front in the GS is found to be slightly displaced (by ~1-3°) north of the SSH front during the coldest months, corresponding to the strongest density gain as cold and dry

continental air masses impinge upon the warmer waters of the GS. SSS front of the OE is much better aligned with SSH in upstream than downstream, indicating that ocean dynamics is a less important process affecting the SSS of downstream.

P1-11 Topographic Beta Spiral and Onshore Intrusion of the Kuroshio Current

Dezhou Yang (Institute of Oceanology, Chinese Academy of Sciences)

The Kuroshio intrusion plays a vitally important role in carrying nutrients to marginal seas. However, the key mechanism leading to the Kuroshio intrusion remains unclear. In this study we postulate a mechanism: when the Kuroshio runs onto steep topography northeast of Taiwan, the strong inertia gives rise to upwelling over topography, leading to a left-hand spiral in the stratified ocean. This is called the topographic beta spiral, which is a major player regulating the Kuroshio intrusion; this spiral can be inferred from hydrographic surveys. In the world oceans, the topographic beta spirals can be induced by upwelling generated by strong currents running onto steep topography. This is a vital mechanism regulating onshore intruding flow and the cross-shelf transport of energy and nutrients from the Kuroshio Current to the East China Sea. This topographic beta spiral reveals a long-term missing link between the oceanic general circulation theory and shelf dynamic theory.

P1-12 Response of surface winds to sea surface temperature perturbations in the Kuroshio-Oyashio Extension region

[1]Jingjing He, [1]Xiaopei Lin, [2]Lisan Yu ([1]Physical Oceanography Laboratory/CIMST, Ocean University of China and Qingdao National Laboratory for Marine Science and Technology, [2]Department of Physical Oceanography, Woods Hole Oceanographic Institution)

The response of the surface wind speed to the sea surface temperature (SST) change in the Kuroshio-Oyashio Extension (KOE) frontal region is studied using 10 years (2002-2011) high-resolution satellite observations and reanalysis data. The local effect of the SST perturbation on the marine atmospheric boundary layer (MABL) height is investigated using the atmospheric sounding observations. Results show that the mean MABL structure is anchored by the SST fronts with higher over the south than the north sides. Moreover, more active warm eddies are found in the north side of SST fronts. The asymmetric distribution of the MABL height and oceanic eddies could explain the observed strong positive SST-surface wind speed correlations (>= 0.4) in the north of 36°N. The SST perturbations induced by the strong warm eddies are large enough to trigger the momentum vertical mixing in MABL to accelerate surface wind speed. In comparison, the MABL is high and the eddy-induced air-sea temperature perturbation is small, so the mesoscale positive SST-surface wind speed correlations are not significant in the south of 36°N.

P1-13 Response of the Kuroshio Extension Path State to Near-Term Global Warming in CMIP5 Experiments with MIROC4h

[1]Rui Li, [2]Zhao Jing, [2]Zhaohui Chen, [2]Lixin Wu ([1]Institute of Oceanology, Chinese Academy of Sciences, [2]Ocean University of China)

In this study, responses of the Kuroshio Extension (KE) path state to near-term (2006−2035) global warming are investigated using a Kuroshio-resolving atmosphere-ocean coupled model. Under the representative concentration pathway 4.5 (RCP4.5) forcing, the KE system is intensified and its path state tends to move northward and becomes more stable. It is suggested that the local anticyclonic

wind stress anomalies in the KE region favor the spin-up of the southern recirculation gyre, and the remote effect induced by the anticyclonic wind stress anomalies over the central and eastern mid-latitude North Pacific also contributes to the stabilization of the KE system substantially. The dominant role of wind stress forcing on KE variability under near-term global warming is further confirmed by adopting a linear 1.5-layer reduced-gravity model forced by wind stress curl field from the present climate model. It is also found that the main contributing longitudinal band for KE index (KEI) moves westward in response to the warmed climate. This results from the northwest- ward expansion of the large-scale sea level pressure (SLP) field.

P1-14 Decadal variation of the Kuroshio intrusion into the South China Sea during 1992-2016

Yicheng Chen, Fangguo Zhai (Ocean University of China)

Decadal variation of the Kuroshio intrusion into the South China Sea (SCS) between 1992 and 2016 is investigated using the high-resolution Hybrid Co- ordinate Ocean Model (HYCOM) reanalysis data. Statistical analysis indicates that the occurrence frequency of Kuroshio intrusion is high during 2003-2005 and 2014-2016, while low during 1998-2000 and 2008-2010. This makes the upper-layer (0-700 m) Luzon Strait transport (LST) being large and small during the former and latter periods, respectively. Both the decadal variations of the occurrence frequency of Kuroshio intrusion and LST are highly correlated with the Pacific Decadal Oscillation (PDO). Besides, the decadal variation of the LST is also highly correlated with that of the meridional sea surface height (SSH) gradient west of the Luzon Strait (LS), which is believed to be an important role affecting the Kuroshio intrusion by previous studies. However, further analyses indicate that the decadal variation of the meridional SSH gradient west of the LS can not be explained by local wind forcing via Ekman dynamics. This implies that the former quite possibly results from that of the Kuroshio intrusion and the latter is not controlled by local wind forcing. Application of the Godfrey's island rule uncovers that the basin-scale wind forcing in the tropical North Pacific Ocean associated with PDO is a major factor regulating the decadal variation of the LST. During the warm phase of PDO, the Aleutian Low intrudes southward, inducing the positive wind stress curl anomalies and contributing to anomalous northward Sverdrup transport in the tropical North Pacific Ocean. In response, anomalous southward flow occurs east of the Philippines so as to balance the entire interior Sverdrup transport anomaly. This leads to weaker northward Kuroshio Current, enhancing the Kuroshio intrusion to the SCS and hence a stronger westward LST. During the cold phase of PDO, the situation is reversed.

P1-15 Baroclinic Instability of Non-zonal Flows and Bottom Slope Effects on Propagation of the Most Unstable Wave

Leng Hengling, Bai Xuezhi (Hohai University)

A linear, two-layer potential vorticity (PV) equation model on a beta-plane is employed to study the baroclinic instability of non-zonal basic currents flowing over a uniform bottom slope. The general characters of unstable perturbations, such as propagation and scale are mainly determined by the background PV gradient consisting of the thermocline depth gradient, planetary vorticity gradient and bottom slope. In a wavenumber coordinate frame, all components of the background PV gradient are projected to the normal direction of the wavenumber vector of initial perturbation. The method has an advantage in simplifying the mathematical expressions of the criteria for instability, phase velocity and growth rate of unstable modes. Case study and theoretical analysis suggest that, in the case of a positive slope (the bottom slope in the same direction as the isopycnal tilt), the fastest-growing wave is capable of escaping from the basic flows and propagating cross the streamlines. On the contrary, in the case of a negative slope (the bottom slope opposed to the isopycnal tilt), the most unstable wave always propagates along the streamlines as if being trapped in the basic flows. In addition, the spatial scale of the most un- stable mode can be heavily reduced by a negative slope.

P1-16 Interannual and inter-decadal variability of the North Equatorial Countercurrent in the Western Pacific

[1]Xiao Chen, [2]BO QIU ([1]Hohai University, [2]University of Hawaii)

Interannual and longer timescale variations of the North Equatorial Countercurrent (NECC) in the western Pacific are investigated using the multi-decade (1960-2014) hindcast by the Ocean general circulation model for the Earth Simulator (OFES). The OFES-simulated sea level and upper ocean circulation changes show favorable comparisons with available tide gauge data and repeat hydrographic surveys along the 137ºE meridian. An empirical orthogonal function (EOF) analysis reveals that the low-frequency NECC variability is dominated by two distinct modes. The first mode fluctuates interannually and shows strengthening and southward migration of the NECC concurrent with the development of El Niño events. Unlike the extra-tropical western Pacific Ocean circulation variability controlled by wind forcing west of the dateline, the interannual NECC variations are forced by equatorial wind forcing cumulative across the entire Pacific basin. The second mode of the NECC variability has a inter-decadal timescale and is characterized by NECC's progressive weakening in strength, migrating poleward, and broadening in width over the past 50 years. These long-term changes in NECC are caused by the corresponding changes in the trade wind system that weakened and expanded poleward in the past half a century across the Pacific basin.

P1-17 Decadal variability of water transport in North Pacific using P-vector method

Shouchang Wu, Hailun He (Second Institute of Oceanography, SOA)

The coupled response of oceans and climate change is a hot topic in global research. Water transport in the North Pacific is one of the important research direction. Based on the climatological temperature and salinity data of the WOA (World Ocean Map), we use the P-vector method to get the water transport related to the potential vorticity and compares it with the Sverdrup transport calculated by wind stress. We check the decadal variability of the water trans- port described by the WOA data set, and its relationship with the decadal variability of the wind stress. This research enriches the study of decadal ocean circulation in the North Pacific Ocean. The results of this research have certain scientific significance for the study of the low-frequency changes of the North Pacific Ocean on the global climate change response.

P1-18 Can errors/bias arising from the ignored acceleration be bounded or even controlled in the Lagrangian Argo trajectory deriving method?

[1]Tianyu Wang, [2]Sarah Gille, [1]Yan Du ([1]South China Sea Institute of Oceanology, CAS, [2] Scripps Institution of Oceanography)

Argo float trajectories are simulated using an eddy-permitting ocean model output from the Estimating the Circulation and Climate of the Ocean, Phase II (ECCO2) project and a Lagrangian particle tracking method programmed to represent the vertical motions of profiling Argo floats. Deep velocity estimates proved by such simulated Lagrangian trajectories, combined with the ambient Eulerian velocity at the reference layer (1000 m) from ECCO2, give qualitative metrics for the bias from the typical trajectory-deriving method. We find in certain regions acceleration measured by the Lagrangian floats becomes important and this can be a bias of the estimates of the Eulerian current velocities. This bias can be inferred from the standard Taylor expansion as a function of the Argo sampling period (although this is generally fixed by the Argo cycle time) and acceptably ignored when there are minimal velocity gradients. However, it becomes significant in western boundary current regions and in the Antarctic Circumpolar Current (ACC) system, where the convergence of simulated floats is colocated with jets and areas of strong Reynold's stress convergence, as it's well known that eddy momentum fluxes maintain these jet like flows. Consequently, during a 9-day parking period, speed bias induced by the

Lagrangian velocity acceleration can be as large as 4 cm s-1, representing roughly 30% of the ambient velocity. If unaccounted for, this could bias velocities inferred from observed float trajectories.

P1-19 Tropical Meridional Overturning Circulation Observed by Subsurface Moorings in the Western Pacific

[1,2]Lina Song, [1,3]Yuanlong Li, [1,3]Jianing Wang, [1,3]Fan Wang, [1,3]Shijian Hu, [1,3]Chuanyu Liu, [1]Xinyuan Diao, [1,2]Cong Guan ([1]Key Laboratory of Ocean Circulation and Waves, Institute of Oceanology, Chinese Academy of Sciences, Qingdao, China, [2]Institute of Oceanographic Instrumentation, Shandong Academy of Sciences, Qingdao, China, [3]Function Laboratory for Ocean Dynamics and Climate, Qingdao National Laboratory for Marine Science and Technology, Qingdao, China)*

Meridional ocean current in the northwestern Pacific was documented by seven subsurface moorings deployed at 142°E during August 2014-October 2015. A sandwich structure of the tropical meridional overturning circulation (TMOC) was revealed between 0°-6°N that consists of a surface northward flow (0-80 m), a thermocline southward flow (80-260 m; 22.6-26.5σ_θ), and a subthermocline northward flow (260-500 m; 26.5-26.9σ_θ). Based on mooring data, along with satellite and reanalysis data, prominent seasonal-to-interannual variations were observed in all three layers, and the equatorial zonal winds were found to be a dominant cause of the variations. The TMOC is generally stronger in boreal winter and weaker in summer. During 2014-2015, the TMOC was greatly weakened by westerly wind anomalies associated with the El Niño condition. Further analysis suggests that the TMOC can affect equatorial surface temperature in the western Pacific through anomalous upwelling/downwelling and likely plays a vital role in the El Niño-Southern Oscillation (ENSO).

ABSTRACT-POSTER-SESSION 2

P2-1 Multi-decadal timeseries of the Indonesian throughflow

[1]Jun Wei, [1]Mingting Li, [2]Arnold Gordon ([1]Peking University, [2]Columnbia University)

NCEP reanalysis wind data from 1948 to 2016 and Makassar Strait transport from 2004 to 2011 are used to construct a multi-decadal timeseries of 0–300 m Makassar Throughflow using a back-propagation (BP) neural network. Based on the 2004–2015 Makassar timeseries, 0–300 m transport accounts for 75% (±8%) of the total Makassar throughflow. Results from the INSTANT program 2004–2006 indicate that the Makassar throughflow provides 78% of the Indonesian Throughflow (ITF) within the upper 1000 m (77% of the full depth ITF). As the ITF is driven largely by North Pacific winds, we use the North Pacific zonal wind to construct a 68-year timeseries of 0–300 m Makassar Throughflow to trace interannual to decadal variability. The constructed timeseries has a mean transport of 9.2 ± 1 Sv within the 0–300 m layer. Using the 2004–2015 statistics this converts to a total Makassar Strait throughflow of 12.2 Sv and using the 2004–2006 INSTANT data, to a total ITF within the upper kilometer of 14.7 Sv. The Makassar throughflow decreases from 1948 to 1995, increases after 1995, then rapidly decreases after 2013, which agrees with the Pacific to Indian inter-ocean pressure difference across the Indonesian seas based on SODA reanalysis with a correlation coefficients of 0.6. The Pacific Decadal Oscillation (PDO) and El Nino-Southern Oscillation (ENSO), have correlation coefficients with the constructed Makassar throughflow of −0.6 and −0.4 respectively.

P2-2 An Argo-derived background diffusivity parameterization for improved ocean simulations in the tropical Pacific

Yuchao Zhu, Rong-Hua Zhang (Institute of Oceanology Chinese Academy of Sciences)

Coupled general circulation models (CGCMs) suffer from the prominent sea surface temperature (SST) biases in the tropical Pacific Ocean, such as the too- cold tongue along the equator. The ocean general circulation models (OGCMs) answer for this bias problem to a large degree, in which the parameterization of the vertical mixing processes is of great uncertainty. The background diffusivity, representing the integrated effects of the diapycnal mixing processes in the ocean interior, is typically assigned with a constant value of 10-5 m2 s-1 in the current OGCMs. However, it goes against the recent evidences that the diffusivity is reduced by an order of magnitude in the tropics. The overestimated mixing in the tropics can degrade the simulations in currents and water mass properties, but the possible biases are not well understood. Thus, in this study, the spatial structure for the background diffusivity in the tropical Pacific Ocean is derived from the Argo data based on the strain-based finescale parameterization, and is then employed into the MOM5-based ocean-only modeling and the CM2.1-based coupled modeling. It reveals that the SST simulations are improved by employing the Argo-derived background diffusivity. In addition, the subsurface warm bias is also alleviated, leading to a more realistic equatorial thermocline. The improved simulations in temperature can be attributed to the regulation in the currents system. In the upper layer, the equatorial upwelling weakens and cooling effects from the vertical advection is reduced. Beneath the thermocline, the cooling is induced both by the reduced heat transfer from the upper layer and by the convergence of the cool water from the off-equatorial regions.

P2-3 Low-Frequency Variability of the South Pacific Subtropical Gyre as Seen from Satellite Altimetry and Argo

[1]Linlin Zhang, [2]Tangdong Qu ([1]Institute of Oceanology, Chinese Academy of Sciences, [2]University of California, Los Angeles)

Low-frequency variability of the South Pacific Subtropical Gyre is investigated using satellite altimeter and Argo data. In most of the region studied, both sea surface height and steric height exhibit a linearly increasing trend, with its largest amplitude in the western part of the basin. Analysis of the Argo data reveals that the steric height increase north of 308S is primarily caused by variations in the upper 500 m, while the steric height increase south of 308S is determined by variations in the whole depths from the sea surface to 1800 m, with contributions from below 1000m accounting for about 50% of the total variance. Most of the steric height increase is due to thermal expansion, except below 1000m where haline contraction is of comparable magnitude with thermal expansion. Correspondingly, the South Pacific Subtropical Gyre has strengthened in the past decade. Within the latitude range between 108 and 358S, transport of the gyre circulation increased by 20%–30% in the upper 1000m and by 10%–30% in the deeper layers from 2004 to 2013. Further analysis shows that these variations are closely related to the southern annular mode in the South Pacific.

P2-4 Trends of Sea Surface Temperature and Sea Surface Temperature fronts in the South China Sea during 2003-2017

Yi Yu, YunTao Wang, Haoran Zhang (Second Institute of Oceanography)

The trends of sea surface temperature (SST) and SST fronts in the South China Sea (SCS) are analyzed during 2003-2017 using high-resolution satellite data. The linear trend of basin averaged SST is 0.31°C/decade with the strongest warming identified at the southeastern Vietnam. Although the rate of warming is comparable in both seasons for the entire basin, the spatial patterns of linear trend are different between summer and winter. SST trend to the west of Luzon Strait is characterized by fast

warming in summer, exceeding about 0.6 °C/decade, but the trend is not significant in winter. While the strongest warming trend occurs in the Southeast of Vietnam in winter with much less pronounced warming in summer. A positive trend of SST fronts is identified in the cost of China, associating with increasing wind stress. The increasing trend SST fronts to the east of Vietnam during summer suggests the northeasterly wind stress anomaly is associated with the warming trend of SST. Large-scale circulation, like El Nino, can influence the trends of SST and SST fronts. A sig- nificant correlation is found between SST anomaly and Nino3.4, and the ENSO signal is leading by eight-month. The basin averaged SST linear trends in- crease after the years of the El Nino event (2009-2010), which is at least due to the fast warming rate causing by the enhanced northeasterly wind. Peaks of positive anomalous SST and negative anomalous SST fronts are found co-occurring with the strong El Nino events (2009-2010, 2015-2016).

P2-5 Eddy generation mechanism in the central South China Sea

Jiajia Chen, Xuhua Cheng (College of Oceanography, HoHai University)

The mesoscale eddy generation mechanisms in the central South China Sea (CSCS) are investigated using altimetry observations and solutions of nonlinear, 11/2-layer reduced-gravity model. We estimate the relative role of the wind forcing in the interior SCS and the remote forcing from the western tropical Pacific (WTP) in eddy generation in the CSCS. Model solutions show that the wind in the interior SCS is the primary forcing, which explains about 69% mesoscale eddies in the CSCS. Signals from the WTP also play an important role. Wind driven equatorial-signals reach the western coast of Luzon Island through the Sibutu Passage and Mindoro Strait. The reflected Rossby waves from the eastern boundary propagate westward, become unstable, and turn to isolated eddies. The signals from WTP explain about 47% mesoscale eddies in the CSCS. The high-frequency wind forcing either in the CSCS or WTP is important in the eddy generations.

P2-6 Long-range Radiation and Dissipation of M2 Internal Tides in the Northwestern Pacific and South China Sea

Yang Wang, Zhenhua Xu, Baoshu Yin, Hang Chang (Institution of Oceanology, Chinese Academy of Scienecs)

Generation and long-range radiation processes of M2 internal tides in the Northwestern Pacific and South China Sea (SCS) are revealed by a set of high- resolution numerical simulations. M2 Internal tides originated from Luzon Strait can both propagate westward into SCS and eastward into the northwestern Pacific. In the SCS, the internal tide field is dominated by the westward baroclinic tides from Luzon Strait. While in the northwestern Pacific, besides Luzon Strait, the M2 internal tides are also effectively generated and radiated by other prominent topographical features including Ryukyu Island chains, Bonin ridge and Mariana Arc. Low mode eastward tidal beams from Luzon Strait radiate into the Western Pacific over thousands of kilometers and interfere with internal tides originate from other sources. Strong dissipation occurs both near the sources and in the deep basin of SCS and Philippine Sea. The remote incident internal tidal dissipation over the deep basin exhibit widespread distribution and thus redistribute the internal tide energy. The modulation effect of Kuroshio on the generation and propagation of internal tides is also discussed.

P2-7 Features of the Equatorial Intermediate Current associated with basin resonance in the Indian Ocean

[1]Dongxiao Wang, [1]Ke Huang, [2]Weiqing Han, [1]Weiqiang Wang, [3]Qiang Xie, [1]Ju Chen, [1]Gengxin Chen

([1]SCSIO, CAS, [2]University of Colorado, UAS, [3]Institute of Deep–Sea Science and Engineering, CAS)

This paper investigates the features of the Equatorial Intermediate Current (EIC) in the Indian Ocean and its relationship with basin resonance at the semiannual time scale by using in–situ observations, reanalysis output, and a continuously stratified linear ocean model (LOM). The observational results show that the EIC is characterized by prominent semiannual variations with velocity reversals and westward phase propagation; and it is strongly influenced by the pronounced 2nd baroclinic–mode structure but with identifiable vertical phase propagation. Similar behavior is found in the reanalysis data and LOM results. The simulation of wind–driven equatorial wave dynamics in the LOM reveals that the observed variability of the EIC can be largely explained by the equatorial basin resonance at the semiannual period, when the 2nd baroclinic Rossby wave reflected from the eastern boundary intensifies the directly forced equatorial Kelvin and Rossby waves in the basin interior. The sum of the first 10 modes can reproduce the main features of the EIC. Among these modes, the resonant 2nd baroclinic–mode makes the largest contribution, which dominates the vertical structure, semiannual cycle, and westward phase propagation of the EIC. The other 9 modes however are also important, and the superposition of the first 10 modes produces downward energy propagation in the equatorial Indian Ocean.

P2-8 Eddy-current interaction in the Leeuwin Current off the lower-west coast of Australia

Qinyan Liu (South China Sea Institute of Oceanology)

The Leeuwin Current (LC) off the west coast of Australia is featured by active eddy activities with prominent seasonal and interannual variability. In this study, we use long-term shelf mooring observations of current velocity and temperature off Two Rocks (31.5°S) and off Fremantle (32°S), combined with numerical model simulations, to provide new insight to the LC eddy energetics off the lower-west coast of Australia. Mooring results show that the maxim- um surface velocity of the LC on the continental shelf occurs in austral winter-spring, and reaches >35 cm s-1 in July and September, in contrast to the austral autumn-winter peak of the overall volume transport of the LC. An unseasonable strengthening of the LC occurred in February-April 2011 (42 cm s-1 at 200 m isobath), during an extreme Ningaloo Niño (marine heatwave) event. Off the lower-west coast of Australia, eddies act to maintain the mean shear of the LC, in contrast with eddy-mean flow interaction in the upstream LC. Eddy- induced Reynolds stress shows significant cross-steam variations, positive on the offshore side and negative on the inshore side of the LC core. The barotropic conversion rate of eddy energy depicts striking along-stream variations: mean flow to eddy conversion on the offshore side upstream from the mooring locations where high eddy kinetic energy is observed; eddy to mean flow conversion downstream from the mooring locations where the mean flow of the LC re-emerges from the active eddy field. The baroclinic conversion of eddy energy also becomes more significant south of 32°S.

P2-9 Decadal and long-term changes in the upper layer salinity in the South China Sea over the past five decades

Lili Zeng (South China Sea Institute of Oceanology, Chinese Academy of Sciences)

A newly assembled South China Sea Physical Oceanographic Dataset (SCSPOD) provides the first observational evidence for mixed layer salinity and subsurface salinity changes in the SCS from 1960 to 2015. The upper layer salinity was more like the Pacific Decadal Oscillation-like changes than a linear decreasing; it freshened in the 1960s, started to salinify in 1974, freshened again from 1993, and then salinified from 2012. A box-average salinity budget shows that the mixed layer freshening was associated with reduced surface freshwater flux and advection through the Luzon Strait, while salinification was driven by enhanced surface freshwater loss. An analysis of the subsurface salinity budget reveals that the main underlying contributors to subsurface salinity are horizontal advection and vertical entrainment. In particular, advection driven by the Luzon Strait transport and vertical entrainment from the mixed layer are the key factors controlling variations on subsurface salinity.

P2-10 Impact of the South China Sea Summer Monsoon on the Indian Ocean Dipole

[1]Yazhou Zhang, [1]Jianping Li, [2]Jiaqing Xue, [1]Juan Feng, [1]Qiuyun Wang, [1]Yidan Xu, and [1]Yuehong Wang ([1]Beijing Normal University, [2]State Key Laboratory of Numerical Modeling for Atmospheric Sciences and Geophysical Fluid Dynamics, Institute of Atmospheric Physics, Chinese Academy of Sciences)

This paper investigates the impact of the South China Sea summer monsoon (SCSSM) on the Indian Ocean Dipole (IOD). The results show that the SCSSM has a significant relationship with the IOD over the boreal summer (June–August, JJA) and fall (September–November, SON). When the SCSSM is strong, more and less precipitation falls over the western North Pacific and Maritime Continent, respectively, and this corresponds with enhanced South China Sea monsoon Hadley circulation (SCSMHC). The precipitation dipole over the western North Pacific and Maritime Continent, as well as the enhanced SCSMHC, lead to intensification of the southeasterly anomalies off Sumatra and Java, which then contribute to the negative sea surface temperature (SST) anomalies in the tropical southeastern Indian Ocean through the positive wind–evaporation–SST and wind–thermocline–SST (Bjerknes) feedbacks. Consequently, a positive IOD develops due to the increased zonal gradient of the tropical Indian Ocean SST anomalies, and vice versa. The SCSSM has a peak correlation with the IOD when the former leads the latter by three months. This implies that a positive IOD can persist from JJA to SON and reach its mature phase within the frame of the positive Bjerknes feedback in SON. In addition, the El Niño–Southern Oscillation (ENSO) has a slight influence on the relationship between the SCSSM and the IOD.

P2-11 Sensitivity experiments of modeling SCSTF-ITF interactions by closing straits and passages in a 0.1° × 0.1° regional ocean model

Mingting Li, Jun Wei (Peking University)

Based on a high-resolution (0.1° × 0.1°) regional ocean model covering the entire northern Pacific, this study investigated impacts of the South China Sea Throughflow (SCSTF) on Indonesian Throughflow (ITF) through a set of sensitivity experiments with closed straits and passages. The results showed that, compared to the control experiment with all straits opened, closing Luzon Strait caused more water flowing into Sulawesi Sea from Mindanao Current and the southward Mindoro–Sibutu flow is reversed. When the Mindoro-Sibutu passage is blocked by closing Sibutu Strait, both Mindanao-Sulawesi flow and ITF transports increased. The correlation coefficient between Mindanao-sulawesi transport and ITF transport increased from 0.75 to 0.99. They almost have same seasonal and interannual variability. This experiment confirms the South China Sea “freshwater plug” mechanism. When closing Luzon-Karimata flow near Makassar Strait, the ITF transport increases by ~3 Sv, while the inflow from Mindanao has no change. This implies that the heap up of low salinity water in Java Sea significantly inhibits the southward Makassar flow.

P2-12 Wind-driven cross equator transport

[1]Junwei Chai, [1]Xiaopei Lin, [2]Jiayan Yang ([1]Ocean University of China, [2]Woods Hole Oceanographic Institution)

Sverdrup relation indicates that the zonally-integrated curl of wind stress may drive a cross-equatorial transport in the oceanic basins, which is satisfied by the tropical observation well. However, the Sverdrup transport includes the geostrophic and Ekman transport parts and both of them have the singular point in the equator, because the coriolis force f equals zero. To investigate the transport in the Equatorial Atlantic, the Regional Ocean Model (ROMS) is used to study the equatorial solution under steady wind forcing. The study region is designed as a rectangle basin with uniform depth and a boundary from 30°S to 30°N. The distribution and quantity of the circulation is similar to the Atlantic ocean. The geostrophic transport and Ekman transport are computed based on the data. The result shows that Ekman transport

is two orders of magnitude larger than that in the mid-latitude. A good agreement is found between the geostrophic transport stream function and the transport derived from the wind field through the Sverdrup relation.

P2-13 Vertical propagation of mid-depth zonal currents associated with surface wind forcing in the equatorial Indian Ocean

[1]Huang Ke, [2]Michael McPhaden, [1]Weiqiang Wang, [3]Qiang Xie, [1]Dongxiao Wang ([1]South China Sea Institute of Oceanology, CAS, [2]NOAA, USA, [3]Institute of Deep−Sea Science and Engineering, CAS)

The vertical propagation of mid-depth (200–1500 m) zonal velocity in the equatorial Indian Ocean and its relationship with surface wind forcing are investigated. We focus on semiannual time scales, using in-situ mooring observations and an oceanic reanalysis product that can reasonably well reproduce the structure and magnitude of the observed mid-depth zonal velocity in the equatorial Indian Ocean. The pronounced semiannual cycle in observed mid-depth zonal currents indicates a clear upward phase propagation with particularly robust signatures between at depths of 500–1000 m between 3°S–3°N, 70–85°E. The main characteristics of the mid-depth currents are consistent with vertically propagating first–meridional–mode Rossby wave at semiannual period. Theory suggests that equatorial Kelvin waves, forced by zonal wind variations in the western half of the basin, transfer energy downward and eastward, reflecting into Rossby waves at the eastern boundary. These Rossby waves transfer energy downward and westward, causing semiannual variability at mid-depth in the equatorial Indian Ocean.

ABSTRACT-POSTER-SESSION 3

P3-1 Strengthened Indonesian Throughflow drives decadal warming in the Southern Indian Ocean

[1]Ying Zhang, [2]Ming Feng, [1]Yan Du, [3]Helen Philips, [3]Nathan Bindoff, [4]Michael McPhaden ([1]South China Sea Institute of Oceanology, Chinese Academy of Sciences, [2]CSIRO Oceans and Atmosphere, [3]Institute for Marine and Antarctic Studies, University of Tasmania, [4]NOAA/Pacific Marine Environmental Laboratory)

Remarkable warming of the Southern Indian Ocean during the recent decade is assessed using a heat budget analysis based on the Estimating the Circulation and Climate of the Ocean version 4 release 3 model results. The annual mean temperature averaged in the upper-700m Southern Indian Ocean during 1998-2015 has experienced significant warming at a rate of 1.03×10-2℃/yr. The heat budget analysis indicates the increase in temperature during 1998- 2015 is collectively driven by the decreased cooling contribution of the net air-sea heat flux and the increased warming contribution of the total heat advection. The increased ITF advection is the largest contributor to warming the upper 700m of the Southern Indian Ocean, while the reduction of surface turbulent heat flux makes a secondary contribution. Understanding the decadal heat balance in the Indian Ocean is important for decadal climate variability in the Indo-Pacific basin.

P3-2 Research on the effects of El Niño events in the typhoon

Weihui Sui ((Public Meteorological Service Center of CMA)

By Using El Nino events and typhoon data in 65 years(1951-2015),Statistics and analysis of El Nino

events including Started to develop, the end of the year influence on the Pacific Northwest (including the South China Sea) typhoon source locations, build landed the number and strength characteristics, At the same time Preliminary Study relationship between the global warming and El Nino intensity, type, frequency, and the typhoon characteristic change .The results show: Number of typhoons generate more and the main performance in the first half of the year in El nino started to develop, Number of typhoons generate fewer and fewer mainly reflects in the first half of El Nino end year; The overall number of typhoons landed less than normal in El Nino events years. The stronger the el nino events less land, Strong typhoon and super typhoon landfall reducing in El Nino end year; Under the background of warmer climate, strengthen the intensity of El Niño events, there is an increasing trend in the frequency of occurrence and a significant reduction in the number of typhoon.

P3-3 Contrasting the intraseasonal variations in the Upper Equatorial Pacific Currents during the 1997-98 and 2015-16 El Niño

Yilong Lv, Yuanlong Li, Xiaohui Tang, Fan Wang (Institute of Oceanology, Chinese Academy of Sciences)

Intraseasonal variations (ISV) of zonal current in the upper equatorial Pacific Ocean during the 1997–1998 El Niño event and 2015–2016 El Niño event is explored using a combination of observations and ocean re-analyses. The ISVs exhibited intensity differences between the two ENSO events of 1997-98 and 2015-16, showing a stronger 1997-98 than 2015-16. According to the composite analysis, the difference in intensity of the ISV of the zonal currents is mainly caused by the difference in intensity of the ISV of zonal wind stress. In 1997-98, the impact of the MJO in the Indian Ocean was stronger than in the 2015-16 event. However, the 2015-16 event was even more affected by the subtropical. This difference in the wind field causes differences in the Intraseasonal variations in the upper equatorial flow field.

P3-4 Oceanic processes of upper ocean heat content associated with two types of ENSO

Junqiao Feng (IOCAS)

The spatiotemporal variability of equatorial Pacific upper ocean heat content (HC)and subsurface heat during two types of El Niño–Southern Oscillation (ENSO), i.e., Eastern and Central Pacific (EP and CP) types, are investigated using subsurface ocean heat budget analysis. Results show that HC tendencies during both types of ENSO are mainly controlled by oceanic heat advection beneath the mixed layer to the thermocline, and the role of net heat flux can be neglected. The most important three terms are the zonal and vertical advections of anomalous heat by climatological currents (QU0T′, QW0T′) and zonal advection of climatological heat by anomalous current (QU′T0). The large contribution of QU0T′extends from west to east along the equatorial Pacific. The considerable contribution of QU′T0 is confined to the east of 160°W, and that of the QW0T′ is observed in the central Pacific between 180°E and 120°W. In particular, a major contribution of QW0T′ is also observed in the far eastern Pacific east of 100°W during EP ENSO. There is also a small contribution from meridional advection of climatological heat by anomalous current (QV′T0). In contrast, the meridional advection of anomalous heat by climatological cur- rents (QV0T′) and vertical advection of climatological heat by anomalous current (QW′T0) are two damping factors in the HC tendency, with the former dominating. Differences in spatial distribution of the heat advection associated with the two types of ENSO are also presented. We define a warm water heat index (WWH) as integrated heat content above 26 kg m−3 potential density (26σ) isopycnal depth within 130°E–80°W and 5°S–5°N. Further examination suggests that the recharge–discharge of WWH is involved in both types of El Niño, though with some differences. First, it takes about 42 (55) months for the evolution of a recharge–discharge cycle during an EP (CP)ENSO. Second, the EP El Niño event peaks during the discharge phase, 7–8 months after the re- charge time. The CP El Niño peaks during the recharge phase, 4–5 months before the recharge time. The locations of HC anomalies in the El Niño mature phase relative to those at recharged time explain why the EP and CP El Niño peak in different stages of the recharge–discharge process.

P3-5 The response of the equatorial Pacific Ocean to the winds during 2014-2015

Jing Wang (IOCAS)

The equatorial wave dynamics of interannual sea level variations between 2014/2015 and 2015/2016 El Niño events are compared using the LICOM forced by the NCEP reanalysis Ⅰ wind stress and heat flux during 2000-2015. And the LICOM can reproduce the interannual variability of 20ºC isotherm depth anomalies and sea level anomalies (SLA) along the equator over the Pacific Ocean in comparison with the D20 anomalies data and the AVISO altimeter SLA data well. The equatorial wave coefficients are extracted from the LICOM simulation to study the role of the propagation and reflections of the equatorial waves in the evolution of SLA during El Niño events. During 2014/2015 El Niño event, upwelling equatorial Kelvin waves from the western boundary in April 2014 reach the eastern Pacific Ocean, which weakened SLA in the eastern Pacific Ocean induced by the downwelling equatorial Kelvin waves. However, no upwelling equatorial Kelvin waves from western boundary in the Pacific Ocean can reach the eastern boundary during 2015/2016 El Niño events. Linear wave model results also demonstrate that upwelling equatorial Kelvin waves in both 2014 and 2015 from the western boundary can reach the eastern boundary. However, stronger westerly-wind-burst-forced downwelling equatorial Kelvin waves overwhelmed the upwelling equatorial Kelvin waves from the western boundary in 2015. Therefore, the western boundary reflection and weak westerly wind burst inhibit the growth of 2014/2015 El Niño event. The disclosed equatorial wave dynamics are important to the simulation and prediction of ENSO event in future study.

P3-6 Computation of the surface wind stress response to the mesoscale SST perturbations in the Peru-Chile sea area Based on the Tikhonov regularization method

[1]Chaoran Cui, [1]Rong-Hua Zhang, [1]Hongna Wang, [2]Yanzhou Wei ([1]Institute of oceanology ,Chinese academy of sciences, [2]Second institute of Oceanography)

The interaction between the mesoscale sea surface temperature (SST) and wind stress perturbations has a great influence on the ocean and atmosphere. However, the simulations of the atmospheric response to SST perturbations still remain a great challenge in the Peru-Chile current system. In this study, the Tikhonov regularization method is applied to the calculation of the wind stress perturbation. Before the calculation, the characteristics of mesoscale SST- wind stress coupling in the Peru-Chile current system are first quantified with the QuikSCAT and AMSR-E data. The result shows that the mesoscale perturbations of the wind stress, divergence and curl of wind stress are positive linear related to the high-pass filtered SST, downwind SST gradients and cross- wind SST gradients respectively. The domain where wind stress and SST perturbations have a high correlation is restricted to the nearshore sea area, which is because there is complicated hydrography structure in this region. The weakest mesoscale SST-wind stress coupling is happening in the southwest part of the Peru-Chile current system. To calculate the wind perturbations that are induced by the mesoscale SST perturbations exactly, the Tikhonov regularization method is applied to this study. This method allows us to compute the wind stress perturbations from the crosswind and downwind component of the SST gradient perturbations, and guarantee the unique solutions in the limited and irregular domains. The computation example is shown in the Peru-Chile cur- rent system and the result shows that the pattern of the reconstructed wind stress perturbations is consistent with the distribution of the SST perturbations, perfectly. This means that the wind stress perturbations calculated by the Tikhonov regularization method are related to the SST perturbations exactly. This method is useful for the mesoscale SST-wind stress coupling studies and improving the model simulations.

P3-7 CMIP5 model biases in the climatological mean state of the western Pacific warm pool

Yuxing Yang, Wang Faming, Zheng Jian (Institute of Oceanology, Chinese Academy of Science)

Biases in coupled general circulation models represent important limits for climate prediction. Based on historical runs of 26 coupled climate models of the Fifth Phase of the Coupled Model Intercomparison Project, the error of the climatological mean of the western Pacific warm pool (WPWP) is investigated. The results show that simulation of the morphology of the WPWP is related to the first inter-model Empirical Orthogonal Function mode of the annual mean sea surface temperature over the tropical Pacific. This is significantly influenced by ocean currents. The upper-ocean heat budget analysis also indicates that heat advection plays a key role in determining the size of the WPWP during simulation. Zonal heat advection bias controls the extension or con- traction of the eastern edge in the equator. Both the zonal heat advection bias caused by zonal ocean currents bias and meridional heat advection bias caused by the meridional sea-surface temperature gradient bias are the crucial factors in determining the southern section size of the WPWP. In the north- ern section of WPWPs, latent heat bias is the most important factor determining size. In addition, in the equator and south section of the WPWP, the advective feedback plays a key role, while in the northern section of WPWPs, the wind-evaporation-sea surface temperature feedback is most important.

P3-8 A hybrid coupled model (HCM) of atmosphere and ocean physics and biology (AOPB) in the tropical Pacific

[1]Feng Tian, [2]Rong-Hua Zhang, [3]Xiujun Wang ([1]Institute of Oceanology, Chinese Academy of Sciences, [2]Institute of Oceanology, Chinese Academy of Sciences;Qingdao National Laboratory for Marine Science and Technology, [3]College of Global Change and Earth System Science, Beijing Normal University;Joint Center for Global Change Studies)

Multiple processes are involved in modulating the El Niño-Southern Oscillation (ENSO) in the tropical Pacific, and these processes are neither well represented nor well understood. A new hybrid coupled model (HCM) of atmosphere and ocean physics and biology (AOPB) is developed for multi-sphere interaction studies in the region. An ocean biology model is coupled with a simplified ocean-atmosphere system consisting of an ocean general circulation model (OGCM) and a statistical atmospheric model for interannual anomalies of wind stress (τ). The HCM AOPB serves as a simple Earth system for the tropical Pacific to represent the coupling among the atmospheric and physical and biological ocean components. Model experiments are performed to illustrate the new model's ability to depict the mean ocean state and interannual variability associated with the ENSO. The relationships among anomaly fields are analyzed to illustrate the ocean biology-induced heating feedback and its modulating effects on the ENSO, which is characterized by a negative feedback. The underlying processes and mechanisms that are illustrated can be attributed to dominant modulation of the penetrative solar radiation through the bottom of the mixed layer (ML). Further model applications to studies on these processes and bio-physical interactions are discussed.

P3-9 The roles of atmospheric wind and entrained water temperature (Te) in the second-year cooling of the 2010–12 La Niña event

Chuan Gao, Rong-Hua Zhang (Institute of Oceanology, Chinese Academy of Sciences)

An intermediate coupled model (ICM) yields a successful real-time prediction of the sea surface temperature (SST) evolution in the tropical Pacific during the 2010-12 La Niña event, whereas many other coupled models fail. It was previously identified that the thermocline effect on the SST (including vertical advection and mixing), as represented by water temperature entrained into the mixed layer (Te) and its relationship with the thermocline fluctuation, is an important factor that affects the second-year cooling in mid-late 2011. Because atmospheric wind forcing is also important to ENSO processes, its role is investigated in this study within the context of real-time prediction of the 2010-12 La Niña event using the ICM in which wind stress anomalies are calculated using an empirical model as a response to SST anomalies. An easterly wind anomaly is observed to persist over the western-central Pacific during

2010-11, which acts to sustain a horse shoe-like Te pattern connecting large negative subsurface thermal anomalies in the central-eastern regions off and on the equator. Sensitivity experiments are conducted using the ICM to demonstrate how its SST predictions are directly affected by the intensity of wind forcing. The second-year cooling in 2011 is not predicted to occur in the ICM if the easterly wind anomaly intensity is weakly represented below certain levels; in- stead, a surface warming can emerge in 2011, with weak SST variability. The results of the current study indicate that the intensity of interannual wind forcing is equally important to SST evolution during 2010-11 compared with that of the thermocline effect. To correctly predict the observed La Niña conditions in the fall of 2011, the ICM needs to adequately represent the intensity of both the wind forcing and the thermocline effects.

P3-10 Spatio-temporal variation of Indian summer monsoon rainfall and associated δ18O variability: Its teleconnections with ENSO

PULLABHATLA KIRAN KUMAR, Arvind Singh, Rengaswamy Ramesh (Physical research Laboratory)

Indian summer monsoon rainfall (ISMR) controls the agricultural productivity and economy of the country by contributing 80% of the total annual precipitation in India. ISM varied at intra annual to Intra seasonal scale which has huge impact on the billions of people. The ISMR variability and its response with respect to El-Nino is revisited. Using the remote sensing rainfall and HadISST derived Niño3.4 datasets, the spatiotemporal correlation patterns of rainfall and Niño3.4, shows a strong negative correlation over the central India (CI) and a positive correlation over the northeast India (NEI) during the summer monsoon. These correlation patterns at monthly scale varies spatially and temporally. The isotope enabled nudged general circulation models (GCM) de- rived rainfall and δ18O of precipitation also shows the similar positive and negative correlation with the Niño3.4 index over CI and NEI rainfall. The observational and GCM simulations shows that the long-term trends in the ISM strength are controlled by the long-term variation in El Niño Southern Oscillation (ENSO) strength in addition to land-Sea temperature gradient. The paleoclimate proxy records from the CI and NEI caves, which shows the opposite variation trends during El- Niño periods, which confirms the paleoclimate proxies are able to reflect the ENSO effect on rainfall variation.

P3-11 Oceanic feedbacks in affecting ENSO asymmetry

[1]Cong Guan, [2]Michael McPhaden, [1]Shijian Hu, [1]Fan Wang ([1]Institute of Oceanology, CAS, [2]NOAA/Pacific Marine Environmental Laboratory)

Based on temperature variance budget, we diagnosed oceanic roles in these ENSO asymmetric features from three aspects: the amplitude of anomalous temperature during the mature phase of El Niño events is larger than La Niña in the Niño3 region; In the Niño4 region, the amplitude in mature La Niña is larger than El Niño; La Niña events basically last longer than El Niños.

In the Niño3 region, the larger temperature amplitude of El Niño than La Niña is attributed to a greater growth rate during El Niño development phase than La Niña events. Stronger positive oceanic feedbacks are found during El Niño development phase with the most contribution from zonal advective feedback (ZAF), following by Ekman feedback (EKF) and thermocline feedback (TCF). Difference of the negative feedbacks between the El Niño and La Niña events is mostly from the damping effects of thermal damping. However, in Niño4, La Niña has greater growth rate than El Niño, which is induced by larger effects of positive TCF in its developing phase while ZAF contributes equally to developing these two events. ENSO asymmetry in duration in the Niño3 region, is be- cause the decay rate in La Niña events is smaller than that of El Niño events by 0.2 °C2 mon-1. Strong positive TCF still persists during the decaying of La Niña, which slows down the fade of the cold events. It is shown that the difference of TCF between El Niño and La Niña decaying phases is induced by zonal-mean thermocline variations across the equatorial Pacific basin, indicating the asymmetry of discharge/ recharge processes between the equator and off-equator.

P3-12 Distinct ENSO regimes enhanced by recent global warming

[1]Ning Jiang, [1]Congwen Zhu, [2]Weihong Qian ([1]State Key Laboratory of Severe Weather (LASW) and Institute of Climate System, Chinese Academy of Meteorological Sciences, [2]School of Physics, Peking University, Beijing)

The diversity of ESNO, especially eastern and central Pacific (EP and CP) El Niño, has been widely concerned. Here we applied the empirical orthogonal function (EOF) and k-means clustering analysis to explore its change under global warming during 1950--2016. Our results suggest ENSO diversities can be determined by the combination of a background mode and two intrinsic modes of SSTA. The recent global warming seems to increase the frequency and amplitude of extreme ENSO events, and to cause more basin-wide warm events and CP La Niña events. The change of ENSO diversity is not only attributed to a slowly intensifying background of west-east SST gradient, but also to the changing combination of intrinsic modes of ENSO. Contrast analysis suggests that the distinction between the cold/moderate warm and extreme warm regimes of ENSO has become more obvious under recent global warming.

P3-13 The Buoyant Equipment for Skin Temperature (BEST), A New Instrument for Measurement of Air-Sea Interactive Temperatures

Chuqun CHEN, Haibin YE, Shilin TANG (LTO, South China Sea Institute of Oceanology, Chinese Academy of Sciences)

The air-sea interaction occurs between the ocean and the atmospheric is the most active and common natural process on the Earth. The Skin Sea Surface Temperatures (SSTskin) and the Bottom Air Temperature(BAT) are the true interacting temperatures of the air-sea interaction, which plays a very important role on climate and global change. However, the SSTskin is hard to measure as the skin layer of the ocean is its topmost layer less than 1 mm thick. With the absence of in-situ measurement of SSTskin and BAT, the temperatures used for air-sea interaction studies, are not the real interacting temperatures (SSTskin and BAT), instead of the bulk temperature of the ocean at depth about 1 m and the air temperature at 4m~20m above the sea surface. In this presentation, The Buoyant Equipment for Skin Temperature (BEST), a new instrument for high resolution measurement of temperatures in the air-sea interfacial layers, is described. The instrument BEST is a pole with thousands of temperature sensors on it. The temperature sensors, thermistors, for standard version of BEST are arrayed from 0.6 mm in the top 1/3 part of the pole to 10 mm in the bottom part of the pole. The pole could be vertically floated in the air-sea interfacial layer, and it can synchronically measure the temperatures of the bottom layer of the air, the skin layer and the surface layer of the water with an accuracy of 0.02K at a vertical spatial resolution up to 0.6mm. And the BEST could continuously work for one week or longer depending on mainly the battery. The measured temperatures can be recorded every second. The in-situ measurement with BEST shows that the temperatures of the lowest layer of the atmosphere is seriously affected by the water temperature, corresponding, the surface temperature of water is also significantly affected by the air temperature . A strong thermocline with several centimetres thick at the topmost layer of the water is always exist (ref.figure 1).

P3-14 Sea surface temperature in the subtropical Pacific boosted the 2015 El Niño and hindered the 2016 La Niña

[1]Jingzhi Su, [1]Renhe Zhang, [1]Xinyao Rong, [2]Qingye Min, [1]Congwen Zhu ([1]Chinese Academy of Meteorological Sciences, [2]Fudan University)

After the quick decaying of the 2015 super El Niño, the predicted La Niña unexpectedly failed to materialize to the anticipated standard in 2016. The diagnosis analyses, as well as numerical experiments, showed that such ENSO evolution of the 2015 super El Niño and the hindered 2016 La Niña may be essentially contributed by the sea surface temperature anomalies (SSTAs) in the subtropical Pacific. The self-sustaining SSTAs in the subtropical Pacific tend to weaken the trade winds during boreal spring-summer, leading to anomalous westerlies along the equatorial region over a period of more than one season. Such

long-lasting wind anomalies provide an essential requirement for the ENSO formation, particularly before a positive Bjerkness feedback is thoroughly built up between the oceanic and atmospheric states. Besides the 2015 super El Niño and the hindered La Niña in 2016, there were several other El Niño/La Niña events that cannot be explained only by the oceanic heat content in the equatorial Pacific. However, the puzzles related with those eccentric El Niño/La Niña events can be well explained by suitable SSTAs in the subtropical Pacific. Thus, the leading SSTAs in the subtropical Pacific can be treated as an independent indicator for ENSO prediction, on the basis of the oceanic heat content inherent in the equatorial region. Because ENSO events have become more uncertain under the background of global warming and the Pacific Decadal Oscillation during recent decades, thorough investigations of the role of the subtropical Pacific in ENSO formation are urgently needed.

P3-15 Impact of atmospheric model resolution on simulation of ENSO feedback processes: a coupled model study

Lijuan Hua (Chinese Academy of Meteorological Sciences)

This study examines El Niño-Southern Oscillation (ENSO)-related air-sea feedback processes in a coupled general circulation model (CGCM) to gauge model errors and pin down their sources in ENSO simulation. Three horizontal resolutions of the atmospheric component (T42, T63 and T106) of the CGCM are used to investigate how the simulated ENSO behaviors are affected by the resolution. We find that air-sea feedback processes in the three experiments mainly differ in terms of both thermodynamic and dynamic feedbacks. We also find that these processes are simulated more reasonably in the highest resolution version than in the other two lower resolution versions. The difference in the thermodynamic feedback arises from the difference in the shortwave-radiation (SW) feedback. Due to the severely (mildly) excessive cold tongue in the lower (higher) resolution version, the SW feedback is severely (mildly) underestimated. The main difference in the dynamic feedback processes lies in the thermocline feedback and the zonal-advection feedback, both of which are caused by the difference in the anomalous thermocline response to anomalous zonal wind stress. The difference in representing the anomalous thermocline response is attributed to the difference in meridional structure of zonal wind stress anomaly in the three simulations, which is linked to meridional resolution.

ABSTRACT-POSTER-SESSION 4

P4-1 Different impacts of two types of El Niño on the yield of early rice of Southern China

Runnan Sun, Jianping Li (Beijing Normal University)

Rice production in Southern China (SC), constituting almost one-third of the total in China, has been proved to be closely associated with climate change. Different effects of the Eastern Pacific (EP) El Niño and the Central Pacific (CP) El Niño on rice yield in SC during boreal spring (May–June–July) is addressed by composite and correlation analyses using grid cell early rice yield data from 1982 to 2006. During EP El Niño events, rice yield in most area of SC is reduced; while during CP El Niño events, it increases mildly. The impacts between the EP and CP El Niño on rice yield show significant differences in nearly half areas of SC. The potential mechanism leading to the significant different effects of EP and CP El Niño on rice yield is investigated. During boreal spring, CP El Niño significantly decreases the rainfall in SC, which favors rice yield in SC; in contrast, EP El Niño significantly increases the precipitation in eastern SC, consequently resulting into an unfavorable condition for rice production.

P4-2 Causes of enhanced SST variability over the equatorial Atlantic and its relationship to Atlantic zonal mode in CMIP5

Yun Yang (Beijing Normal University)

A spurious band of enhanced sea surface temperature (SST) variance (SBEV) is identified over the northern equatorial Atlantic in Geophysical Fluid Dynamics Laboratory (GFDL) coupled model version 2.1. The SBEV is especially pronounced in boreal spring and due to the combined effect of both anomalous atmo- spheric thermal forcing and oceanic vertical upwelling.

The SBEV is a common bias in Coupled Model Intercomparison Project 5 (CMIP5), found in 14 out of 23 models. The SBEV in CMIP5 is associated with the atmospheric thermal forcing and the oceanic vertical upwelling, similar to GFDL CM2.1. While the tropical North Atlantic variability is only weakly correlated with the Atlantic Zonal Mode (AZM) in observations, the SBEV in CMIP5 produces conditions that drive and intensify the AZM variability via triggering the Bjerknes feedback. This partially explains why AZM is strong in some CMIP5 models even though the equatorial cold tongue and easterly trades are biased low.

P4-3 Mesoscale SST Perturbation-induced Impacts on Precipitation Climatology in the Kuroshio-Oyashio Extension Region, as Revealed by the WRF Simulations

Jiaxiang Gao, Rong-Hua Zhang, Hongna Wang (Institute of Oceanology, Chinese Academy of Sciences)

Mesoscale coupling between perturbations of mesoscale sea surface temperature (SST) and low-level winds has been extensively studied using available high-resolution satellite observations. However, the climatological impacts of mesoscale SST perturbations (SSTmeso) on the free atmosphere have not been fully understood. In this study, the rectified effect of SSTmeso on local precipitation climatology in the Kuroshio-Oyashio Extension (KOE) region is investigated using the Weather Research and Forecasting (WRF) Model; two runs are performed, one forced by 1° × 1° SST fields and another by additional SSTmeso extracted from satellite observations. Climatological precipitation response to SSTmeso is characterized mainly by enhanced precipitation on the warmer flank of three oceanic SST fronts in this region. The results show that the positive correlation between the 10-m wind speed perturbations and SSTmeso is well captured by the WRF model with a reasonable spatial pattern but relatively weak strength. The addition of SSTmeso improves the climatologic- al precipitation simulated by WRF with a better representation of fine-scale structures compared with satellite observations. A closer examination on the underlying mechanism suggests that while the pressure adjustment mechanism can explain the climatological precipitation enhancement along the fronts and the relatively high contribution of the convective precipitation, other factors such as synoptic events should also be taken into consideration to account for the seasonality of the precipitation response, especially its disappearance in summer.

P4-4 Simulating the IPOD, East Asian summer monsoon, and their relationships in CMIP5

[1]Yu Miao, [1]Li Jianping, [2]Zheng Fei, [3]Wang Xiaofan, [4]Zheng Jiayu ([1]College of Global Change and Earth System Sciences, [2]Institute of Atmospheric Physics, [3] Centre for Communication and Outreach, [4]State Key Laboratory of Tropical Oceanography)

This paper evaluates the simulation performance of the 37 coupled models that from the Coupled Model Intercomparison Project Phase 5 (CMIP5) with respect to the East Asian summer monsoon (EASM) and the Indo-Pacific warm pool and North Pacific Ocean dipole (IPOD) and also the interrelationships between them. The results show that the majority of the models are unable to accurately simulate the interannual variability and long-term trends of the EASM, and their simulations of the temporal and spatial variations of the IPOD are also limited. Further analysis showed that the correlation coefficients between

the simulated and observed EASM index (EASMI) is proportional to those between the simulated and observed IPOD index (IPODI); that is, if the models have skills to simulate one of them then they will likely generate good simulations of another. Based on the above relationship, this paper proposes a conditional multi-model ensemble method (CMME) that eliminates those models without capability to simulate the IPOD and EASM when calculating the multi-model ensemble (MME). The analysis shows that, compared with the MME, this CMME method can significantly improve the simulations of the spatial and temporal variations of both the IPOD and EASM as well as their interrelationship, suggesting the potential for the CMME approach to be used in place of the MME method.

P4-5 Decadal variability of temperature in the Pacific ocean

Hongna Wang (IOCAS)

The Pacific decadal oscillation (PDO) has important impacts on the atmosphere and ocean. The decadal variability of temperature in Pacific is important to the weather and climate variations. Here we use the method of ensemble empirical mode decomposition (EEMD) to research the decadal variability of temperature in the Pacific. Using the EEMD to decompose the PDO index, we obtained ten components. The individual components exhibit preferred mean period of 4 months (C1), 1 year (C2), 2-3 years (C3), 5 years (C4), 10 years (C5), 15-20 years (C6), 30-50 years (C7), 60-80 years (C8), and 100 years or longer (C9 and R). According to the sums of EEMD C6-8 of PDO index, we can know that the amplitude of PDO in decadal time scale is decreasing after the 2000 year. The decadal variations of temperature in North Pacific are weakened too. The decadal variability of temperature in North Pacific is obviously different from the temperature in Equatorial Pacific. The relation between the PDO and ENSO is different in the different time periods. Before the 1978 year, the variation of PDO is ahead of the ENSO, but it's reverse after the 2000 year.

P4-6 Contrasting the impacts of the 1997–1998 and 2015–2016 extreme El Niño events on the East Asian winter atmospheric circulation

[1]Jian Zheng, [2]Qinyu Liu, [3]Zesheng Chen ([1]Institute of Oceanology, Chinese Academy of Sciences, [2]Ocean University of China, [3]South China Sea Institute of Oceanology, Chinese Academy of Sciences)

This study investigates how the Indian Ocean Dipole (IOD) modulated the influence of the 1997–1998 and 2015–2016 El Niño events on the East Asian winter atmospheric circulation. Due to the extreme IOD in the fall of 1997, the tropical Indian Ocean (TIO) displayed higher sea surface temperature (SST) anomalies in the western basin than in the eastern basin during the following winter. As a result, the Walker circulation weakened in the TIO and tropical Pacific, leading to a zonal rainfall dipole in the Indo-Western Pacific (IWP), which triggered a wave train pattern over East Asia with positive geopotential height anomalies in the upper-level troposphere over northeastern China and Japan during the winter of 1997–1998. In contrast, there was no IOD in the fall of 2015, and the winter rainfall anomaly in the western TIO was weak that year. The geopotential height anomalies were negative around northeastern China and the Sea of Japan—the opposite of those during the winter of 1997–1998. Comparing the historical El Niño events with the high IOD index and low IOD index indicates that the IOD is a crucial contributor to the dipole rainfall in the IWP and, thus, the circulation anomalies in East Asia.

P4-7 Increasing threat of landfalling typhoons in the western North Pacific between 1974 and 2013

Shoude Guan (Key Laboratory of Ocean Circulation and Waves, Institute of Oceanology, Chinese

Academy of Sciences)

Long-term changes between 1974 and 2013 were investigated in western North Pacific typhoons making landfall in East and Southeast Asia. Landfalling typhoon parameters, including the percentage of typhoons making landfall, the annual mean landfall intensity (LFI), and the annual accumulated power dissipation index at land, all increased significantly (at the 99% confidence level), by 14%, 17%, and 94%, respectively, over the study period. The increase in probability of a typhoon making landfall was attributed to an eastward shift of the typhoon genesis location. The LFI was decomposed into the product of the intensification rate and intensification duration. The product reproduced variations in the observed LFI well, and the correlation coefficient was high at 0.82. Although the intensification duration decreased slightly, an unprecedented increase in the intensification rate was observed, this increased the LFI. Warming of the upper ocean in the western North Pacific typhoon main intensification region, giving a higher tropical cyclone heat potential, yielded better oceanic conditions and overcame the worsening atmospheric conditions (increasing vertical wind shear), allowing typhoons to intensify. The increase in the annual accumulated power dissipation index was mainly caused by the increase in the LFI, and the annual number of typhoons and typhoon duration contributed much less. Increasing typhoon landfalling activities might heighten the threat posed by typhoons to populations and infrastructure in coastal regions.

P4-8 Wintertime global warming hiatus tied to negative phase of cold ocean-warm land pattern

[1]Jun-Chao Yang, [1]Xiaopei Lin, [2,1]Shang-Ping Xie, [1,2]Yu Zhang, [3]Yu Kosaka ([1]Physical Oceanography Laboratory/CIMST, Ocean University of China and Qingdao National Laboratory for Marine Science and Technology, [2]Scripps Institution of Oceanography, University of California, [3]Research Center for Advanced Science and Technology, The University of Tokyo)

Global mean surface temperature (GMST) warming undergoes a near-decadal slowdown during the 2000s, termed recent global warming “hiatus.” For annual-mean GMST, cold tropical eastern Pacific (TEP) and its forced surface air temperature cooling particularly damp the warming effect of radiative forcing. But in boreal winter when the hiatus is prevalent, a recent study argues that atmospheric internal variability (AIV) shows comparable contribution as the TEP-related component. As AIV includes a lot of modes, how it influences GMST and hiatus seems to be complex.

Here, we use observations and model realizations to show that total contribution of AIV to GMST is closely associated with the so-called Cold Ocean-Warm Land (COWL) pattern. This pattern features two temperature anomaly centers of same sign in northern Eurasia and northwestern North America. The corresponding time series of the COWL pattern dominates wintertime AIV-related GMST and shows comparable ability to the TEP in modulating GMST trend from interannual to interdecadal time scales. Moreover, COWL-related variability is able to eliminate the recent hiatus and create new hiatus cases in different model realizations. Under intense human-induced warming, negative phase of COWL pattern often contributes to substantial continental cooling in the model hiatus, in line with the case of recent observational one. Since the COWL pattern is a combination of AIV effect, it is unpredictable and hence seriously limits the predictability of wintertime hiatus.

P4-9 Simulating the Pacific Decadal Mode and its impact on ENSO in ACCESS model

[1]Arnold Sullivan, [2]Jing-Jia Luo, [3]Jin-Yi Yu, [4]Bodman Roger, [1]Wenju Cai, [1]Arnold Sullivan, [2]Jing-Jia Luo, [3]Jin-Yi Yu, [4]Bodman Roger, [1]Wenju Cai ([1]CSIRO oceans and atmosphere, [2]Bureau of Meteorology, [3]University of California Irvine, [4]4)School of Earth Sciences, University of Melbourne)

Previous studies have shown that decadal variability in the tropical Pacific may affect the occurrence and characteristics of El Nino-Southern Oscillation (ENSO). For instance, the frequent occurrence of central-Pacific (CP) type of El Nino in recent decades, which exerts distinct impacts on global climate and socio-

economics from those of eastern-Pacific (EP) El Nino, has been linked to decadal/multi-decal background change in the Pacific. It has been found that decadal Pacific modes such as Pacific Meridional Mode (PMM) or North Pacific Oscillation (NPO) may play an important role in triggering the development of CP El Nino. However, the exact mechanism remains unclear.

To understand the linkage between the Pacific decadal modes and the El Nino behaviour, two set of three simulations from the atmospheric general circulation model (AGCM) experiments has been setup from the Australian Community Climate and Earth-System Simulator (ACCESS-AM) version 1.3 and version 2. The first set use period based on 1952 to 2005, and the second set use period based on 1950 to 2016. In the first experiments, monthly raw sea surface temperature (SST) is used to force the ACCESS-AM. In the second and third experiment, band-pass filtered (5-month to 7 years) and low-pass filtered (greater than 7 years) SST forcing is used. Separating the interannual and decadal SST forcing allows a better understand the role of the interannual ENSO and decadal modes generates distinct atmospheric winds that influence the evolution of El Nino events.

P4-10 Why was the western Pacific subtropical anticyclone weaker in late summer after the 2015/16 super El Niño?

Boqi Liu, Congwen Zhu, Jingzhi Su, Lijuan Hua, Yihong Duan (Chinese Academy of Meteorological Sciences)

The western Pacific subtropical anticyclone (WPSA), which bridges the El Niño events and the East Asian summer monsoon, is generally enhanced in boreal summer after El Niño events. However, it becomes weaker in boreal late summer (July–August) of 2016, following the 2015/16 super El Niño event, indicating failure of the previous experience. Our results suggest that the weaker WPSA in late summer 2016 is associated with the extinction of the Indian Ocean capacitor effect, presenting the cold sea surface temperature anomalies (SSTAs) in the western tropical Indian Ocean (WTIO) after the fast decaying of the 2015/16 super El Niño in spring. Compared with the case in 1982/83 and 1997/98, both data analysis and numerical experiments indicate that the cold WTIO SSTAs could induce an anomalous zonal circulation, with its descending branch over the WTIO and the ascending branch over the western North Pacific (WNP). Afterwards, the thermal structure in the upper troposphere of the WNP is altered to enhance the local wave guide, which facilitate the equator- ward propagation of the mid-latitudinal wave train into the WNP. Consequently, the abnormal ascending over the WNP weaken the WPSA in conjunction with the anomaly of the upper-tropospheric cyclone due to the southward intrusion of the wave train during late summer 2016. This implicates the possible influence of El Niño evolution in spring on the WPSA intensity in the subsequent summer.

P4-11 withdrawn

P4-12 Evaluating of cooling tower scheme in high resolution regional model

Miao Yu (Institute of Urban Meteorology, China Meteorological Administration, Beijing, China)

A new cooling tower scheme considering quantitative sensible and latent heat flux released from air condition was implemented in building energy model (BEM) and coupled to the regional model (WRF). Two simulations using default WRF/BEP+BEM and improved WRF/BEP+BEM to estimate the effects improvement effect focusing on dry day and wet day respectively. The new cooling tower system in commercial area not only induces the significant increase the anthropogenic heat partition by 90% of the total heat flux releasing as latent but also further change the surface heat flux feature. When cooling tower is introduced, averaged surface latent heat flux in urban area is increased to about 64.3 W•m-2

with the peak of 150 W•m-2 in dry day and 40.35 W•m-2 with the peak of 150 W•m-2 in wet day. Further new cooling tower scheme improve the model performance of temperature and humidity. Maximum and minimum temperature error improves 2-3 degree especially in dry day. In the vertical, model performance of boundary layer structure in rural area is much better than urban area.

P4-13 A Study of Wind Wave Prediction of Binary Typhoons over the Northwestern Pacific Ocean with a Coupled Atmosphere-Ocean-Wave Model

[1]Weiwei Ding, [2]linlin qi, [2]Huijie Wang, [1]Tianju Wang ([1]National University of Defense Technology, [2]Academy of Air Force)

The coupled atmosphere-ocean-wave model was introduced and its forecast performance for wind wave parameters over the northwestern Pacific Ocean was evaluated by using the GFS and the Northwest Pacific ocean forecasting data. We carried out a 72-h forecasting experiment for 5 days, when the binary typhoons took place over the northwestern Pacific Ocean, and examine the distribution characteristics and predictability of the wind wave field. The results showed that the typhoon tracks as well as the characteristics of wave distribution and evolution can be well forecasted. It is found that the forecasted significant wave height increases with increasing maximum wind and decreasing minimum surface pressure near the typhoon center. The forecasted significant wave height field is well consistent with the satellite altimeters observations of Jason-3. Because of the intensity and location, the forecast performance of wind wave parameters over the open sea is better than that over the offshore areas and that during the abrupt changing period of typhoon intensity. In this paper, the related conclusions can provide some useful reference for operational quantitative forecasts of typhoon waves by using coupled atmo- sphere-ocean-wave model.

P4-14 Interannual variability and dynamics of intraseasonal wind rectification in the equatorial Pacific Ocean

Xia Zhao (IOCAS)

The rectification of intraseasonal wind forcing on interannual sea surface temperature anomalies (SSTA) and sea level anomalies (SLA) associated with El Niño-Southern Oscillation (ENSO) during 1993-2016 are investigated using the LICOM ocean general circulation model forced with daily winds. The comparisons of the experiments with and without the intraseasonal wind forcing have shown that the rectified interannual SSTA and SLA by the intraseasonal winds are much weaker than the total interannual SSTA and SLA in the cold tongue, due to the much weaker rectified than the total interannual Kelvin and Rossby waves in the equatorial Pacific Ocean. The dynamics of the rectification are through the nonlinear zonal and vertical advection by the background currents, which produces downwelling equatorial Kelvin waves during El Niño. The meridional advection is much smaller than the zonal and vertical advection, suggesting that the rectification is not induced by the Ekman dynamics or the thermocline rectification. The rectified interannual Kelvin waves are found to be much smaller than reflected at the Pacific western boundary and those forced by the interannual winds, suggesting that the latter two play a much more important role in ENSO dynamics than the intraseasonal winds. The results of this study suggest an unlikely significant role of oceanic nonlinear rectification by intraseasonal winds during the onset and cycling of El Niño.

P4-15 Relationship between the western North Pacific Ocean and the East Asian summer monsoon and its non-stationarity

[1]Pei-long Yu, [1]Li-feng Zhang, [2]Quan-jia Zhong, [1]Han-xiao Yin, [1]Ming-yang Zhang ([1]College of Meteorology and Oceanography, National University of Defense Technology, [2]State Key Laboratory of

Numerical Modeling for Atmospheric Sciences and Geophysical Fluid Dynamics (LASG), Institute of Atmospheric Physic, Chinese Academy of Sciences; College of Earth Science, University of Chinese Academy of Sciences)

In this study, the relationship between the western North Pacific Ocean (WNPO; 0–55°N, 100–165°E) and the East Asian summer monsoon (EASM) and its non-stationarity are investigated. It is found that the WNPO-EASM connection experiences a well-defined interdecadal change in the late 1980s and early 1990s. The EASM-related WNPO sea surface temperature anomaly (SSTA) pattern changes from the dipole pattern [WNPO dipole (WNPOD)] that develops over the period between 1968 and 1987 (P1) to a tripole pattern [WNPO tripole (WNPOT)] between 1991 and 2010 (P2). The positive (negative) phase of the WNPOD is characterized by warm (cold) SSTAs in the Japan Sea and Kuroshio–Oyashio Extension region, and cold (warm) SSTAs in the subtropical WNPO, whereas the positive (negative) phase of the WNPOT shows warming (cooling) in the Kuroshio Extension region (KER), and cooling (warming) in the south of Kamchatka Peninsula (SKP) and Philippine Sea (PS). During P1 (P2), the WNPOD (WNPOT) can be regarded as the first (second) leading mode of summer WNPO SST variability, and its positive phase is associated with a weakened WNPO subtropical high and thereby the deficient summer rainfall in the Yangtze River valley, together with a strong EASM, and vice versa. The change in the WNPO–EASM relationship may be caused by interdecadal changes in the relationship of the equatorial central Pacific (ECP) with the WNPO and EASM, and an increase in summer KER SST variability associated with an enhanced PDO. During P2, because the ECP warming-induced cyclonic anomalies move northwestwards and intensify, summertime ECP warming is able to generate a strong EASM and significant cooling over the two poles of the WNPOT (SKP and PS). These strengthened impacts of the ECP on the WNPOT and EASM con- tribute to the strengthened WNPOT–EASM relationship during P2. In addition, the increased KER SST variability associated with an enhanced PDO in summer between 1991 and 2010 changes the KER-related atmospheric circulation over East Asia and thus the KER–EASM relationship during P2. These two factors probably cause the EASM-related WNPO SSTA pattern to change from the WNPOD in P1 to the WNPOT in P2.

P4-16 Atmospheric Energetic over the Tropical Indian Ocean during the IOD Event

Yuehong Wang, Jianping Li (1.College of Global Change and Earth System Sciences (GCESS), Beijing Normal University)

The atmospheric layer perturbation potential energy (LPPE) over the tropical Indian Ocean is calculated and analyzed in a composite IOD event using reanalysis datasets for the period 1848–2015. The LPPE anomalies in the lower troposphere (1000–850 hPa) showing a dipole pattern responding to the anomalous variation of surface sea temperature (SST) are more significance than that in the upper troposphere (700–200 hPa) during the IOD event. Negative LPPE anomalies in the lower troposphere induces less energy is converted to atmospheric kinetic energy (KE) over the eastern Indian Ocean, leading to weakened Walker circulation over the Indian Ocean.1–2 month later, opposite motion over the western Indian Ocean further to weaken Walker circulation, causing the easterly anomalies in the equatorial Indian Ocean develop, and easterly anomalies further maintain the SST gradient of the Indian Ocean. The response of the Walker circulation forced by the reverse situation of occurs in the two poles of IOD provides a positive feedback during the IOD event.

P4-17 Decadal variations of salinity in western tropical Pacific

Guanghui Zhou, Rong-Hua Zhang (Key Laboratory of Ocean Circulation and Waves, Institute of Oceanology, Chinese Academy of Sciences, Qingdao 266071, China)

El Niño–Southern Oscillation (ENSO) is the most dominant air–sea interaction phenomenon in the tropical Pacific on an interannual (2–7-yr periodicity) time scale. In addition to the interannual ENSO signal, previous studies have pointed out that decadal variability exists in the tropical Pacific. It has been

shown that the decadal-scale sea surface temperature (SST) and sea level pressure (SLP) show similar spatial patterns to those of ENSO. Furthermore, previous studies used historical data to show that decadal-scale upper-ocean heat content (OHC) propagates from the western tropical Pacific toward the eastern tropical Pacific along the equator, similar to that of ENSO. Such OHC propagation of the decadal scale was also found in a 200-yr simulation of the ocean–atmosphere coupled model. Exploration of decadal-scale salinity change is important for a better understanding of decadal-scale climate variability because salinity variations influence oceanic density related to the subduction process from the midlatitudes to the tropics and also by generating a salinity barrier layer that affects the thermal condition of the upper ocean. Along with temperature, salinity determines the oceanic density, which influences the vertical stratification and vertical mixing. In the past, most previous studies have focused on the thermal field since it typically represents the dominate in- fluence in the eastern equatorial Pacific. The importance of salinity to the tropical Pacific climate system has not been getting much attention; the active role of decadal varying salinity in the coupled climate system also has been less studied. In the western tropical Pacific, salinity variability has been shown to influence the oceanic density, the vertical stability of the water column, and ultimately the thermal field. This salinity effect is an important factor that may contribute to the decadal-to-interannual evolution of the ocean and thus can affect the developing of ENSO events.

P4-18 Evolution of the Madden–Julian Oscillation in Two Types of El Niño

[1]Xiong Chen, [2]Jian Ling, [1]Chongyin Li ([1]College of Meteorology and Oceanography, National University of Defense Technology, [2]LASG, Institute of Atmospheric Physics, CAS)

Evolution characteristics of the Madden–Julian oscillation (MJO) during the eastern Pacific (EP) and central Pacific (CP) types of El Niño have been investigated. MJO activities are strengthened over the western Pacific during the predeveloping and developing phases of EP El Niño, but suppressed during the mature and decaying phases. In contrast, MJO activities do not show a clear relationship with CP El Niño before their occurrence over the western Pacific, but they increase over the central Pacific during the mature and decaying phases of CP El Niño. Lag correlation analyses further confirm that MJO activities over the western Pacific in boreal spring and early summer are closely related to EP El Niño up to 2–11 months later, but not for CP El Niño. EP El Niño tends to weaken the MJO and lead to a much shorter range of its eastward propagation. Anomalous descending motions over the Maritime Continent and western Pacific related to El Niño can suppress convection and moisture flux convergence there and weaken MJO activities over these regions during the mature phase of both types of El Niño. MJO activities over the western Pacific are much weaker in EP El Niño due to the stronger anomalous descending motions. Furthermore, the MJO propagates more continuously and farther eastward during CP El Niño because of robust moisture convergence over the central Pacific, which provides adequate moisture for the development of MJO convection.

P4-19 Impact Of South Indian Ocean Dipole On Tropical Cyclone Genesis Over The South China Sea

Teng Wang, Lu Xi, Song Yang (Sun Yat-sen University)

This study investigates the impact of the South Indian Ocean Dipole (SIOD) on the frequency of tropical cyclones (TCs) over the South China Sea (SCS) in summer (May-August) and winter (September-December) for 1975-2012. The frequency of TCs over the SCS shows significant interannual variations in the two seasons and relatively obvious interdecadal variability in summer. A prominent relationship occurs between the TC generation over the SCS and the SIOD, and the latter can be regarded as a good predictor of the former on interannual scale. In winter, vertical circulation is obvious due to a strong SIOD induces intensified ascending motions and high sea surface temperature over the northern SCS with sufficient moisture that supplies a favorable environment for TC formation. The impact of SIOD is weaker in summer but a convergent zone with upward motion also can be found over northeastern SCS. In addition, the SIOD and El Niño-Southern Oscillation are two primary impacting factors in winter and TC numbers increase when La Niña and positive SIOD events occur simultaneity.

However, the SIOD is a dominant and independent impacting factor in summer and El Niño events just play a secondary role.

ABSTRACT-POSTER-SESSION 5

P5-1 Effects of wave-current interactions on suspended-sediment dynamics during strong wave events in Jiaozhou Bay, Qingdao, China

GUANDONG GAO (Institute of Oceanology, Chinese Academy of Science)

Wave-current interactions are crucial to suspended-sediment dynamics but the roles of the associated physical mechanisms, the depth-dependent wave radiation stress, Stokes drift velocity, vertical transfer of wave-generated pressure transfer to the mean momentum equation (form drag), wave dissipation as a source term in the turbulence kinetic energy equation, and mean current advection and refraction of wave energy, have not yet been fully understood. Therefore, in this study, a computationally-fast wave model developed by Mellor et al. (2008), an FVCOM hydrodynamics model and the sediment model developed by the University of New South Wales are two-way coupled to study the effect of each wave-current interaction mechanism on suspended-sediment dynamics nearshore during strong wave events in a tidally dominated and semi-closed bay, Jiaozhou Bay, as a case study. Comparison of Geostationary Ocean Colour Imager data and model results demonstrates that the inclusion of just the combined wave-current bottom stress in the model, as done in most previous studies, is clearly far from adequate to model accurately the suspended-sediment dynamics. The effect of each mechanism in the wave-current coupled processes is also investigated separately through numerical simulations. It is found that, even though the combined wave-current bottom stress has the largest effect, the combined effect of the other wave-current interactions, mean current advection and refraction of wave energy, wave radiation stress and form drag (from largest to smallest effect), are comparable. These mechanisms can cause significant variation in the current velo- cities, vertical mixing and even the bottom stress, and should obviously be paid more attention when modelling suspended-sediment dynamics during strong wave events.

P5-2 The Value of the Greenhouse Gas Monitoring System for Climate Change in the China Sea

Dan Wang, Honggang Lv, Yifei Jiang, Tiejun Ling, Dongdong Xia (Key Laboratory of Research on Marine Hazards Forecasting, National Marine Environment Forecasting Center)

Coastal ocean carbon is an important component of global carbon cycling. In many of these coastal systems, spatial and temporal changes in air-sea CO2 fluxes remain with large uncertainties, which are often associated with the present evaluation of CO2 fluxes in individual coastal ocean system, which would in turn influence the evaluation of global fluxes. CO2 is one of the most important greenhouse gases that cause global warming. After the sea absorbs excessive CO2, the composition of carbonate system will change. Consequently, the pH of the seawater will decrease and in result damage the marine ecological environment. In this study, the authors focus on the South China Sea (SCS) and atmospheric CO2 is observed on greenhouse gas monitoring station of Xisha. Based on the analysis of historical and in-situ data, seasonal changes in air-sea CO2 fluxes (pCO2) and the capacity of carbon fixation in SCS are assessed, and meanwhile, the controlling mechanism and main influential factors of air-sea CO2 fluxes are studied. The results of the CO2 background con- centration in Xisha indicated the obvious diurnal and seasonal variations. The CO2 concentration was lower during daytime and higher during nighttime in four seasons. Our results also showed that the CO2 background concentration in Xisha was much higher in spring and winter but much lower in summer and autumn. The diurnal variation of

background concentration is mainly influenced by the sunlight, temperature and biological photosynthesis and respiration in this region. However, its seasonal variation is controlled by monsoon, atmospheric circulation, primary productivity, and source or sink of the sea-air interface. Otherwise, the authors also introduce the capacity construction of greenhouse gas monitoring system for climate change in the China Sea.

P5-3 Ocean hydrography of the Yap seamount and its adjacent sea area in the tropical Western Pacific in autumn 2014

XINGYU SHI, ZHENYAN WANG (Institute of Oceanography, Chinese Academy of Sciences)

Seamount, as the topography inundated in the ocean, has small top area and higher uplift height than 1000m. It can partly influence the movements of cur- rents and water masses, leading to different hydrographic characteristics with other area. The special hydrographic characteristics of seamount will exert a massive impact on the biogeochemical environment, sedimentary process, and marine ecological system, and contribute to unique biological communities and sedimentary environment in the seamount area. There are many seamounts distributed in the Yap subduction zone, Western Pacific. This paper aims at analyzing the hydrographic characteristics at Yap seamount and its adjacent area in the western Pacific, using in situ hydrological data, Argo floats data and sea surface height anomaly data. The surface layer of the study area is mainly affected by the North Equatorial Current (NEC), and the western current velocity is about 0.15 to 0.45m/s. Below the halocline layer, water is mainly controlled by the North Equatorial Undercurrent (NEUC), the eastward velocity is about 0.05 to 0.25m/s. Water masses analysis revealed that the subsurface layer of the study area is occupied by the North Pacific Tropical Water (NPTW), and the Antarctic Intermediate Water (AAIW) and its mixed water masses with North Pacific Intermediate Water (NPIW) comprised the intermediate layer. In addition, the mesoscale eddy activities are frequent in the study area. Cold and warm eddies exist at the same time with 8°N-10°N as the boundary. There are mainly cold eddy activities in the northern area, and warm eddy activities in the south area. The analysis of ocean hydrography in the Yap seamount and its adjacent will provide more scientific supports for deeper analysis of the formation mechanism about marine biological community and sedimentary environment at Yap seamount.

P5-4 Spatial and temporal variability of surface chlorophyll and particulate organic carbon in the North Pacific Ocean during 2003-2016: Physical and biogeochemical controls

Jun Yu, Xiujun Wang (Beijing Normal University)

The North Pacific Ocean is a significant sink region for carbon with large variability driven by physical and biogeochemical processes related to climate fluctuations. In this study, we analyzed the 14-year time series (2003-2016) of surface chlorophyll and particulate organic carbon (POC) derived from MOD- IS-Aqua. Chlorophyll and POC show a similar spatial pattern, with the highest values seen in the northwest and the lowest in the subtropical region to the south. Both chlorophyll and POC reveal a large interannual variability, with considerably higher values post 2014. Our analysis shows a strong positive correlation ($P<0.001$) between POC and chlorophyll, indicating the dominant role of biological activity in regulating the variability of surface POC. There is a weak positive relationship between POC and SST north of 45N, but a strong negative correlation ($P<0.001$) south of 40N, implying that physical processes may play a large role in driving biological processes thus the variability of POC in the North Pacific. Our study suggests that the temporal variation of sur- face POC may be influenced by the climate modes of the Pacific Decadal Oscillation (PDO), El Nino–Southern Oscillation (ENSO) and North Pacific Gyre Oscillation (NPGO). In addition, the Blob might be responsible for the significant POC increase in the subarctic Pacific post 2014.

P5-5 Comparative study of the adaptive characteristics of zooplankton in deep (500-3500 m) and shallow (0-200 m) layers in the Western Tropical Pacific Ocean

Lei Chen, Chaolun Li, Zhencheng Tao, Fangping Cheng, Xiaocheng Wang (Institute of Oceanology, Chinese Academy of Sciences)

The deep sea has limited food resources and is considered one of the most rigorous environments on Earth. In contrast, zooplankton and their food sup- plies are abundant in shallow sea layers. In this study, the different adaptive characteristics of zooplankton taxa in the deep and shallow layers were explored from the aspects of feeding type, trophic niche partition among taxa and growth performance. Our results showed that wider ranges of δ15N and δ13C values were detected in the deep-layer taxa, indicating various feeding types. This characteristic is crucial for zooplankton in deep-sea ecosystems to make full use of limited resources (e.g., marine snow and fecal pellets). Lower trophic niche overlap among taxa was revealed in the shallow layer, indicating a higher level of trophic niche partitioning. This is a fundamental mechanism that minimizes the inter-taxa competition and sustains the co-existence of zooplankton in the shallow layer. From an ecological stoichiometry perspective, most taxonomic groups in the deep layer exhibited higher C:P and N:P ratios than the taxa with similar taxonomic statuses in the shallow layer, suggesting lower maximal growth rates in the deep layer. Lower growth rates potentially reduce the consumption of limited resources in the deep layer, and higher growth rates facilitate the rapid exploitation of abundant resources and allow zooplankton in the shallow layer to flourish.

P5-6 Influence of the Mindanao Undercurrent on terrigenous material transport of the tropical western Pacific

Zhenyan Wang, Wei Gao (Institute of Oceanology, Chinese Academy of Sciences)

The Mindanao Undercurrent plays a significant role in transporting material and energy at intermediate depths in the tropical western Pacific; this role is vital to global thermohaline circulation and climate change. The spatial structure of the Mindanao Undercurrent (MUC) has attracted the attention of physical oceanographers. However, there has been a great deal of discussion regarding whether the MUC is a quasi-permanent flow with a certain scale. This study reveals the potential ability of this undercurrent to transport terrigenous materials and provides new sedimentological evidence for its permanence from the perspective of material transport in the ocean. The contents of eight trace elements (Ca, Ti, Fe, Mn, Cu, Zn, Sr and Zr) in the SPM in the upper 1000-dbar depth of the water column are semi-quantitatively measured via synchrotron radiation micro-beam X-ray fluorescence (μ-XRF) analysis based on suspended particulate matter samples collected along a survey section during a marine cruise in December 2014. The lithogenic elements Ti, Mn, Fe and Zr can be traced to inputs from external terrigenous sources, whereas the biogenic elements Ca, Cu, Zn and Sr are related to internal biogenic sources. The results of water mass analysis and statistical analysis suggest that the offshore core of the northward-flowing Mindanao Undercurrent transports relative hypersaline subsurface water, which is rich in terrigenous particle materials at density surfaces of 26.2-27.0 σθ. This inference that the MUC can achieve long-distance material transport provides support for the MUC as a quasi-permanent current in the western Pacific.

P5-7 Lead behavior in the Western Tropical Pacific

Shuo Jiang, Yan Chang, Jing Zhang (State Key Laboratory of Estuarine and Coastal Research, East China Normal University)

Lead (Pb) is one of the main trace elements in GEOTRACES project. The behavior of Pb in the open-ocean environment can be used to study ocean metal transport and reactivity under human perturbation, and to trace and quantify ocean physical transport. During the cruise in 2016, we collected seawater

samples along 130°E section from 2°N to 19°N and gave the first systematical description of Dissolved Lead (DPb) distributions in western Tropical Pacific. In the studying area, DPb concentration was highly influenced by hydrologic regimes. In the surface water, DPb concentration ranged from 22 pM to 60 pM, and DPb concentrations in the southern of 5°N were lower than in the north, maybe influenced by surface currents and eddies. In the upper 500 m, DPb concentration ranged from 16 pM to 68 pM, higher DPb concentrations were presented in the depth of 200 m to 500 m at the north of 10°N, influenced by North Equatorial Current which originated near the center of the Western North Pacific with a high atmospheric DPb deposition, while the lower concentrations showed in the deeper layers at southern of 5°N, maybe affected by New Guinea Coastal Undercurrent which originated from Southern Pacific. Two full-depth stations both showed a typical scavenging profile, similar with that of North Pacific with a subsurface maximum at 250 m to 400 m. From 2000 m to bottom, DPb concentration decreased to less than 10 pM, larger than that of central Tropical Pacific and Southern Ocean, demonstrating the large hu- man impact on this area.

P5-8 Impact of Mesoscale Eddies on Bioavailability and Composition of Dissolved Organic Matter in West Pacific Ocean

Miao Zhang, Ying Wu, Fuqiang Wang (East China Normal University)

Mesoscale eddies can influence the production and export of dissolved organic matter (DOM) in marine euphotic and mesopelagic zone. Bacteria com- munity and nutrient limitation could also be modified by cyclonic mesoscale eddies. An on-board incubation experiment was carried out in west Pacific Ocean to assess the impact caused by the bacteria and nutrient addition brought with seawater in mesopelagic layer to surface on bioavailability and com- position of DOM. Three groups were prepared, with mixing of seawater from different layers with bacteria. Dissolved organic carbon (DOC) decreased sharply in the first half day, while 9.34%, 14.2% and 11.0% DOC was degraded in group Ⅰ, Ⅱ, Ⅲ respectively. After 140 days, DOC in group II was most de- composed (20.7%), while more DOC in group I (16.4%) was degraded than group III (15.4%). Five individual fluorescent components were identified: three humic-like (C1, C2, C3) and two protein-like (C4, C5) components. C1 was low molecular weight (LMW) component increasing continuously during incubation experiment. C2 was high molecular weight (HMW) component, which in the groups with deep seawater showed higher intensity. C2 in group II de- creased in the first 10 days and decrease afterwards. Group I and III, however, didn't fluctuate similarly. C3 showed HMW feature with different changes between three groups. C3 in group II decreased while increased in group I and III. We speculate that there are some certain bacteria with the function to de- grade aromatic and fulvic acid components in surface, which could work just with abundant nutrient. This certain bacteria, however, didn't exist in 400m. C4 was tryptophan-like component which was degraded most in Group II during incubation period. C5 was tyrosine-like component showing more fluctuate in the groups with deep seawater. Thus we hypothesis the mesoscale process especially the cyclonic eddies can bring nutrient and microbe to the sur- face or subsurface layer and modify the nutrient limitation and bacteria community, which could accelerate the degradation of DOM and change the com- position. Such modification could modulate regional carbon cycle and oceanic microbial carbon pump finally.

P5-9 Carbon Chemistry in the Mainstream of Kuroshio Current in Eastern Taiwan and Its Transport of Carbon into the East China Sea Shelf

Qu Baoxiao, Song Jinming, Yuan Huamao, Li Xuegang, Li Ning (Institute of Ocenology, Chinese Academy of Sciences)

Comprehensive carbon chemistry data were measured from the mainstream of Kuroshio, off eastern Taiwan, in May 2014. Results indicated that variations of pH@25 °C, POC, ΩCa, DIC, pCO2 and RF were closely related to the characteristics of various water types. Phytoplankton photosynthesis played important roles in DIC variation in Kuroshio Surface Water (KSW), whereas the DIC variation in Kuroshio Subsurface Water (KSSW) was probably influenced by the external transport of DIC-enriched water from

the South China Sea. Vertical profiles of hydrological parameters and carbonate species indicated that the Kuroshio Current off eastern Taiwan could intrude into the ECS shelf as far as 27.9° E, 125.5° N in spring. What is more, the KSW, KSSW and Kuroshio Intermediate Water (KIW) could convey DIC into the East China Sea (ECS) with flux of 285, 305 and 112 Tg C/half year (1 Tg = 1012 g), respectively. The relevant flux of POC was 0.16, 2.93 and 0.04 Tg C/half year, respectively. Consequently, the intrusion of Kuroshio could probably exert a counteracting influence on the potential of CO2 uptake in the ECS, which needs further study.

P5-10 The temporal and spatial distribution and dynamic of dissolved carbon and the particulate organic carbon in the East China Sea

Lei He, Jianle Li, Kedong Yin (Sun Yat-Sen University)

The continental shelf is one of the most active regions in the marine carbon cycle. The East China Sea (ECS) is crucial to the global carbon cycle for having one of the largest continental shelves in the world. The dissolved inorganic carbon (DIC), dissolved organic carbon (DOC) , particulate organic carbon (POC) and other environmental factors such as nutrients, temperature, salinity, dissolved oxygen (DO) were analyzed on spring (May-June, 2014), summer (June-July, 2013), autumn (August, 2011), winter (January, 2015). In horizontal distribution, the highest DOC and POC concentration were in the coastal zones and tend to decrease toward the far shore because of the terrestrial input and biological activity. The DOC and POC concentration were significantly higher in spring and summer than in autumn and winter. On the contrary, the concentration of DIC was increased from inshore to offshore. Except DIC was highest in the Yangtze estuary and decreased towards the outer sea in the bottom in summer because of the thermocline. According to the correlation analysis, DOC has a significant correlation with different biological factors in different seasons, such as TN, PON and silicate. However, the high values of DOC were mainly attributed to the terrestrial sources in spring, which was proved by the significant negative correlation of DOC and salinity. POC has a significant positive correlation with Chla in four seasons, which suggested primary production is an important origin for POC. DIC has a significant correlation with temperature and AOU all through the year, which indicated the gas solubility and bacterial respiration have great influence on DIC, and the global warming may be a significant limitation to absorption of carbon dioxide by the ocean. Meanwhile, DIC has a significant negative correlation with Chla, DO and nutrients, which mean that the active photosynthesis of phytoplankton plays an important role in carbon sinking in spring and summer in ECS.

PATTICIPANTS LIST

	Name	Institute	Region	Email
1	BOYLE, Edward	Massachusetts Institute of Technology	USA	eaboyle@mit.edu
2	BUESSELER, Ken	Woods Hole Oceanographic Institution	USA	kbuesseler@whoi.edu
3	CAI, Wenju	CSIRO	Australia	Wenju.Cai@csiro.au
4	CAI, Yanjun	Institute of Earth Environment, CAS	China	yanjun_cai@ieecas.cn
5	CAI, Yongqing	Second Institute of Oceanography, SOA/Zhejiang University	China	caiyongqing@sio.org.cn
6	CHAI, Fei	Second Institute of Oceanography, SOA	China	fchai@sio.org.cn
7	CHAI, Junwei	Ocean University of China	China	meetingcjw@163.com
8	CHANG, Hang	Institute of Oceanology, CAS	China	changhag@foxmail.com
9	CHEN, Chen-Tung Arthur	National Sun Yat-sen University	China	ctchen@mail.nsysu.edu.tw
10	CHEN, Chuqun	South China Sea Institute of Oceanology, CAS	China	cqchen@scsio.ac.cn
11	CHEN, Guixing	Sun Yat-Sen University	China	chen_guixing@mail.sysu.edu.cn
12	CHEN, Haiying	Institute of Oceanology, CAS	China	hychen@qdio.ac.cn
13	CHEN, Jiajia	College of Oceanography, HoHai University	China	jiajia2016@hhu.edu.cn
14	CHEN, Lei	Institute of Oceanology, CAS	China	leichen815902132@126.com
15	CHEN, Lu	Institute of Oceanology, CAS	China	502958667@qq.com
16	CHEN, Meixiang	Hohai University	China	chenmeixiang@hhu.edu.cn
17	CHEN, Xianyao	Ocean Univeristy of China	China	chenxy@ouc.edu.cn
18	CHEN, Xiao	Hohai University	China	chenxiao1231@hhu.edu.cn
19	CHEN, Xiong	College of Meteorology and Oceanography, National University of Defense Technology	China	chenx_zc_mail@sina.com
20	CHENG, Lijing	Institute of Atmospheric Physics, CAS	China	chenglij@mail.iap.ac.cn
21	CHI, Jie	Institute of Oceanology, CAS	China	chijie@qdio.ac.cn
22	CUI, Chaoran	Institute of Oceanology, CAS	China	crcui@qdio.ac.cn
23	DAI, Minhan	Xiamen University	China	mdai@xmu.edu.cn
24	DANABASOGLU, Gokhan	Climate and Global Dynamics Division, NESL, National Center for Atmospheric Research	USA	gokhan@ucar.edu
25	DING, Weiwei	National University of Defense Technology	China	993837570@qq.com

26	DING, Yang	Ocean University of China	China	dingyangpol@ouc.edu.cn
27	DONG, Wenjing	Ocean University of China	China	945732544@qq.com
28	DU, Mei	Institute of Oceanology, CAS	China	dumei15@mails.ucas.ac.cn
29	DU, Meishan	Institute of Oceanology, CAS	China	msdu@qdio.ac.cn
30	DU, Yan	South China Sea Institute of Oceanology, CAS	China	duyan@scsio.ac.cn
31	DUAN, Jing	Institute of Oceanology, CAS	China	jingduan@qdio.ac.cn
32	ENIAFE, Basit Akanni	Amanpour Royal Nigeria Limited	Nigeria	amanpourroyalniglimited@gmail.com
33	FENG, Junqiao	Institute of Oceanology, CAS	China	fengjunqiao@qdio.ac.cn
34	FENG, Ling	Institute of Oceanology, CAS	China	lingfeng0219@163.com
35	FENG, Ming	CSIRO	Australia	ming.feng@csiro.au
36	FU, Gang	Ocean University of China	China	fugang@ouc.edu.cn
37	GAN, Bolan	Ocean University of China	China	gbl0203@ouc.edu.cn
38	GAN, Jianping	The Hong Kong University of Science and Technology	China	magan@ust.hk
39	GAO, Chuan	Institute of Oceanology, CAS	China	gaochuan@qdio.ac.cn
40	GAO, Guandong	Institute of Oceanology, CAS	China	guandonggao@qdio.ac.cn
41	GAO, Jiaxiang	Institute of Oceanology, CAS	China	gaojiaxiang15@mails.ucas.ac.cn
42	GAO, Jing	Institute of Oceanology, CAS	China	gaojingiocas@126.com
43	GAO, Kunshan	Xiamen University	China	ksgao@xmu.edu.cn
44	GAO, Tianxiang	Ocean University of China	China	987718954@qq.com
45	GAO, Wei	Institute of Oceanology, CAS	China	gaowei880121@sina.com
46	GENG, Yu	Institute of Oceanology, CAS	China	gengyu115@mails.ucas.ac.cn
47	GHASSEM, Asrar	University of Maryland	USA	Ghassem.Asrar@pnnl.gov
48	GORDON, Arnold L.	Lamont-Doherty Earth Observatory, Columbia University	USA	agordon@ldeo.columbia.edu
49	GU, Pinting	Ocean University of China	China	849614094@qq.com
50	GUAN, Cong	Institute of Oceanology, CAS	China	congguan@qdio.ac.cn
51	GUAN, Shoude	Institute of Oceanology, CAS	China	guanshoude@qdio.ac.cn
52	GUAN, Yuping	South China Sea Institute of Oceanology, CAS	China	guan@scsio.ac.cn
53	GUO, Haihong	Ocean University of China	China	oucguohaihong@qq.com
54	GUO, Li	Chinese Academy of Meteorological Sciences	China	guoli01001@126.com
55	GUO, Lijuan	Institute of Oceanology, CAS	China	guolijuan@qdio.ac.cn
56	GUO, Lingrui	Ocean University of China	China	glr2010@126.com
57	HALPERN, David	Scripps Institution of Oceanography	USA	dhalpern@ucsd.edu

58	HAO, Yuqian	Chinese Academy of Meteorological Sciences	China	yuqianhao0315@163.com
59	HE, Hailun	Second Institute of Oceanography, SOA	China	hailunhe777@gmail.com
60	HE, Jingjing	Ocean University of China	China	hejj17@163.com
61	HE, Lei	Sun Yat-Sen University	China	helei23@mail.sysu.edu.cn
62	HOU, Huaqian	Institute of Oceanology, CAS	China	samhou4177@foxmail.com
63	HOU, Xia	Ocean University of China	China	houx@ouc.edu.cn
64	HOU, Yinglin	Institute of Oceanology, CAS	China	haidahyl@163.com
65	HU, Dunxin	Institute of Oceanology, CAS	China	dxhu@qdio.ac.cn
66	HU, Rou	Ocean University of China	China	546016697@qq.com
67	HU, Shijian	Institute of Oceanology, CAS	China	sjhu@qdio.ac.cn
68	HU, Xiaoming	Sun Yat-Sen University	China	huxm6@mail.sysu.edu.cn
69	HU, Zifeng	Hohai University	China	zifeng.hu@qq.com
70	HUA, Lijuan	Chinese Academy of Meteorological Sciences	China	hualj@cma.gov.cn
71	HUANG, Ke	South China Sea Institute of Oceanology, CAS	China	kehuang@scsio.ac.cn
72	HUANG, Ying	Institute of Oceanology, CAS	China	879092015@qq.com
73	HUI, Chang	Ocean University of China	China	huichang@stu.ouc.edu.cn
74	ILOMO, Ophery	University of Dar Es Salaam	Tanzania	ilomo67@gmail.com
75	JEON, Chanhyung	Inha University	South Korea	chanhyungjeon@gmail.com
76	JIA, Fan	Institute of Oceanology, CAS	China	jiafan@qdio.ac.cn
77	JIANG, Dabang	Institute of Atmospheric Physics, CAS	China	jiangdb@mail.iap.ac.cn
78	JIANG, Ning	Chinese Academy of Meteorological Sciences	China	jiangn@cma.gov.cn
79	JIANG, Shuo	East China Normal University	China	jiangshuo1020@163.com
80	JIANG, Zhipeng	Ocean University of China	China	15063969590@163.com
81	JIAO, Nianzhi	Xiamen University	China	jiao@xmu.edu.cn
82	JIN, Xin	Institute of Atmospheric Physics, CAS	China	aosl@mail.iap.ac.cn
83	JIN, Yi	Ocean University of China	China	jinyi.ocean@gmail.com
84	KESSLER, William	NOAA/PMEL	USA	william.s.kessler@noaa.gov
85	KIRAN, Kumar Pullabhatla	Physical Research Laboratory	India	kiranp@prl.res.in
86	LAN, Jian	Ocean University of China	China	lanjian@ouc.edu.cn
87	LEE, Jae Hak	Korea Institute of Ocean Science and Technology	South Korea	jhlee@kiost.ac.kr
88	LENG, Hengling	Hohai University	China	161331010005@hhu.edu.cn
89	LI, Ailian	Institute of Oceanology, CAS	China	1030213857@qq.com

90	LI, Bo	South China Sea Institute of Oceanology, CAS	China	libo@scsio.ac.cn
91	LI, Jianping	Beijing Normal University	China	ljp@bnu.edu.cn
92	LI, Jingkai	Ocean University of China	China	ljk1105@ouc.edu.cn
93	LI, Junlu	The Hong Kong University of Science and Technology	China	jliaw@connect.ust.hk
94	LI, Lijuan	Institute of Atmospheric Physics, CAS	China	ljli@mail.iap.ac.cn
95	LI, Mingkui	Ocean University of China	China	mkli@ouc.edu.cn
96	LI, Mingting	Peking University	China	limingting@pku.edu.cn
97	LI, Qiuxian	Ocean University of China	China	1404448299@qq.com
98	LI, Rui	Institute of Oceanology, CAS	China	lirui@qdio.ac.cn
99	LI, Shujun	Ocean University of China	China	lishujunouc@163.com
100	LI, Tiegang	First Institute of Oceanography, SOA	China	tgli@fio.org.cn
101	LI, Xinyue	Ocean University of China	China	xinyueli_ouc@163.com
102	LI, Yan	South China Sea Institute of Oceanology, CAS	China	yanl@scsio.ac.cn
103	LI, Yanqin	Ocean University of China	China	liyanqin@stu.ouc.edu.cn
104	LI, Yanqing	Institute of Oceanology, CAS	China	liyanqing@qdio.ac.cn
105	LI, Yuanlong	Institute of Oceanology, CAS	China	liyuanlong@qdio.ac.cn
106	LI, Yunyu	Institute of Oceanology, CAS	China	lyy@qdio.ac.cn
107	LI, Zhuoran	Ocean University of China	China	lzrtibet@126.com
108	LI, Ziguang	Ocean Univeristy of China	China	ziguangli@ouc.edu.cn
109	LIN, Li	Institute of Oceanology, CAS	China	dorislin@qdio.ac.cn
110	LIN, Xiaopei	Ocean University of China	China	linxiaop@ouc.edu.cn
111	LIU, Boqi	Chinese Academy of Meteorological Sciences	China	lbq@lasg.iap.ac.cn
112	LIU, Chuanyu	Institute of Oceanology, CAS	China	chuanyu.liu@qdio.ac.cn
113	LIU, Cong	Ocean University of China	China	liucong175@gmail.com
114	LIU, Hengchang	Institute of Oceanology, CAS	China	liuhengchang16@mails.ucas.ac.cn
115	LIU, Hongwei	Institute of Oceanology, CAS	China	liuhongwei@qdio.ac.cn
116	LIU, Jingwu	Ocean University of China	China	liujingwu@126.com
117	LIU, Lingling	Institute of Oceanology, CAS	China	liull@qdio.ac.cn
118	LIU, Qinyan	South China Sea Institute of Oceanology, CAS	China	qyliu66@scsio.ac.cn
119	LIU, Qinyu	Ocean University of China	China	liuqy@ouc.edu.cn
120	LIU, Yang	Institute of Oceanology, CAS	China	liuyang@qdio.ac.cn
121	LIU, Yi	Ocean University of China	China	liuy_1996@163.com
122	LIU, Yu	Institute of Earth Environment, CAS	China	liuyu@loess.llqg.ac.cn
123	LUO, Yiyong	Ocean University of China	China	yiyongluo@ouc.edu.cn
124	LV, Haibin	Huai Hai Institute of Technology	China	kjxlhb@126.com

125	LV, Mingkun	Institute of Oceanology, CAS	China	qdlvmingkun@126.com
126	LV, Yilong	Institute of Oceanology, CAS	China	lvyl90@163.com
127	MA, Jinfeng	Institute of Atmospheric Physics, CAS	China	jfma@lasg.iap.ac.cn
128	MA, Junying	Institute of Oceanology, CAS	China	majy@ms.qdio.ac.cn
129	MA, Qian	Ocean University of China	China	oucmaqian@163.com
130	MA, Qiang	Institute of Oceanology, CAS	China	mqiocas@gmail.com
131	MA, Shuangmei	Institute of Climate System, Chinese Academy of Meteorological Sciences	China	masm@cma.gov.cn
132	MA, Yixin	Institute of Oceanology, CAS	China	mayixin@qdio.ac.cn
133	MEI, Huan	College of Oceanography, Hohai University	China	hmei@hhu.edu.cn
134	MIAO, Yu	College of Global Change and Earth System Sciences (GCESS), Beijing Normal University	China	273171128@qq.com
135	MIN, Wenjia	Institute of Oceanology, CAS	China	minwenjia@163.com
136	MINOBE, Shoshiro	Hokkaido University	Japan	minobe@sci.hokudai.ac.jp
137	MULLUNGAL, Muhammed Nayeem	Qatar University	India	nayeemmuhamed@gmail.com
138	NAGARAJAH, Rajkumar	University of Colombo	Sri Lanka	rajacqueline@yahoo.com
139	NAN, Feng	Institute of Oceanology, CAS	China	nanfeng0515@qdio.ac.cn
140	OKA, Eitarou	Atmosphere and Ocean Research Institute, The University of Tokyo	Japan	eoka@aori.u-tokyo.ac.jp
141	OLADEINDE, Suraju Olanrewaju	Amanpour Royal Nigeria Limited	Nigeria	louisy2k.2001@yahoo.com
142	OLAMILEKAN, Ajadi Rasheed	Amanpour Royal Nigeria Limited	Nigeria	louisy2k.2001@gmail.com
143	PARK, Jae-Hun	Inha University	South Korea	jaehunpark@inha.ac.kr
144	PEI, Lin	Institute of Urban Meteorology, CMA	China	lpei@ium.cn
145	QI, Jifeng	Institute of Oceanology, CAS	China	jfqi@qdio.ac.cn
146	QIN, Huiling	Sun Yat-Sen University	China	qinhling@mail.sysu.edu.cn
147	QIU, Bo	University of Hawaii	USA	bo@soest.hawaii.edu
148	QU, Baoxiao	Institute of Oceanology, CAS	China	qubx@qdio.ac.cn
149	REN, Qiuping	Institute of Oceanology, CAS	China	renqiuping17@mails.ucas.ac.cn
150	RHINES, Peter B.	University of Washington	USA	rhinesp@gmail.com
151	RICHET, Océane	CSIRO	Australia	oceane.richet@csiro.au
152	RUAN, Ruomei	Ocean University of China	China	ruanruomei@126.com
153	SANTOS, Jose	International CLIVAR Project Office	USA	jose.santos@clivar.org

154	SCHNEIDER, Niklas	University of Hawaii	USA	nschneid@hawaii.edu
155	SEN GUPTA, Alexander	University Of New South Wales	Australia	a.sengupta@unsw.edu.au
156	SHAO, Yu-Xian	Editorial Office of Advances in Climate Change Research/National Climate Center	China	shaoyx@cma.gov.cn
157	SHI, Fei	Ocean University of China	China	994940228@qq.com
158	SHI, Huangyuan	Ocean University of China	China	1464061484@qq.com
159	SHI, Xingyu	Institute of Oceanology, CAS	China	353398133@qq.com
160	SONG, Lina	Institute of Oceanology, CAS	China	linasong1987@126.com
161	SPEICH, Sabrina	Laboratoire de Météorologie Dynamique (LMD), Institut Pierre-Simon Laplace (IPSL)	France	speich@lmd.ens.fr
162	SPRINTALL, Janet	Scripps Institution of Oceanography	USA	jsprintall@ucsd.edu
163	SU, Jingzhi	Chinese Academy of Meteorological Sciences	China	sujz@cma.gov.cn
164	SUI, Weihui	Public Meteorological Service Centre, CMA	China	suiweihui@hotmail.com
165	SULLIVAN, Arnold	CSIRO	Australia	arnold.sullivan@csiro.au
166	SUN, Bingrong	Ocean University of China	China	sunbingrong@stu.ouc.edu.cn
167	SUN, Changfeng	Institute of Earth Environment, CAS	China	suncf@ieecas.cn
168	SUN, Fan	Institute of Oceanology, CAS	China	sunfansunshine@163.com
169	SUN, Runnan	Beijing Normal University	China	1531462597@qq.com
170	SUN, Yan	Institute of Oceanology, CAS	China	yansun@qdio.ac.cn
171	SUN, Yue	Ocean University of China	China	1327357381@qq.com
172	TANG, Xiaohui	Institute of Oceanology, CAS	China	tangxiaohui@qdio.ac.cn
173	TANG, Zhijia	Institute of Oceanology, CAS	China	tangzj123@foxmail.com
174	TAO, Shuhao	Ocean University of China	China	1592189885@qq.com
175	TIAN, Feng	Institute of Oceanology, CAS	China	tianfeng777@hotmail.com
176	WANG, Bin	Hohai University	China	wangbinzwsx@hhu.edu.cn
177	WANG, Bin	University of Hawaii	USA	wangbin@hawaii.edu
178	WANG, Chunzai	South China Sea Institute of Oceanology, CAS	China	cwang@scsio.ac.cn
179	WANG, Dan	National Marine Environmental Forecasting Center	China	saisaiwang@163.com
180	WANG, Dongxiao	South China Sea Institute of Oceanology, CAS	China	dxwang@scsio.ac.cn
181	WANG, Faming	Institute of Oceanology, CAS	China	faming_wang@qdio.ac.cn
182	WANG, Fan	Institute of Oceanology, CAS	China	fwang@qdio.ac.cn

183	WANG, Fujun	Institute of Oceanology, CAS	China	fujunwang@qdio.ac.cn
184	WANG, Guojian	CSIRO	Australia	Guojian.Wang@csiro.au
185	WANG, Hanshi	Ocean University of China	China	595059418@qq.com
186	WANG, Hongna	Institute of Oceanology, CAS	China	wanghongna@qdio.ac.cn
187	WANG, Jianing	Institute of Oceanology, CAS	China	wjn@qdio.ac.cn
188	WANG, Jing	Institute of Oceanology, CAS	China	candywang@qdio.ac.cn
189	WANG, Jing	Institute of Oceanology, CAS	China	wangjing@qdio.ac.cn
190	WANG, Jinping	Ocean University of China	China	clytie159@yeah.net
191	WANG, Kai	Institute of Oceanology, CAS	China	949172284@qq.com
192	WANG, Min	Institute of Oceanology, CAS	China	wangmin@qdio.ac.cn
193	WANG, Qingye	Institute of Oceanology, CAS	China	wangqy@qdio.ac.cn
194	WANG, Ran	Hohai University	China	wangr@hhu.edu.cn
195	WANG, Tianyu	Ocean University of China	China	skytwang@153.com
196	WANG, Tianyu	South China Sea Institute of Oceanology, CAS	China	wty_927@hotmail.com
197	WANG, Weidong	Institute of Oceanology, CAS	China	wangweidong215@mails.ucas.ac.cn
198	WANG, Xiaowei	Institute of Oceanology, CAS	China	wangxiaowei@qdio.ac.cn
199	WANG, Xin	South China Sea Institute of Oceanology, CAS	China	wangxin@scsio.ac.cn
200	WANG, Xiuqin	Ocean University of China	China	wangxq@ouc.edu.cn
201	WANG, Yang	Institute of Oceanology, CAS	China	effwang@126.com
202	WANG, Yuehong	College of Global Change and Earth System Sciences (GCESS), Beijing Normal University	China	201521490011@mail.bnu.edu.cn
203	WANG, Yuntao	Second Institute of Oceanography, SOA	China	yuntao.wang@sio.org.cn
204	WANG, Zhenyan	Institute of Oceanology, CAS	China	zywang@qdio.ac.cn
205	WANG, Zhuoyue	Institute of Oceanology, CAS	China	wangzhuoyue16@mails.ucas.ac.cn
206	WEI, Jun	Peking University	China	junwei@pku.edu.cn
207	WIJFFELS, Suan	CSIRO	Australia	Susan.Wijffels@csiro.au
208	WU, Baolan	Ocean University of China	China	wubaolan@stu.ouc.edu.cn
209	WU, Bo	Institute of Atmospheric Physics, CAS	China	wubo@mail.iap.ac.cn
210	WU, Lixin	Ocean University of China	China	lxwu@ouc.edu.cn
211	WU, Shouchang	Second Institute of Oceanography, SOA	China	shouchangwu@163.com
212	XI, Lu	Sun Yat-Sen University	China	luxi5@mail.sysu.edu.cn
213	XIAO, Kai	hohai university	China	1550809212@qq.com
214	XIE, Shang-Ping	Scripps Institution of Oceanography	USA	sxie@ucsd.edu
215	XIE, Shuyi	Hohai University	China	shuyixie@163.com
216	XIE, Tiejun	Beijing Normal University	China	xietiejunhn@163.com

217	XIU, Peng	South China Sea Institute of Oceanology, CAS	China	pxiu@scsio.ac.cn
218	XU, Anqi	Institute of Oceanology, CAS	China	anqi1212@126.com
219	XU, Lingjing	Institute of Oceanology, CAS	China	418132374@qq.com
220	XU, Lixiao	Ocean University of China	China	xulixiao2004@126.com
221	XU, Tengfei	First Institute of Oceanography, SOA	China	xutengfei@fio.org.cn
222	XU, Yongsheng	Institute of Oceanology, CAS	China	yongsheng.xu@qdio.ac.cn
223	XU, Zhenhua	Institute of Oceanology, CAS	China	xuzhenhua@qdio.ac.cn
224	XUE, Huijie	South China Sea Institute of Oceanology, CAS	China	huijiexue@scsio.ac.cn
225	YAMAGATA, Toshio	JAMSTEC	Japan	yamagata@jamstec.go.jp
226	YAN, Jie	Institute of Oceanology, CAS	China	yanjie16@mails.ucas.ac.cn
227	YANG, Dezhou	Institute of Oceanology, CAS	China	yangdezhou@qdio.ac.cn
228	YANG, Fengfan	Institute of Oceanology, CAS	China	fengfanyang@qdio.ac.cn
229	YANG, Jing	Ocean University of China	China	707933428@qq.com
230	YANG, Jun-Chao	Ocean University of China	China	yangjunchao1991@163.com
231	YANG, Liu	Ocean University of China	China	2422197447@qq.com
232	YANG, Wenlong	Institute of Oceanology, CAS	China	yangwenlong16@mails.ucas.ac.cn
233	YANG, Yun	Beijing Normal University	China	yunyang@bnu.edu.cn
234	YANG, Yuxing	Institute of Oceanology, CAS	China	yangyx@qdio.ac.cn
235	YIN, Baoshu	Institute of Oceanology, CAS	China	bsyin@qdio.ac.cn
236	YU, Jin-Yi	University of California, Irvine	USA	jyyu@uci.edu
237	YU, Jun	Beijing Normal University	China	962898226@qq.com
238	YU, Miao	Institute of Urban Meteorology, CMA	China	yumiao0926@126.com
239	YU, Minjie	Chinese Academy of Meteorological Sciences	China	yuminjie_1994@163.com
240	YU, Pei-long	College of Meteorology and Oceanography, National University of Defense Technology	China	ypl_cli@sina.cn
241	YU, Tan	Shanghai Ocean University	China	tyu@shou.edu.cn
242	YU, Xiaojing	Institute of Desert Meteorology, CMA	China	yxj1301@126.com
243	YU, Yi	Second Institute of Oceanography, SOA	China	yiyu@sio.org.cn
244	YU, Yongqiang	Institute of Atmospheric Physics, CAS	China	yyq@lasg.iap.ac.cn
245	YUAN, Dongliang	Institute of Oceanology, CAS	China	dyuan@qdio.ac.cn
246	ZANG, Nan	Institute of Oceanology, CAS	China	zangnan@qdio.ac.cn
247	ZELLER, Mathias	Monash University	Australia	mathias.zeller@monash.edu
248	ZENG, Lili	South China Sea Institute of Oceanology, CAS	China	zenglili@scsio.ac.cn

249	ZHAI, Fangguo	Ocean University of China	China	gfzhai@ouc.edu.cn
250	ZHANG, Haoran	Second Institute of Oceanography, SOA	China	zhanghaoran22@163.com
251	ZHANG, Li	Ocean University of China	China	lzhang@qnlm.ac
252	ZHANG, Ling	Institute of Oceanology, CAS	China	zhangling@qdio.ac.cn
253	ZHANG, Linlin	Institute of Oceanology, CAS	China	zhanglinlin@qdio.ac.cn
254	ZHANG, Miao	East China Normal University	China	zhangmiaohh@126.com
255	ZHANG, Ningning	Nanjing University of Information Science and Technology	China	znn.happy@163.com
256	ZHANG, Rong-Hua	Institute of Oceanology, CAS	China	rzhang@qdio.ac.cn
257	ZHANG, Weiwei	Xiamen University	China	wwzhangxmu@xmu.edu.cn
258	ZHANG, Yazhou	College of Global Change and Earth System Sciences (GCESS), Beijing Normal University	China	201531490008@mail.bnu.edu.cn
259	ZHANG, Ying	South China Sea Institute of Oceanology, CAS	China	zhangying@scsio.ac.cn
260	ZHANG, Yueqi	Ocean University of China	China	zyq@stu.ouc.edu.cn
261	ZHANG, Zhengguang	Ocean University of China	China	zhengguang@ouc.edu.cn
262	ZHAO, Bo	Institute of Oceanology, CAS	China	zb00808099@163.com
263	ZHAO, Xia	Institute of Oceanology, CAS	China	zhaoxia@qdio.ac.cn
264	ZHENG, Jian	Institute of Oceanology, CAS	China	zhengjian@qdio.ac.cn
265	ZHENG, Jie	Institute of Oceanology, CAS	China	zhengjie@qdio.ac.cn
266	ZHONG, Wenxiu	Ocean University of China	China	doriszhong60@163.com
267	ZHOU, Guanghui	Institute of Oceanology, CAS	China	zhough@qdio.ac.cn
268	ZHOU, Hui	Institute of Oceanology, CAS	China	147824248@qq.com
269	ZHOU, Li	Institute of Oceanology, CAS	China	zhoulihenu@163.com
270	ZHOU, Xin	Institute of Atmospheric Physics, CAS	China	njudaqizhouxin@sina.com
271	ZHU, Congwen	Chinese Academy of Meteorological Sciences	China	zhucw@cma.gov.cn
272	ZHU, Ruichen	Ocean University of China	China	zrc@stu.ouc.edu.cn
273	ZHU, Yuchao	Institute of Oceanology, CAS	China	yuchaozhu@qdio.ac.cn
274	ZHUANG, Wei	Xiamen University	China	wzhuang@xmu.edu.cn

LOGISTICS

Name	Email	Cell Phone	Affairs
ZHOU, Hui	zhouhui@qdio.ac.cn	+86 18953286497	General
MA, Yixin	mayixin@qdio.ac.cn	+86 18724761399	Meeting Venue
WANG, Jianing	wjn@qdio.ac.cn	+86 18561681378	Transportation
HU, Shijian	sjhu@qdio.ac.cn	+86 18105321381	Sheraton Hotel Accommodation
WANG, Jing	candywang@qdio.ac.cn	+86 13589203052	Registration
ZHANG, Linlin	zhanglinlin@qdio.ac.cn	+86 18562712171	Poster & Booth
MA, Junying	majy@qdio.ac.cn	+86 13583217288	Dining
ZHENG, Jie	zhengjie@qdio.ac.cn	+86 13127005703	Volunteers

Local Organizing Room: 830, 831

Please dial 0 and transfer to room 830 or room 831 through hotel telephone for any conference related queries.